

NATIONAL BUREAU OF STANDARDS
MICROCOPY RESOLUTION TEST CHART

AD-A162 994

12

AFWAL-TR-85-2055



*FLOW TRANSITION IN GAS TURBINE AIRFOIL BOUNDARY
LAYERS: FUNDAMENTALS AND EMPIRICISMS

Gregory S. West and Lit S. Han

Department of Mechanical Engineering
The Ohio State University
Columbus, Ohio 43210



September 1985

Final Report for Period 29 March 1982 - 28 December 1984

Approved for public release; distribution unlimited.

AERO PROPULSION LABORATORY
AIR FORCE WRIGHT AERONAUTICAL LABORATORIES
AIR FORCE SYSTEMS COMMAND
WRIGHT-PATTERSON AIR FORCE BASE, OHIO 45433

(*Funded in Part by NASA Lewis Research Center.)

DTIC FILE COPY

6 1 8 099

When Government drawings, specifications, or other data are used for any purpose other than in connection with a definitely related Government procurement operation, the United States Government thereby incurs no responsibility nor any obligation whatsoever; and the fact that the government may have formulated, furnished, or in any way supplied the said drawings, specifications, or other data, is not to be regarded by implication or otherwise as in any manner licensing the holder or any other person or corporation, or conveying any rights or permission to manufacture use, or sell any patented invention that may in any way be related thereto.

This report has been reviewed by the Office of Public Affairs (ASD/PA) and is releasable to the National Technical Information Service (NTIS). At NTIS, it will be available to the general public, including foreign nations.

This technical report has been reviewed and is approved for publication.

Charles D MacArthur

CHARLES D. MACARTHUR
Project Engineer

Michael E Stefkovich

MICHAEL E. STEFKOVICH, Major, USAF
Chief, Components Branch

FOR THE COMMANDER

Robert W. Baker

ROBERT W. BAKER, Major, USAF
Deputy Director
Turbine Engine Division
Aero Propulsion Laboratory

"If your address has changed, if you wish to be removed from our mailing list, or if the addressee is no longer employed by your organization please notify AFWAL/POTC, W-PAFB, OH 45433 to help us maintain a current mailing list".

Copies of this report should not be returned unless return is required by security considerations, contractual obligations, or notice on a specific document.

Unclassified

SECURITY CLASSIFICATION OF THIS PAGE

REPORT DOCUMENTATION PAGE

1a. REPORT SECURITY CLASSIFICATION Unclassified		1b. RESTRICTIVE MARKINGS	
2a. SECURITY CLASSIFICATION AUTHORITY		3. DISTRIBUTION/AVAILABILITY OF REPORT Approved for public release; distribution unlimited	
2b. DECLASSIFICATION/DOWNGRADING SCHEDULE			
4. PERFORMING ORGANIZATION REPORT NUMBER(S) 714467/763057		5. MONITORING ORGANIZATION REPORT NUMBER(S) AFWAL-TR-85-2055	
6a. NAME OF PERFORMING ORGANIZATION The Ohio State University Research Foundation	6b. OFFICE SYMBOL (If applicable)	7a. NAME OF MONITORING ORGANIZATION Air Force Wright Aeronautical Laboratories Aero Propulsion Laboratory (AFWAL/POTC)	
6c. ADDRESS (City, State and ZIP Code) 1314 Kinnear Road Columbus, Ohio 43212		7b. ADDRESS (City, State and ZIP Code) Wright-Patterson AFB, OH, 45433	
8a. NAME OF FUNDING/SPONSORING ORGANIZATION * Aero Propulsion Laboratory (see item 16)	8b. OFFICE SYMBOL (If applicable) AFWAL/POTC	9. PROCUREMENT INSTRUMENT IDENTIFICATION NUMBER In part under M1PR-C-79073-D* F33615-82-K-2218	
8c. ADDRESS (City, State and ZIP Code) Wright-Patterson Air Force Base, Ohio 45433		10. SOURCE OF FUNDING NOS.	
11. TITLE (Include Security Classification) ** see reverse		PROGRAM ELEMENT NO. 62203F	PROJECT NO. 3066
12. PERSONAL AUTHOR(S) Gregory S. West and Lit S. Han		TASK NO. 14	WORK UNIT NO. 11
13a. TYPE OF REPORT Final	13b. TIME COVERED FROM 3/29-82 TO 12-28-84	14. DATE OF REPORT (Yr., Mo., Day) September 1985	15. PAGE COUNT 169
16. SUPPLEMENTARY NOTATION *Funded in Part by NASA Lewis Research Center, Cleveland Ohio 44135			
17. COSATI CODES		18. SUBJECT TERMS (Continue on reverse if necessary and identify by block number)	
FIELD 21	GROUP 05	gas turbine; airfoil boundary layer, transition.	
19. ABSTRACT (Continue on reverse if necessary and identify by block number) Transition prediction in gas turbine boundary layer flows is critical in assessing the cooling requirements for gas turbine vanes and blades. This report summarized the classical, fundamental findings in transition prediction for simplified geometrics and discusses the empirical rules currently in use for the gas turbine environments.			
20. DISTRIBUTION/AVAILABILITY OF ABSTRACT UNCLASSIFIED/UNLIMITED <input checked="" type="checkbox"/> SAME AS RPT. <input type="checkbox"/> DTIC USERS <input type="checkbox"/>		21. ABSTRACT SECURITY CLASSIFICATION Unclassified	
22a. NAME OF RESPONSIBLE INDIVIDUAL Charles D. MacArthur		22b. TELEPHONE NUMBER (Include Area Code) (513) 255-4830	22c. OFFICE SYMBOL AFWAL/POTC

Unclassified

SECURITY CLASSIFICATION OF THIS PAGE

**Block 11. Title
Flow Transition in Gas Turbine Airfoil Boundary Layers: Fundamentals and Empiricisms

Unclassified

SECURITY CLASSIFICATION OF THIS PAGE

FOREWORD

The contents of this report constitute one phase of a two-part research program sponsored by the Air Force Wright Aeronautical Laboratories, Aero Propulsion Laboratory, USAF, Contract No. F33615-82-K-2218. The program, administered through The Ohio State University Research Foundation, was monitored by Dr. Kervyn Mach and by Mr. Charles MacArthur of AFWAL. The program is part of an overall effort to achieve two objectives in enhancing the cooling technology in the hot sections of gas turbine engines.

The first objective ^{of this study} concerns the phenomenon of flow transition in boundary layers on turbine airfoils--from the onset of turbulence to the transition completion. Transition studies, though fundamental to fluid mechanics, are unique in gas turbine cascades because of the compounding factors that act not in individual isolation, but as a collective group and that constitute by-pass mechanisms not amenable to linear analyses from a mathematical point of view.

The second objective is to evolve an engineering methodology to account for ~~the~~ surface roughness effects on heat transfer and turbulent boundary layer analyses, which have heretofore been studied in fragments. → 2 1 4)

Because these two research phases are distinct from each other, it is advisable to document their results in separate reports. Hence, this presentation focuses on the results of transition study. As part of their continuing interest in propulsion technology, NASA Lewis Research Center partially supplied funding for this phase of the research effort. Their financial assistance is hereby acknowledged.

TABLE OF CONTENTS

	<u>Page</u>
I. INTRODUCTION: THE NATURE OF TRANSITION IN A BOUNDARY LAYER FLOW	1
II. LINEAR STABILITY THEORY	7
III. NONLINEAR STABILITY INVESTIGATIONS	11
IV. FLAT PLATE BOUNDARY LAYER TRANSITION AND THE TOLLMIEN-SCHLICHTING INSTABILITY	13
4.1 Freestream Disturbance Effects	15
4.2 Pressure Gradient Influence	25
4.3 Heat Transfer Influence	31
4.4 Compressibility Influence	37
V. TRANSITION ON STREAMWISE CURVED SURFACES AND THE GÖRTLER INSTABILITY	41
5.1 Linear Analyses of Görtler Instability	46
5.2 Nonlinear Analyses of Görtler Instability	63
5.3 Experimental Results on Transition Over Streamwise Curved Flow Surfaces	64
VI. INSTABILITY AND TRANSITION IN PERIODICALLY UNSTEADY NONREVERSING BOUNDARY LAYERS	77
VII. PREDICTING TRANSITION	89
7.1 Linear Theory Approaches	90
7.2 Turbulence Models	93
7.3 Empirical Correlations	96
7.4 Abu-Ghannam and Shaw's Correlation	99
7.5 Abu-Ghannam and Shaw's Method and its Operational Features	113

TABLE OF CONTENTS
(Continued)

	<u>Page</u>
VIII. HEAT TRANSFER IN THE TRANSITION REGIME	125
IX. THE GAS TURBINE ENVIRONMENT	129
9.1 Basic Cascade Flow Conditions	129
9.2 Flow Disturbances	130
9.3 Leading Edge Flow Stagnation	134
9.4 Secondary Flows	135
9.5 Flow Surface Roughness	136
9.6 Film Cooling	136
X. TURBINE CASCADE MODEL TRANSITION INVESTIGATIONS	139
XI. CONCLUDING REMARKS	143
BIBLIOGRAPHY	145

Accession For	
NTIS CRA&I	<input checked="" type="checkbox"/>
DTIC TAB	<input type="checkbox"/>
Unannounced	<input type="checkbox"/>
Justification	
By	
Distribution/	
Availability Codes	
Dist	Avail and/or Special
A-1	

LIST OF FIGURES

<u>Figure</u>		<u>Page</u>
1	Laminar boundary layer as a linear and nonlinear operator	2
2	Idealized sketch of instability and transition processes on a flat plate	16
3	Transition Reynolds number as a function of freestream disturbance intensity	18
4	Marginal stability locus for the Blasius flow	19
5	Marginal stability diagrams for some Falkner-Skan flows	27
6	Marginal stability diagrams for subsonic flow over isothermal surfaces	34
7	Effect of plate temperature on transition	36
8	Distributions of temperature, density, and viscosity in compressible boundary layers on an insulated wall	38
9	Effect of Mach Number on the stability of flow over an insulated surface	40
10	Görtler vortex instability in the boundary layer flow over a concave wall	42
11	Marginal Görtler vortex instability of Blasius flow - displacement thickness effects	49
12	Marginal Görtler stability of Blasius flow - decaying streamline curvature effects	51
13	Marginal Görtler stability of some Falkner-Skan flows	52
14	Potential flow net configuration for Floryan-Saric analysis	54
15	Curves of constant amplification rate for the Görtler instability in Blasius flow	55
16	Effect of Mach number on Görtler stability in flow over an insulated wall	57

LIST OF FIGURES

(Continued)

<u>Figure</u>		<u>Page</u>
17	Effect of Mach number and heat transfer on Görtler stability in flow over an isothermal wall	59
18	Variations of $G_{\theta c}$ with temperature ratio T_w/T_∞ under isothermal conditions	60
19	Marginal stability curves for combined Görtler and buoyancy instabilities	62
20	Transition measurements on 2.5-foot radius concave plate at three freestream turbulence levels	66
21	Effect of concave and convex streamwise wall curvature on transition	68
22	Transition measurements at various effective concave curvatures	70
23	Effects of pressure gradient on transition over a 20-foot radius convex surface	71
24	Effect of pressure gradient on transition over a 2.5-foot radius concave surface	72
25	Transition Reynolds number as function of amplitude and mean pressure gradient in periodically unsteady boundary layer flows	81
26	Overview of flow and instability regimes expected in the presence of zero mean pressure gradient flow oscillations	84
27	Effect of freestream turbulence level on the momentum thickness Reynolds numbers for transition onset and completion	102
28	Influence of freestream turbulence level and pressure gradient on the transition onset momentum thickness Reynolds number	103

LIST OF FIGURES

(Continued)

<u>Figure</u>		<u>Page</u>
29	Pressure distributions for the Abu-Ghannam and Shaw experiments	105
30	Relation between length Reynolds numbers for onset and completion of transition	106
31	Influence of pressure gradient on transition completion momentum thickness Reynolds number	108
32	Distribution of the normalized momentum thickness parameter in the transition regime	110
33	Distribution of the normalized shape factor parameter in the transition regime	111
34	Intermittency distribution in the transition regime	112
35	Friction coefficient variations by finite-difference calculations, van Driest model, flat plate	116
36	Momentum thickness variations by finite-difference calculations, van Driest model, flat plate	117
37	Friction coefficient variations by finite-difference calculations, exponential model, flat plate	119
38	Momentum thickness variations by finite-difference calculations, exponential model, flat plate	120
39	Blade-A suction surface velocity and heat transfer data, $U_i = 22$ fps.	122
40	Calculated friction coefficient, blade-A suction surface, $U_i = 22$ fps.	124
41	Schematic of a section of a turbine blade row and associated convective phenomena	131
42	Hot wire trace of unsteady flow	133

NOMENCLATURE

(Infrequently used symbols are defined in the text.)

<u>Symbol</u>	<u>Definition</u>
C_f	Local coefficient of skin friction, $\tau_w / \frac{1}{2} \rho U_o^2$
C_p	Pressure coefficient, $(p - p_\infty) / \frac{1}{2} \rho U_o^2$
F	Viscously nondimensionalized instability frequency, $\beta v / U_o^2$
G_θ	Görtler parameter, $(U_o \theta / \nu) \sqrt{\theta / r}$
$G_{\theta-t}$	Görtler parameter at transition onset
$G_{\delta-r}$	Görtler parameter based on δ_r , $(U_o \delta_r / \nu) \sqrt{\theta / r}$
H	Boundary layer velocity profile shape factor, δ^* / θ
M_∞	Freestream MACH number
Nu	Nusselt number
p	Local surface static pressure
P_∞	Reference freestream static pressure
Pr	Prandtl number
\dot{q}	Local heat transfer rate
r	Radius of streamwise flow surface curvature
Re_{ns}	Nonsteady Reynolds number, $(U_o \Delta U_o / \omega \nu)$
Re_x	Length Reynolds number, $(U_o x / \nu)$
Re_{δ^*}	Displacement thickness Reynolds number, $(U_o \delta^* / \nu)$
Re_θ	Momentum thickness Reynolds number, $(U_o \theta / \nu)$
$Re_{\theta-t}$	Momentum thickness Reynolds number at transition onset

NOMENCLATURE
(Continued)

<u>Symbol</u>	<u>Definition</u>
$Re_{\theta-T}$	Momentum thickness Reynolds number at transition completion
T	Local static temperature
T_{fs}	Freestream turbulence level, $1/3(u'^2 + v'^2 + w'^2)/U_\infty$
T_r	Adiabatic wall temperature (recovery temperature)
T_w	Wall temperature
T_∞	Reference freestream static temperature
u	Local streamwise component of boundary layer edge
u'	Streamwise component of disturbance velocity
U_0	Streamwise velocity at boundary layer edge
U_∞	Reference freestream velocity
v'	Wall-normal component of disturbance velocity
w'	Transverse component of disturbance velocity
x, y, z	Streamwise, wall-normal, and traverse Cartesian coordinates

Greek Symbols

$\alpha_{\delta-r}$	Nondimensional wavenumber, $2\pi\delta_r/\lambda_{G/TS}$
α_{δ^*}	Nondimensional wavenumber, $2\pi\delta^*/\lambda_{G/TS}$
α_θ	Nondimensional wavenumber, $2\pi\theta/\lambda_{G/TS}$

Greek Symbols

(Continued)

β	Circular frequency of Tollmien-Schlichting disturbances
β_{FS}	Hartree pressure gradient parameter for Falkner-Skan flows
γ	Intermittency factor for transitioning flow
δ	Boundary layer thickness
δ_r	Boundary layer similarity variable, $\sqrt{vx/U_0}$
δ_*	Boundary layer Displacement thickness
θ	Boundary layer Momentum thickness
κ	Acceleration parameter, $v(dU_0/dx)/U_0^2$
λ	Pohlhausen parameter, $(\delta^2/v)(dU_0/dx)$
λ_θ	Modified Pohlhausen parameter, $(\theta^2/v)(dU_0/dx)$
λ_G	Wavelength of Görtler disturbances
λ_{TS}	Wavelength of Tollmien-Schlichting disturbances
μ	Absolute viscosity
ν	Kinematic viscosity
ρ	Density
τ	Freestream turbulence level (percent), $T_{fs} \times 100$
τ_w	Wall shear stress
ω	Circular frequency of freestream oscillation, $2\pi f$

NOMENCLATURE
(Continued)

Subscripts

c	Critical
∞	Freestream
l	Laminar
mc	Minimum critical
o	Edge of boundary layer
t	Transition onset
tr	Transition region
tb	Turbulent region
T	Transition end
w	Wall

Reshotko
SRK

I. INTRODUCTION: THE NATURE OF TRANSITION IN A BOUNDARY LAYER FLOW

↳ Reshotko [4]* has suggested that transition may be viewed as the response of a very complex three-dimensional nonlinear oscillator (the laminar boundary layer) to a random and often statistically nonuniform forcing function (the disturbances). Morkovin [2] has proposed a unified view of the processes leading to transition, shown in Figure 1, which will aid in analyzing this description. *> to iii*

In Figure 1, the box labeled "A.C. INPUT = DISTURBANCES" indicates that the activation of the instability-transition mechanism requires a disturbance (see [3] and Gaster's paper in [4]) that is always present, at least infinitesimally. Furthermore, the response of the boundary layer is very strongly dependent on the magnitude and spectral distribution, and even somewhat on the orientation of the unsteady disturbances.

The arrows from the input box to "LINEAR AMPLIFICATION" denote the "receptivity" of the boundary layer. Receptivity, a term applied by Morkovin, refers to the means by which disturbances couple with, and are assimilated by, the boundary layer. Morkovin's analog for the receptivity mechanism is a variable band-pass filter-preamplifier.

In small disturbance flows over smooth walls, the available disturbance environment tends to excite a selected frequency of boundary layer

*Numbers in brackets refer to references in the Bibliography.

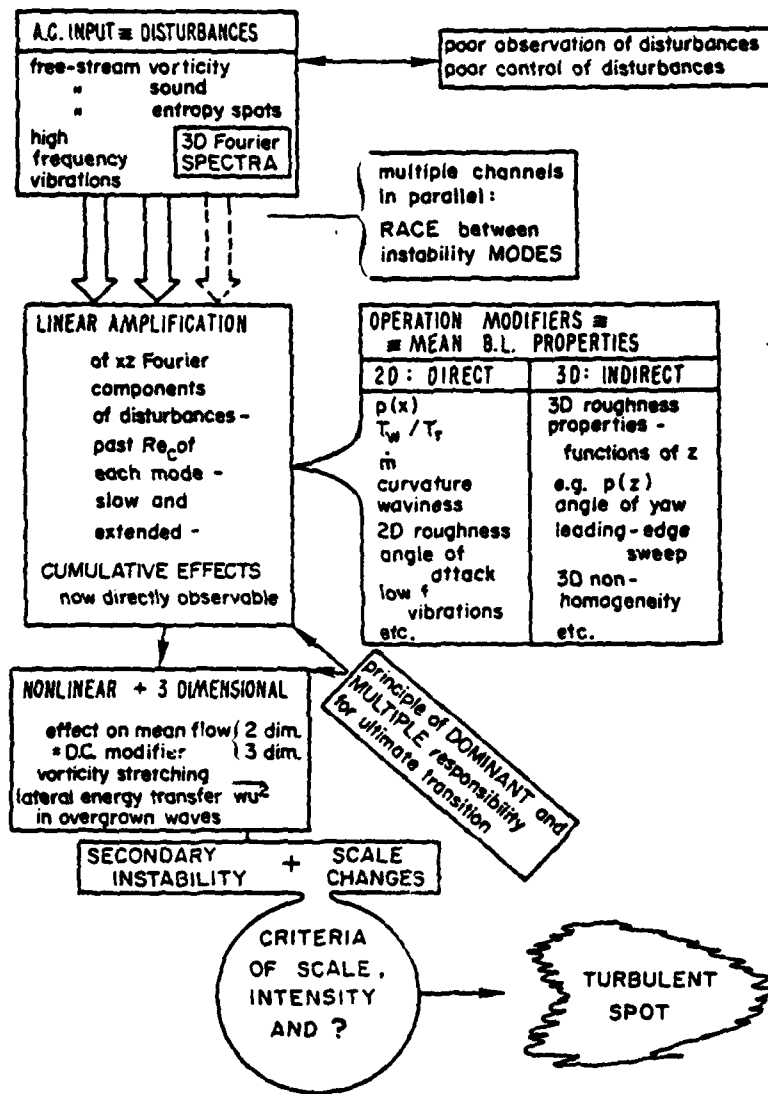


Figure 1. Laminar boundary layer as a linear and nonlinear operator. [181]

instability. The instability is amplified above a certain critical Reynolds number in a distinctive filter-amplifier action that allows its growth to rapidly outpace all others. This aspect is incorporated in the box labeled "LINEAR AMPLIFICATION." For nominally two-dimensional boundary layers, two normal modes of instability have been predicted and later identified experimentally. These are the downstream traveling Tollmien-Schlichting (T-S) waves and the body-force induced steady streamwise vortices. The former mode was modeled theoretically in an original analysis by Tollmien and later in a refined analysis by Schlichting (see Schlichting [5]). Its presence in a Blasius boundary layer in a benign environment was first confirmed by the experiments of Schubauer and Skramstad [6]. The latter modes include the centrifugal Görtler [7] instability for flows over streamwise concavely curved surfaces and buoyancy instabilities (see Schlichting [5]) in boundary layers with unstable density stratification. The characteristics of these instabilities will be discussed more fully in subsequent sections.

The box in Figure 1 labeled "OPERATION MODIFIERS = MEAN BOUNDARY LAYER PROPERTIES" refers to those properties of the flow that act to rearrange the vorticity in the boundary layer. Their influence on the instability is either steady or may be considered so. As a consequence of their action, the receptivity character of the boundary layer is changed and the ascendancy and amplification rates of an instability are determined. Another operator, which does not fit directly in this box, is mean flow unsteadiness. This topic will be addressed in a separate section.

Subsequent to linear amplification of small disturbances, the boundary layer begins nonlinear, three-dimensional development. A "secondary instability" then appears, which promotes a reduction in disturbance scale to

a range more commensurate with turbulence. Transition starts with the appearance of downstream traveling turbulent "bursts" or "spots" which grow and coalesce as the flow continues, forming a fully turbulent boundary layer.

In this presentation, transition "onset" will be used in reference to the first appearance of these bursts, or to the first appearance of the irregular, fine-scale random velocity fluctuations characteristic of turbulence. Transition "completion" will refer to the coalescence of the turbulence to form a fully turbulent boundary layer for all time. In the region between these two locations, the term "intermittency" [8] is used to describe the statistical average of the time that the boundary layer is locally turbulent. Intermittency is usually denoted by the symbol γ , and its value ranges from 0 for laminar flow to 1 for fully turbulent flow. As indicated by Morkovin [3], though, a consistent means of measuring the onset and end of transition, or the intermittency, has not yet been defined. Partially, this is because of the often random nature of the appearance of the turbulent bursts and the variety of techniques used to detect transition. Additionally, transition is sometimes more continuous than intermittent, particularly for low Reynolds number or "bypass" transitions. (The term "bypass" will be defined later in this section.)

Returning to Figure 1, the box labeled "PRINCIPLE OF DOMINANT AND MULTIPLE RESPONSIBILITY FOR ULTIMATE TRANSITION" can be noted. In some cases, the influence on transition of an operation modifier working in concert with the disturbance environment may be singly dominant. Identification of such occurrences may aid in determining a criterion for evaluating transition onset or in deciding how to move the transition region, depending upon the objective. However, in general the location of transition will depend

strongly on the nonlinear combination of influences from several operation modifiers and the unsteady disturbance input. Morkovin's pertinent observation on this matter is that ". . . there are always some freestream disturbances (turbulence, temperature spottiness, random or regular sound), some roughness, some three-dimensionality of the flow, some unevenness of leading edge, some waviness of the skin, some vibrations, some heat transfer, some pressure gradients, and so forth (all very hard to measure). . . ." The singular nature of combined influences, especially those which are irregular or three-dimensional, plus the lack of ability to properly characterize the disturbance environment and the lack of understanding of the selectively sensitive receptivity mechanism lends a very nondeterministic quality to the ultimate transition process. In fact, it is these qualities of the forcing function and the boundary layer oscillator that have foiled or clouded many experimental attempts at evaluating parametrically the various influences on the instability-transition process [2, 3, 9].

Although many incidents of transition are preceded by the development of instabilities identified by linear theory, it is clearly evident that this is not always the case [2, 3]. Such occurrences are labeled "bypasses" by Morkovin and are tentatively denoted by arrows directly from the disturbance box to the secondary instability or turbulent spot in Figure 1. In bypass transitions, any semblance of the linear instability modes is apparently preempted by a more direct and rapid nonlinear response of the boundary layer. Identifiable causes of bypasses include large distributed 3-D roughness [2, 9], localized flow separations [9], and possibly high-level freestream disturbances of the proper scale [2]. Another somewhat special case is the Charters' [10] transverse contamination mechanism. This phenomena

is engendered either by cross-flow between the upper and lower surfaces of a plate at a free side-edge, or by side-wall boundary layer interference at a side-edge juncture [9].

The preceding sketch serves primarily to introduce the complexities of boundary layer transition and to establish a vocabulary for some of the more general features of the process. (For more comprehensive insight into the nature and mechanisms of transition, the excellent reviews of Morkovin [2, 3, 11], Reshotko [1], Tani [12, 13], and Loehrke, et al., [9] should be consulted.)

II. LINEAR STABILITY THEORY

The complexity of the boundary layer oscillator traditionally has rendered it intractable to all but the most simplified theoretical analyses. As a result, the theoretical studies of boundary layer behavior have been limited substantially to linearized infinitesimal perturbation theories. These theories establish marginal stability conditions for, and growth/decay rates of, infinitesimal amplitude periodic boundary layer disturbances. In the process, receptivity considerations are avoided because the disturbances are initialized within the boundary layer.

Physically, infinitesimal disturbances are those whose amplitude is so small as to not change the characteristics of the laminar flow being studied. Functionally, the limits may be set as $A^2 Re \ll 1$, where A is the perturbation velocity to local freestream velocity ratio and Re is a thickness Reynolds number. If, however, the disturbance amplitude is sufficient to modify the time-independent or time-averaged flow quantities for the laminar boundary layer, the disturbances are referred to as being finite [1].

Reshotko [1], Mack [14], and White [15] have delineated the approach and clarified the necessary concepts for applying infinitesimal perturbation stability theory in the case of traveling wave (T-S type) disturbances. (Also, see Gaster in [4].) Typical methods for the case of the centrifugally induced Gortler vortex disturbances can be found in the papers of Ragab and Nayfeh [16] and Floryan and Saric [17]. Therefore, for the purposes of this

survey it is more appropriate to brief some of the salient simplifications and assumptions made in applying the linear theories.

Solutions for the linearized perturbation equations are usually assumed to be of the simplest normal modes form (single frequency sinusoids) and are applied to one or more of the independent variables. For the T-S type disturbances in two-dimensional subsonic flows, the greatest instability is streamwise (see Mack's review in Chapter XVII of Schlichting [5]) thus requiring only a two-dimensional wave for evaluating the marginal stability conditions. Modeling of the three-dimensional streamwise vortex instabilities, on the other hand, demands concurrently acting perturbations in each of the orthogonal coordinate directions.

Other prevalent simplifications in the linear theories usually entail neglecting some of the streamwise derivatives of mean flow quantities. Under some conditions (primarily at large Reynolds numbers), it has sometimes been assumed that all longitudinal derivatives of mean flow quantities as well as the wall normal mean velocity component could be neglected. Thus, the base boundary layer flow is treated as being locally parallel (without growth) or "quasi-parallel." The propriety of this treatment will not be discussed here, but it is enlightening to refer to the nonparallel stability results of Saric and Nayfeh [18, 19] for the T-S instabilities, and Ragab and Nayfeh [16] and Floryan and Saric [17] for the Görtler instabilities as well as the investigations of Gaster [20, 4] and Hall [21]. From these papers, it is evident that nonparallel effects are important for analytically establishing the marginal stability conditions. Nevertheless, the results, with the sole exception of Saric and Nayfeh's [18, 19] for the Blasius boundary layer, are apparently quantitatively unconfirmed.

Provided that the assumptions utilized in the linear theory are appropriate, the resulting marginal (neutral) stability solutions represent the demarcations between damped and amplified "infinitesimal" disturbances in a particular flow. For T-S modes in a subsonic two-dimensional flow, the results are usually plotted as dimensionless wavenumber $\alpha_{\delta^*} = 2\pi\delta^*/\lambda_{TS}$ or $\alpha_{\theta} = 2\pi\theta/\lambda_{TS}$ or dimensionless frequency $F = \beta_{\nu} = U_0^2$ versus the displacement or momentum thickness Reynolds number, yielding a "thumb" shaped locus. Similarly, marginal stability curves for the Görtler modes are plotted as dimensionless wavenumber versus a thickness Görtler parameter, as will be seen later. Points on these curves denote the "critical" Reynolds or Görtler numbers for a particular frequency or wavelength of disturbance. The smallest Reynolds or Görtler number from these curves, regardless of disturbance wavelength, is referred to as being "minimum critical."

Linear stability results will be addressed in this review, partially because they provide some information on the initial processes preceding some cases of boundary layer transition. Particularly, from them knowledge can be garnered about the effectiveness of some operation modifiers, such as pressure gradients and heat transfer, in promoting or delaying instability. Also, they indicate which disturbance frequencies are most effective in destabilizing the boundary layer. Finally, the importance of the nondimensional parameters obtained from linear theory analyses cannot be ignored, since they have often provided the means for correlating transition data. However, the relevance of any results from linear stability theory in considerations of the occurrence of transition is, at best, indistinct and is, in many cases, nil. On this subject Reshotko [1] comments, ". . . the relationship between transition Reynolds number and some representative Reynolds number from infinitesimal-

disturbance stability theory is weak quantitatively and only moderately strong qualitatively." His statement was, nevertheless, focused on cases of post-critical transition driven by relatively small amplitude freestream disturbances. No such relationship can realistically be expected to apply to precritical or bypass transition, in which there is no apparent operation of a linear amplification mechanism. Mack [14] and Morkovin [3] both acknowledge that transition or even turbulent boundary layers have been observed in situations that were supposedly stable laminar flows according to linear theory.

III. NONLINEAR STABILITY INVESTIGATIONS

Investigations of the nonlinear stability of boundary layers are very much in their infancy due to the formidable problems, either mathematical or numerical, associated with analyzing such a complex three-dimensional oscillating system. Many of the analyses have been motivated by the approaches of Stuart [22, 23] and Watson [24] for parallel flow stability. Essentially, they extend the results of linear parallel stability theory into the weakly nonlinear regime by nonlinear small perturbation methods. As discussed by Stuart [25] for T-S type instabilities and Hall [21] for Görtler type instabilities, though, they are not appropriate for application to boundary layer flows, whose growth is characterized as being both nonparallel and diffusive. At any rate, analytical methods are, as yet, inadequate for extending analyses into the regions of highly nonlinear instability development.

Numerical investigations, on the other hand, have their own set of difficulties beginning with the demand for increasingly higher (and three-dimensional) resolution as the nonlinearities in the boundary layer response increase. Additionally, there is the possibility of introducing or suppressing instability through the method itself, coupled with the uncertainty in downstream boundary conditions [26].

In nonlinear stability investigations, as with the linear stability analysis, receptivity is usually not considered (e.g., see [4, 26, 27, 28,

29])). Reshotko [1] and Morkovin [3] review various aspects of the receptivity mechanisms studied through 1976. Rogler [30] presents a more current modelization of some facets of the receptivity phenomena.

The following review of the influence of disturbances and "operation modifiers" on instability and transition will not be mechanistic but primarily parametric. Although this will not lead to the understanding of the nonlinear interactions among the various influences, it will provide some insight into the nature and order of their effects, which may be useful in determining dominance.

IV. FLAT PLATE BOUNDARY LAYER TRANSITION AND THE TOLLMIEN-SCHLICHTING INSTABILITY

If all sources of disturbance (i.e., turbulence, acoustic waves, and vibrations) are very small and the flow surface is smooth, the unstable Blasius boundary layer evolves continuously from the amplification of the 2-D T-S instability modes to the appearance of localized turbulent "spots." The sequence of events has been elucidated by the experiments of researchers, including Schubauer and Skramstad [6], Schubauer and Klebanoff [31], Klebanoff and Tidstrom [32], Klebanoff, Tidstrom and Sargent [33], Kovaszny, Komoda and Vasudeva [34], Hama, Long and Hegarty [35], and Hama and Nutant [36]. Tani [12, 13] has reviewed and interpreted these and other investigations. Although there is yet some uncertainty in the developments immediately preceding the emergence of turbulent spots, the processes may be outlined as follows:

- (1) Past the marginal stability location, downstream traveling (ideally two-dimensional T-S waves (the primary instability) begin to amplify exponentially deep within the boundary layer. Their velocity is roughly one-third that of the freestream and the wavelength is several times the boundary layer thickness (see Gaster in [4] for a discussion of the spatial and temporal nature of the waves). This stage is the object of investigations by linearized stability theory.

- (2) Gradually, nonlinear finite amplitude development takes over, leading to a spanwise varying rate of growth. This pronounced three-dimensionality is attributable to the production of streamwise vortices (the secondary instability) along the swept-back front of the T-S waves, resulting in redistribution of the wave momentum.
- (3) The upward fluid motion caused by two adjacent contrarotating vortices produces a "high shear" layer nearer the outer edge of the boundary layer. Subsequently, the high shear layer sheds smaller scale, intense, discrete vortex loops in cascade, which break apart and individually tangle to produce high frequency fluctuations at scales more commensurate to that of turbulence (see [36]). From this melee, growing localized turbulence emerges and moves downstream at approximately two-thirds of the freestream velocity. Tentatively, these events are interpreted as indicating that the large scale T-S wave instability must combine with the secondary (velocity profile inflection producing) vortex instability as a prerequisite to the disturbance scale reduction and three-dimensionalization required for turbulence [9]. The importance of velocity profile inflections in the reduction of the T-S instability scale will become clearer in the subsection on pressure gradient influence.

The features of turbulent spot formation and growth following breakdown have been the subject of investigations by Emmons [37], Schubauer and Klebanoff [31], Dhawan and Narasimha [8], Elder [38], McCormick [39], and more recently by Wygnanski, Sokolov and Friedman [40]. Dhawan and Narasimha's [8] analysis of Blasius boundary layer intermittency data produced the result that

the inception of turbulent spots is random in time and very nearly along a discontinuous spanwise line in the flow. Nevertheless, the insensitivity of the intermittency development to the exact streamwise ascent spot distribution makes this result less pertinent [40]. With the exception of a short period in the initial growth, the spanwise and streamwise development of each spot is uniform and independent of the existence of other spots [38]. The speeds of the leading and trailing edges are around 0.5 and 0.88 of the freestream, respectively [31], and the spanwise spread subtends an angle of about 20° in the flow [40]. All of the spots apparently have similar streamwise axisymmetric arrowhead shapes with downstream pointing vertices [31, 38, 40]. In addition, they are followed by regions of "becalmed" laminar flow in which another spot is not generated [31].

A schematic plane view of the foregoing events, from T-S instability to coalescence of the turbulent spots is given in Figure 2. To be noted is the solid angle of turbulence, corresponding to Charters' [10] transverse contamination bypass, which is swept out along the sides of the plate.

4.1 Freestream Disturbance Effects

Freestream disturbances represent part of the input to the boundary layer oscillator, as can be noted from Morkovin's diagram. Included in this category are vorticity (eddy velocity fluctuations, which are referred to as freestream turbulence), "sound" (pressure fluctuations which are transformed into velocity fluctuations in the fluid), and entropy variations. Much of the freestream disturbance energy in subsonic flows is exhibited as either turbulence or acoustic phenomena, the latter of which can be both traveling and standing pressure waves. Generally, increasing levels of freestream

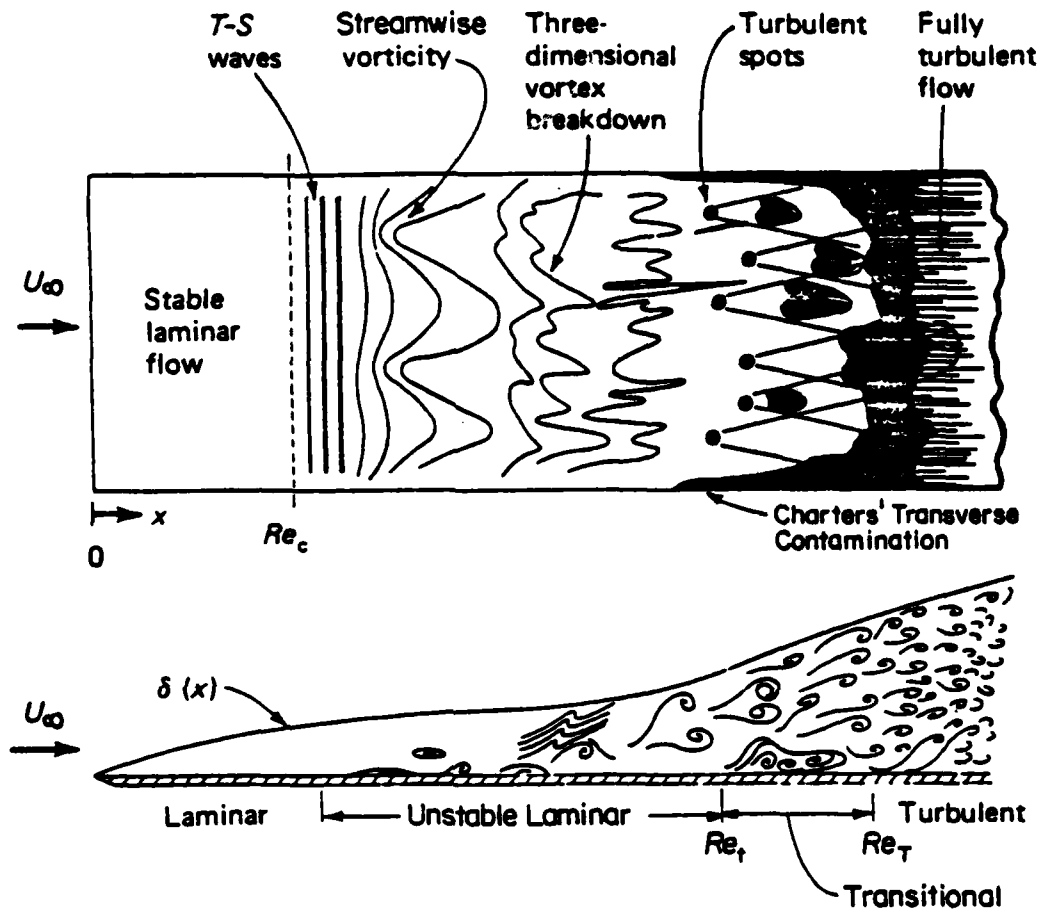


Figure 2. Idealized sketch of instability and transition processes on a flat plate. [15]

disturbances move transition to smaller Reynolds numbers, with the effect at very low disturbance intensities being drastic. However, freestream disturbances in most cases of practical interest are nonhomogeneous and anisotropic, and the spectral distribution of disturbance energy can influence transition onset through the filter-amplifier nature of the boundary layer. In nonbypass transitions, particularly those which are preceded by substantial instability amplification through a linear mechanism, the occurrence of transition depends strongly on the frequencies, and even possibly on the orientations of disturbance spectra in relation to the amplifiable boundary layer oscillation frequencies.

Tani [12] has stated that freestream turbulence appears to control the rate at which the remainder of the boundary layer spectrum feeds on the most amplified component. That is, it hastens breakdown of the unstable laminar layer. Discrete frequencies, on the other hand, which closely match the amplifiable *normal modes* seem in some sense to drive their amplification, or at least to influence their initial amplitude (see [14]). Regardless of the interaction mechanisms (receptivity), though, freestream disturbance frequencies which are close to the frequencies of the amplifiable normal modes can be considerably more efficient at promoting transition than those which are mismatched.

The effects of nonuniform disturbance spectrums were illustrated lucidly by the transition experiments of Spangler and Wells [41]. Figure 3 shows the dramatic differences they obtained for transition Reynolds numbers in Blasius flow when various acoustic and vortical (grid generated) disturbances were introduced. At this point, it is helpful to examine the marginal stability curve for the Blasius flow shown in Figure 4. Note that there is a range of

⊙	Grid generated freestream turbulence
□	Principal Acoustic Freq. (Hz) 27
◇	Principal Acoustic Freq. (Hz) 43
△	Principal Acoustic Freq. (Hz) 76
▽	Principal Acoustic Freq. (Hz) 82

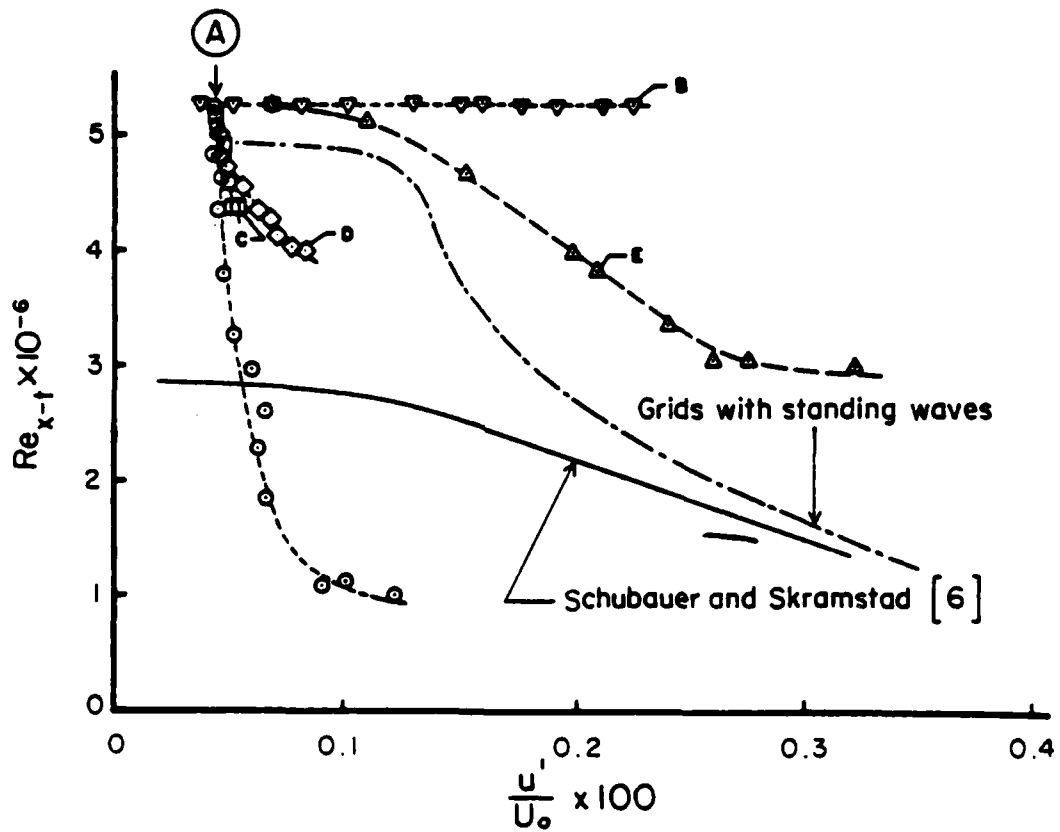


Figure 3. Transition Reynolds number as a function of freestream disturbance intensity. [41]

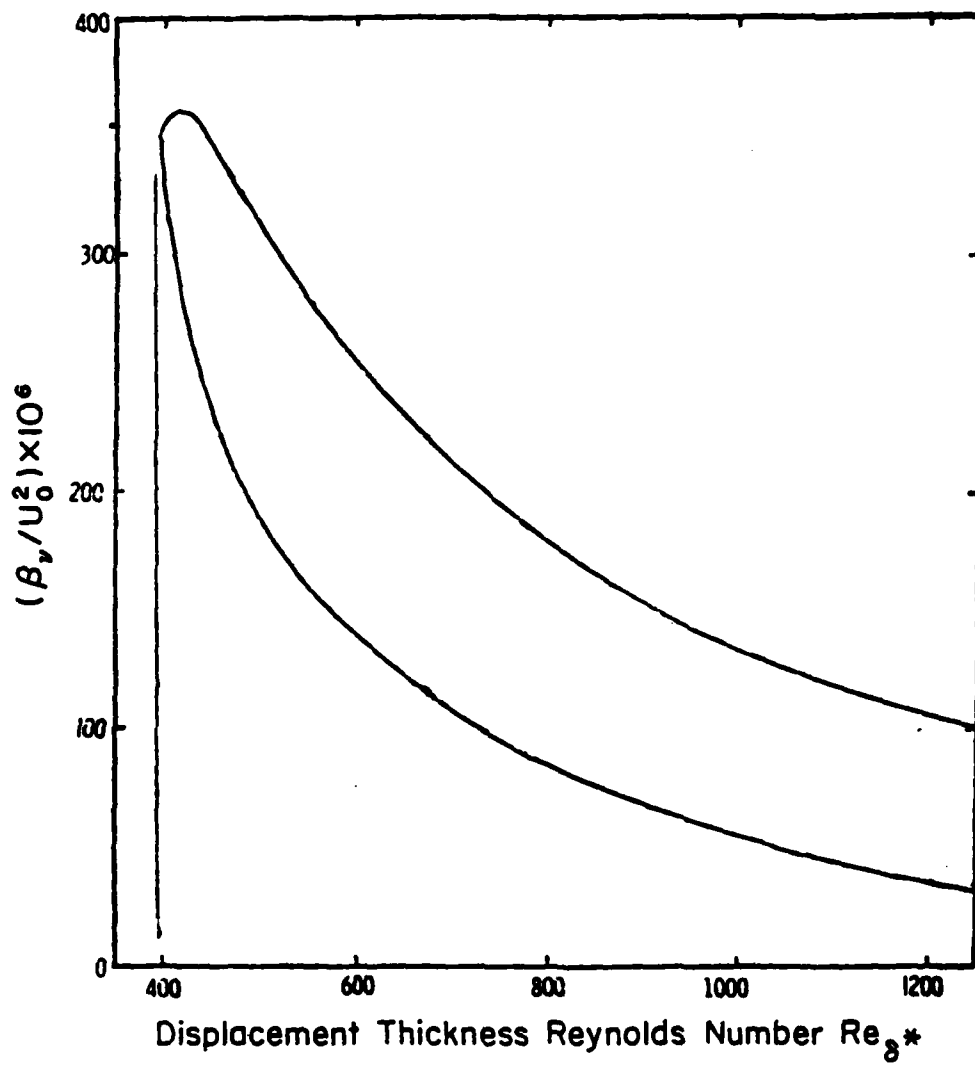


Figure 4. Marginal stability locus for the Blasius flow. [18]

dimensionless amplifiable T-S frequencies for each Reynolds number greater than minimum critical. Those frequencies with the greatest (spatial) rates of amplification will be in the middle of and down into the thumb. Spangler and Wells chose their acoustic disturbance frequencies such that they fell approximately within these amplifiable bandwidths predicted by linear theory.

Also shown in Figure 3 is Schubauer and Skramstad's [6] wind tunnel transition results for various levels of grid generated disturbances. It is of importance to note the difference in length Reynolds number of transition onset at the lowest disturbance levels for the Spangler and Wells (5.25×10^6) and the Schubauer and Skramstad (2.8×10^6) experiments. Spangler and Wells were able to achieve this higher Reynolds number by carefully controlling acoustic disturbances in their wind tunnel, while Schubauer and Skramstad's limiting Reynolds number was apparently the result of fan noise contributions.

Another important lesson is illustrated in locus AB (top line in Figure 3) for which high sound levels (in the range of 90 to 135 db) were ineffective in reducing the Reynolds number of transition. Concerning this phenomena, Loehrke, Morkovin and Fejer [9] commented, "However, this occurrence is almost surely associated with the mismatch between the acoustic spectrum and the spectrum of amplifiable Tollmien-Schlichting instability waves." Observations such as this about the amplifiable dimensionless frequencies ($\beta v/U^2$) and wavelengths ($U_0 \lambda_{TS}/v c_r$, where the disturbance phase velocity $c_r = \beta v/2\pi U_0$) of stability theory and the occurrence of transition in a spectrally nonuniform disturbance environment lead Reshotko [1] to conclude that the relationship (or lack of it) could very possibly account for the so-called "unit-Reynolds-number effect."

As the freestream disturbance levels increase from infinitesimal in the spectrums relevant to stability and transition, the region of linear development of the boundary layer instability decreases. For turbulence levels greater than about 0.1 percent of freestream, the velocity fluctuations begin to mask the T-S wave development through interaction with the boundary layer [42]. Gradually, then, the problem must become one of the nonlinear stability of the (randomly) disturbed flow. Nevertheless, Bennett [43] was able to detect, using a boundary layer hot wire and a spectral analyzer, selected amplification of approximately those frequencies predicted by linear theory in a Blasius flow at a freestream turbulence level of 0.42 percent.

When considering very high level disturbances, the experiments of Schubauer and Klebanoff [31] and Elder [38] become of interest. Following the approach of Mitchner [44], they utilized intense local boundary layer disturbances produced by an electrical spark in studying the growth of turbulent spots. Schubauer and Klebanoff were able to generate a local turbulent spot in a nominally Blasius wind tunnel boundary layer at Reynolds numbers substantially below critical. Although the growth of the spot was retarded until the Reynolds number reached approximately minimum critical, it was not damped. Elder performed a similar experiment in a low disturbance wind tunnel Blasius layer (see Morkovin [2, 3]). In his experimental length Reynolds number range of 2×10^4 to 1×10^6 , he was able to generate a growing turbulent spot whenever the local streamwise disturbance intensity, u'/U_0 , exceeded a value of roughly 0.18. Note that the lower Reynolds number, corresponding to a momentum thickness Reynolds number of 94, is well below minimum critical for the Blasius boundary layer (154 according to the weakly nonparallel results of Saric and Nayfeh [19]). These results substantiate the

conclusion that turbulence formation and growth do not necessarily have a linear amplification mechanism as a prerequisite. In particular, if the intensity and scales of the three-dimensional forcing disturbances are close enough to their ultimate turbulent target, turbulence can be generated through a very rapid nonlinear instability mechanism [2].

To insure a balanced perspective, it should be pointed out that some authors have implicitly opined that true growing turbulence cannot exist in Blasius flow below the minimum critical Reynolds number of linear stability theory. The basis for this opinion rests in the experimental results of Schubauer and Klebanoff [31] and Klebanoff, Schubauer, and Tidstrom [45] who observed retardation of spot growth at Reynolds numbers less than minimum critical. As Morkovin [3] notes of the redirection of thought subsequent to the Schubauer-Klebanoff experiments, ". . . the belief grew that the rapid damping shown by linear theory below O-S (Orr-Sommerfeld) critical conditions was associated in some way with the quenching of nonlinear turbulent phenomena as well." However, he calls attention to the fact that the formation of turbulence has been observed at significantly precritical Reynolds numbers in accelerated boundary layer flows.

As to the question of the existence of true turbulence, one should be cognizant of the artificiality of the spark disturbances and should also recognize equally well that such disturbances, unlike free-stream turbulence, are local and instantaneous. Perhaps Coles' [46] observation that "the main difficulty in the case of boundary-layer flow is that the inherent increase in Reynolds number with distance may act to convert a temporary abnormal response to a strong disturbance into a permanent one" is the most appropriate viewpoint for these cases.

It may be said, though, that there is no distinct minimum Reynolds number for the occurrence of transition, since such limits depend greatly on the character and intensity of the disturbances, as well as the presence of operation modifiers, particularly the bypass inducing distributed roughness, and the stability character altering crossflows. In the latter case, the spanwise pressure gradients can lead to skewed T-S wave fronts and, thus, steady vortex formations oriented essentially in the streamwise direction [2, 47]. The result is that transition can occur at much smaller Reynolds numbers than that observed if only T-S waves are present. Such three dimensionality is unavoidable near the corners of finite width flow surfaces [3]. Conversely, there is no distinct maximum Reynolds number for the occurrence of transition, either, depending on one's success in eliminating all possible sources of flow irregularity and disturbances.

In transition experiments, freestream turbulence correlations are usually based on the R.M.S. disturbance velocity of the combined Fourier spectra normalized to the local freestream velocity.

$$T_{fs} = \frac{(\overline{u'^2} + \overline{v'^2} + \overline{w'^2})/3}{U_0} \quad (1)$$

If the disturbances are considered to be isotropic, only the normalized R.M.S. streamwise component may be given. From the results of the Spangler-Wells' [41] experiments it is evident that such a description is adequate only if the disturbances are homogeneous in the spectrums of relevance to stability and transition. Loehrke, Morkovin, and Fejer [9] comment, "Clearly more than the single parameter u'/U_0 is required to characterize adequately the disturbance input such as the separate amplitudes, spectra, and orientations of the turbulence and sound fields. Such a description of the initial disturbances

has not been attempted even under research laboratory conditions and is hardly practicable under field conditions." Figure 3 clearly demonstrates that in addition to freestream turbulence defined by equation (1), there is at least one more parameter of equal dominance in affecting transition: a parameter involving the principal acoustical frequency of the disturbances. Its exact formulation is undetermined as of to-date but can be expected to be of a Strouhal-type combination.

If the disturbance field is "homogenous and isotropic," transition trends are fairly reproducible, provided other irregularities are controlled (e.g., see [48]). In general, experiments in two-dimensional boundary layers indicate rapidly decreasing effectiveness of turbulence in moving transition as the levels are increased. Also, increased levels of freestream turbulence reduce relatively the effects of operation modifiers such as wall normal temperature gradients and streamwise pressure gradients. Furthermore, at higher turbulence levels (and thus smaller Reynolds numbers) the transition regime becomes shorter and more continuous (less intermittent) due to the increase of the number of turbulent sources.

As a final comment on the freestream turbulence effect on transition it must be brought out that the kind of freestream turbulence in a real gas turbine environment is uniquely different from those, say, in the boundary layers on aircraft surfaces. Flow through gas turbine cascades is characterized by turbulence emanating from combustors; and superimposed on this base-line turbulence is the wake-cutting fluctuation of the freestream velocity. The wake-cutting fluctuation is sometimes viewed as a cyclic variation of the basic flow but not as a turbulence contribution. Its effect on transition, however, has yet to be established or refuted.

4.2 Pressure Gradient Influence

Longitudinal pressure gradients are one of the more prevalent "operation modifiers" in unstable and transitioning boundary layer flows. Fundamentally, they affect the T-S stability and transition response of the boundary layer through changes in the velocity profile and the boundary layer growth rate, and through stretching or contraction of stream tubes. The effects of velocity profiles were first augured through inviscid stability theory, which indicated instability for velocity profiles with an inflection point. White [15] reviews the important historical results from inviscid stability theory. Linear (viscous) stability theory provided the additional important result that, because of viscosity effects, all boundary layer flows become unstable at finite Reynolds numbers [50]. Linear stability theory indicates that accelerated (negative or favorable pressure gradient) boundary layer flows, which exhibit more velocity profile fullness than zero-pressure gradient flows, are stabilized to disturbances. Conversely, the velocity profiles in decelerated (positive or adverse pressure gradient) flows have an inflection point, which renders them less stable. For these flows, the inflection occurs at the wall for very small decelerations, moving outward for increasing deceleration (see Schlichting [5]). In addition to velocity profile effects, the pressure gradients influence the rate of growth of small amplitude T-S disturbances with the rate for adverse and favorable pressure gradients being greater than and less than, respectively, that for a zero pressure gradient flow.

The qualitative validity of the linear stability theory predictions was demonstrated in the experiments of Schubauer and Skramstad [6]. Saric and

Nayfeh's [18] linear (weakly) nonparallel marginal stability results for some of the Falkner-Skan flow family are shown in Figure 5, along with the parallel flow results. Note the increase in bandwidth for amplified frequencies, especially the shift to higher frequencies, as the pressure gradient changes from favorable to zero and becomes progressively more adverse. Note also that the most adverse gradient ($\beta_{FS} = -0.1988$), corresponding to incipient flow separation, does not seem to show a minimum critical Reynolds number. For this case, though, Saric and Nayfeh anticipated significant error since the boundary layer growth at such low Reynolds numbers is rapid (highly non-parallel). Within these marginal stability curves, the frequencies and Reynolds numbers at which the greatest growth rates occur will fall down into and along the center of the "thumb" (see [1, 5, 9]).

As observed by Tani [12] pressure gradients are considerably less influential on the Reynolds number for transition onset than on the minimum critical Reynolds number. For a very small disturbance environment, this difference may be explained partially by the fact that the cumulative growth of unstable frequencies at any Reynolds number is less affected by pressure gradients than the minimum critical Reynolds number. However, as the freestream turbulence level increases, pressure gradient influence becomes even less pronounced. This is largely borne out by the more recent heat transfer test results on turbine blades with varying degrees of freestream turbulence. No quantitative values will be given here since such values are substantially dependent on the parameter used as a measure of pressure gradient.

If freestream disturbances are small, flow surfaces are smooth, and the pressure gradients are moderate, the sequence of instability developments in

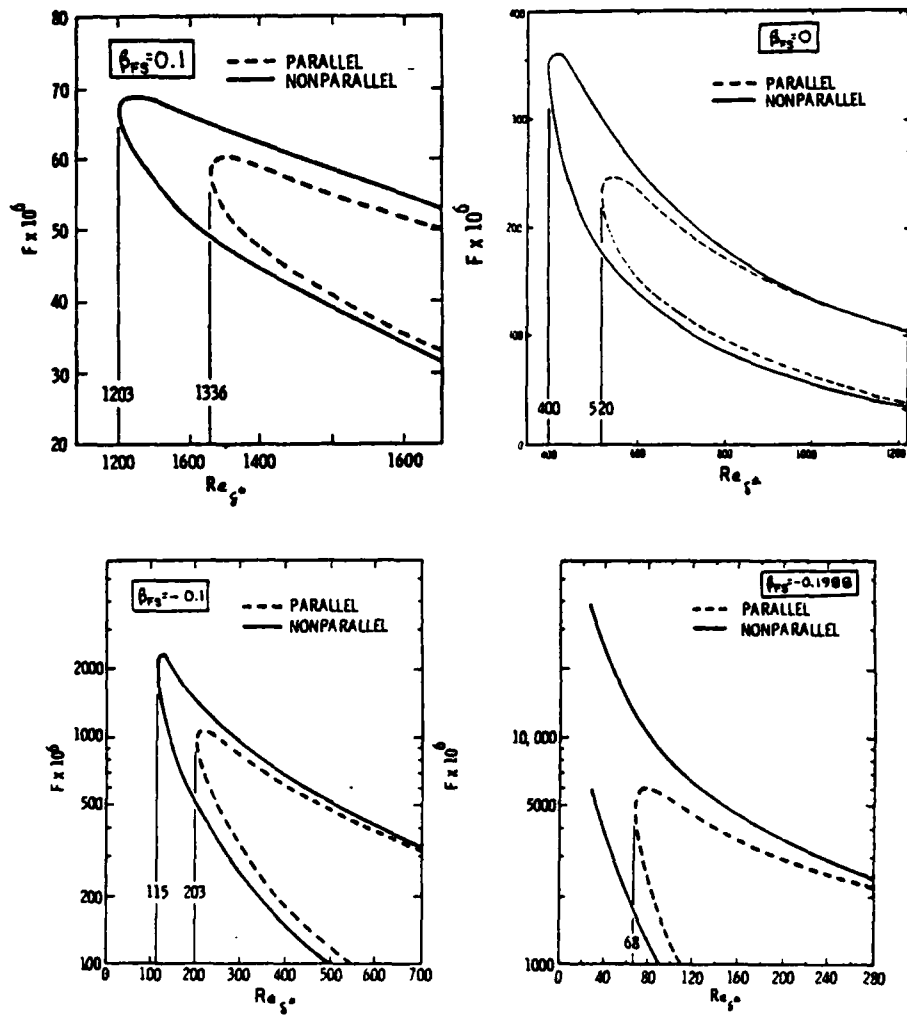


Figure 5. Marginal stability diagrams for some Falkner-Skan flows. [18]

boundary layers with a pressure gradient are similar to those for the zero pressure gradient boundary layers [12]. However, in cases for which the pressure gradients are not moderate, especially in decelerating flows, the processes can be radically different. Nearly separating flows exhibit very abrupt transition without the vortex breakdown and turbulent spots observed in moderate gradients. Separating flows usually become turbulent upon reattachment, without the occurrence of turbulent spots [12]. At the other extreme, it is possible to accelerate the flow so rapidly that it retains its laminar structure. Alternately, a turbulent boundary layer can be accelerated rapidly enough so that it gradually becomes laminar-like. This phenomenon is known as "laminarization," "relaminarization," or "reverse transition." Nevertheless, there are practical limitations on the stabilization afforded by acceleration, since the effects of residual roughness or surface irregularities become more important as the boundary layer is thinned [3]. This is due to the parametric combination $(k_s U_\tau / \nu)$, in which the surface roughness protrusion k_s appears; increasing frictional velocity caused by boundary layer thinning has the same effect as increased roughness. In addition, the profile stability and stream tube stretching are offset by the localized profile inflections, and the larger wall normal velocity and greater random three-dimensional distribution of vorticity resulting from roughness. Also, regardless of the acceleration, any flow is unstable for sufficiently large Reynolds numbers.

Many theoretical and experimental investigations of boundary layer relaminarization phenomena have been directed toward determining suitable parameters or criteria for correlating its occurrence. Probably the clearest experimental indications of relaminarization onset are a sudden increase in

the shape factor, $H (\Delta \delta^*/\theta)$, and a decrease in skin friction [3]. (The converse of this statement would hold for transition onset, at least over flat and moderately streamwise curved surfaces.) However, this provides no empirical or analytical criteria for predicting relaminarization onset.

Two of the parameters suggested as being useful in correlating relaminarization are the "velocity gradient factor" or "acceleration parameter",

$$\kappa = \frac{v}{U_o} \frac{dU_o}{dx} \quad (2)$$

and the momentum thickness Reynolds number, $Re_\theta (\Delta U_o \theta / \nu)$. Narasimha and Sreenivasan [51] thoughtfully and critically evaluate the merits of these and other parameters proposed for use in correlating relaminarization. In particular, κ has been suggested for use not only in correlating relaminarization, but also for transition [52]. As an aid in judging the applicability of κ to relaminarization, it is helpful to understand the origin of this parameter. This parameter κ was obtained from analyses of asymptotic sink-flow boundary layers that are characterized in the limit as having a constant momentum thickness Reynolds number and a self-preserving mean velocity profile shape in both laminar and turbulent boundary layers. In these flows, for which κ is constant, the momentum thickness decreases and the local velocity increases at the same rate. Physically, the flow is asymptotically produced in a convergent, plane wall channel [53]. Critical values for extinction of turbulence were obtained by comparing the results of such analyses with experiment. Although a critical value may be useful on an ad hoc basis in comparable flow situations, the presence of roughness or

streamwise vortices constitutes a possible threat to such a criteria. (Similar comments would apply also to the use of an Re_θ criteria in accelerating turbulent flows.) For general nonsimilar flows in which κ would be used as a local stand-alone criteria, its value is questionable. Patel and Head [54] note that there can be a substantial lag between the application of a supposedly "critical" value and the onset of relaminarization. Zysina-Milozhen, Medvedeva and Rohst [55] observed such a lag in flow relaminarization on a model turbine blade in cascade. They suggested that a critical value of the product of the local thickness Reynolds number and κ might be more suitable. Other investigators [52] have suggested designing turbine blades such that κ is always larger than some "critical" value.

So far the discussion has implicitly centered on flows that are similar or on special cases. However, for nonsimilar boundary layers in general, the transition onset and completion as well as the spatial intermittency distribution depend on the unique pressure gradient history of the boundary layer. As yet under these circumstances, no single pressure gradient parameter has been proven to be adequate as a local criteria in correlating transition. Therefore, the choice of a parameter for correlating the effects of pressure gradient on transition or relaminarization is both experiential and dependent on the pressure gradient magnitude and variation. In many empirical correlations for transition onset, the Pohlhausen parameter

$$\lambda_\delta = \frac{\delta^2}{\nu} \frac{dU_o}{dx} \quad (3)$$

or its momentum thickness variant

$$\lambda_{\theta} \left(= \frac{\theta^2}{\nu} \frac{dU_o}{dx} \right) \quad (4)$$

is used as the local measure of pressure gradient. The preferred form is the latter because, once the freestream velocity distribution is known, the local momentum thickness of most laminar boundary layers can be determined accurately by a simple relationship. Additionally, the use of momentum thickness circumvents the problems associated with use of the ill-defined boundary layer thickness. Another interesting aspect of the modified Pohlhausen parameter is that a critical value in the range of -0.082 to -0.09 serves as a rough estimate for the occurrence of laminar separation (see White [15], p. 318 and Dunham [56]). Finally, as indicated by Liepmann [57], the momentum thickness is more closely related to the wall shear stress, and thus to the slope of the velocity profile at the wall, which is important in characterizing the degree of instability to T-S type disturbances.

As will be seen later from the transition experiments of Abu-Ghannam and Shaw [48], the modified Pohlhausen parameter is inadequate for use as a local parameter in general transition correlations. Also from this data, it may be deduced that the length of the transition region in similar flows (or more generally those with moderate pressure gradients which do not rapidly vary) is a fairly strong function of the Reynolds number for transition onset. Usually, adverse pressure gradients lead to smaller transition Reynolds numbers and shorter transition regions, and vice versa [12].

4.3 Heat Transfer Influence

The addition of heat transfer makes the Prandtl number and wall-to-freestream temperature ratio important parameters in describing the T-S stability and transition response of the boundary layer. For subsonic flows,

a boundary layer transverse temperature gradient operates basically through the viscosity gradient induced by the thermal boundary layer. In addition, if body forces are present, the density stratification in the boundary layer can strongly influence stability and transition.

The viscosity variation induced by the thermal boundary layer is reflected in the boundary layer velocity profiles, yielding either more full (more stable) or inflected (less stable) profiles. With gases, the absolute viscosity increases with increase in temperature, while liquids have the opposite tendency. Therefore, heat transfer to the wall is stabilizing in gas flows and destabilizing in liquid flows. Since this survey is directed toward gas turbine applications, water boundary layers will not be considered. Suitable references on stability and transition of water boundary layers with heat transfer would include Aroesty et. al. [58], Wazzan and Gazley [59], Straziar and Reshotko [60], Barker and Jennings [61], Wazzan et. al. [62], and Wazzan, Okamura, Smith [63,64].

If body forces and density stratification are such as to produce a buoyancy force directed away from the flow surface, the stability characteristics of the laminar flows may be radically altered. Such "unstably stratified" flows exhibit a three-dimensional instability in the form of streamwise vortex rows. These vortex formations are analogous to the Görtler vortices observed in boundary layer flows over concavely curved surfaces [65]. On the other hand, stable stratification suppresses turbulence production. In either case, the stratification stability of the flow is expressed in the Richardson number, which is defined as follows:

$$Ri = - \left(g \frac{d\rho}{dy} / \rho \right) / \left(\frac{du}{dy} \right)_{wall}^2 \quad (5)$$

This parameter represents the buoyancy to inertia force ratio, with $Ri > 0$ corresponding to stabilization, $Ri = 0$ indicating a homogeneous fluid, and $Ri < 0$ corresponding to destabilization. Schlichting [5] gives a more complete review of the limited literature on the stability of stratified flows.

Lees and Lin [66] developed, and Lees [50] used, an asymptotic parallel flow approach for evaluating the effects of heat transfer (isothermal wall) and Mach number on the linearized T-S stability of the compressible laminar boundary layer. Since their method was asymptotic (i.e., introduction of small viscosity - very large Reynolds numbers - to an inviscid compressible fluid), the results are valid only when the wavenumber - thickness Reynolds number product is very large [67]. However, based on the analyses and comments of Mack [68], it is expected that the results of the asymptotic theory will be satisfactory for qualitative information on the influence of compressibility and heat transfer on subsonic boundary layer stability.

In the Lees-Lin analysis, the Prandtl number was constant and the viscosity variation was incorporated via a power law. The resultant marginal stability curves for various wall-to-freestream temperature ratios are given in Figure 6. In this plot, the solid loci are for calculations at a freestream Mach number of 0.7, while the dashed locus is for the Blasius flow. As a comparison, the minimum critical momentum thickness Reynolds number from the latter curve is 150, while Jordinson's [69] accurate numerical calculations for the quasiparallel Blasius flow yielded the value 200. To be noted in this plot, however, is the indication of significant stability changes with change in temperature ratios, even for the midsection

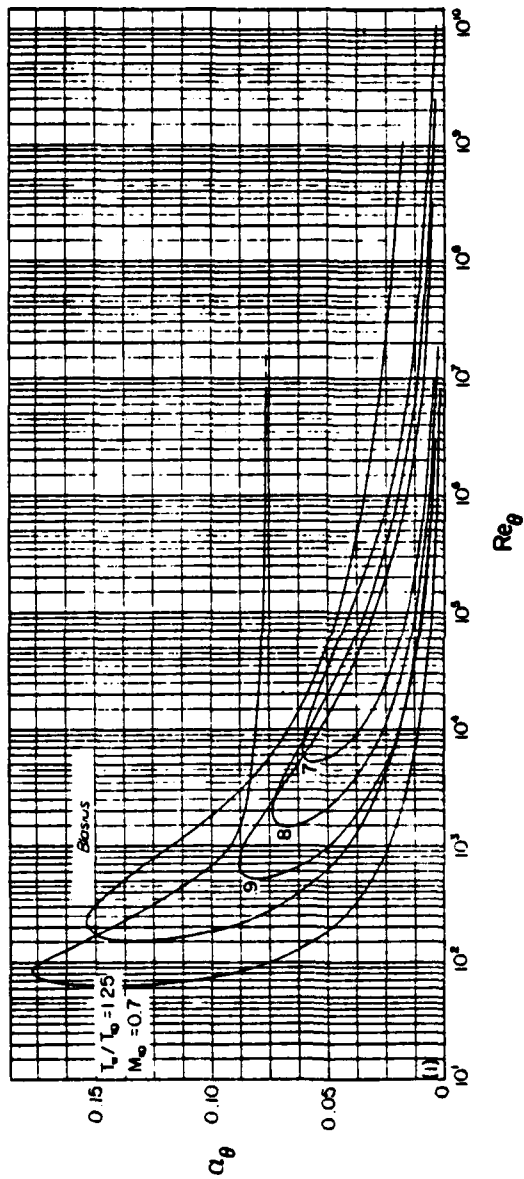


Figure 6. Marginal stability diagrams for subsonic flow over isothermal surfaces. [50]

of the "thumb," within which the greatest rate of amplification occurs. The minimum critical momentum thickness Reynolds numbers corresponding to these curves are 5150, 1440, 523, and 63 at temperature ratios of 0.70, 0.80, 0.90, and 1.25, respectively. As a reference, the temperature ratio for an adiabatic wall at Mach 0.7 is 1.10.

Liepmann and Fila [70] verified experimentally the expected trends for transition onset in a zero pressure gradient boundary layer influenced by heat transfer from the wall. Their experimental set-up consisted of a smooth plate with a sharp leading edge, the plate being mounted vertically in the wind tunnel to nullify boundary layer transverse buoyancy effects. Figure 7 shows the results they obtained with a freestream velocity and temperature of 8.19 m/sec and 20°C, respectively. The other two components of R.M.S. freestream disturbance intensity at the lowest disturbance level ($u'/U_0 = 0.0005$) were $v'/U_0 = w'/U_0 = 0.0008$, while the higher disturbance intensity was presumably uniform. Hot wire anemometry was used to identify transition, and its onset was defined by the first appearance of turbulence bursts on an oscilloscope screen. The authors attributed the low value of length transition Reynolds number ($= 5 \times 10^5$) for the adiabatic flow to the influence of secondary flows resulting from plate edge effects. Although there was a possibility of buoyancy influence (cross-flow) in the heated air layer close to the plate for the nonadiabatic results, the authors concluded, based on velocity profile checks, that it was negligible. Furthermore, transition trends similar to these were noted in Ref. [71].

In published literature, there is little quantitative information pertaining to transition in gas boundary layer flows with heat transfer to the wall. However, the qualitative results that exist, such as Kercher, Sheer,

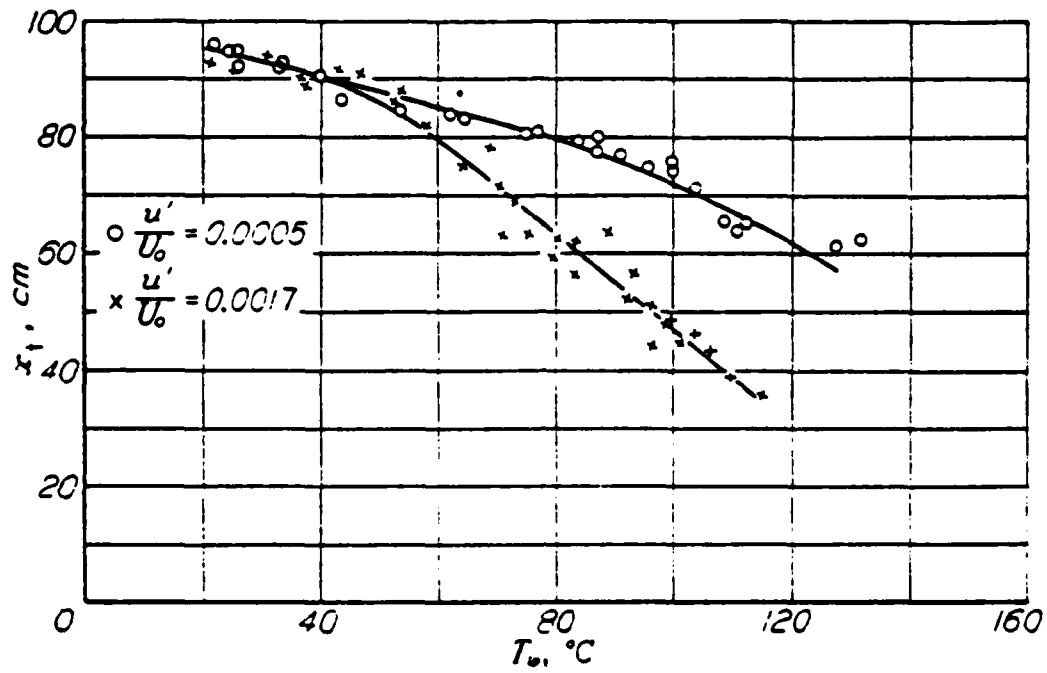


Figure 7. Effect of plate temperature on transition. [70]

and So [72], indicate that the effect is not negligible at relatively low freestream disturbance levels. Furthermore, the stabilization and increased transition Reynolds numbers somewhat parallel that observed in water boundary layers with heat transfer from the wall, provided that the wall-to-freestream temperature ratios are not large. Therefore, the influence of such conditions is expected to be significant, at least for low freestream disturbance levels and smooth flow surfaces. As with pressure gradients, though, the influence of heat transfer on the transition Reynolds number is substantially less than that calculated for the minimum critical Reynolds number, even at very low disturbance levels [73].

4.4 Compressibility Influence

In compressible flows, the temperature rise due to frictional heating in the boundary layer plays a role in determining stability and transition characteristics. An effect on the T-S stability might be anticipated from examination of Figure 8, taken from Kobayashi and Kohama [74], which displays the variations through the boundary layer in viscosity, density, and temperature at three values of Mach number. These profiles were computed by applying Sutherland's viscosity formula to an ideal gas which was assumed to have a constant specific heat and Prandtl number. To be noted in these curves is the fact that the viscosity variation leads one to suspect that increasing Mach numbers might result in inflected velocity profiles. The analytical result of Lees [50] verify this, although the effect in the subsonic flow regime is not great.

Lees [50] calculated the marginal stability curves for subsonic, zero pressure gradient, insulated boundary layers under the assumptions noted

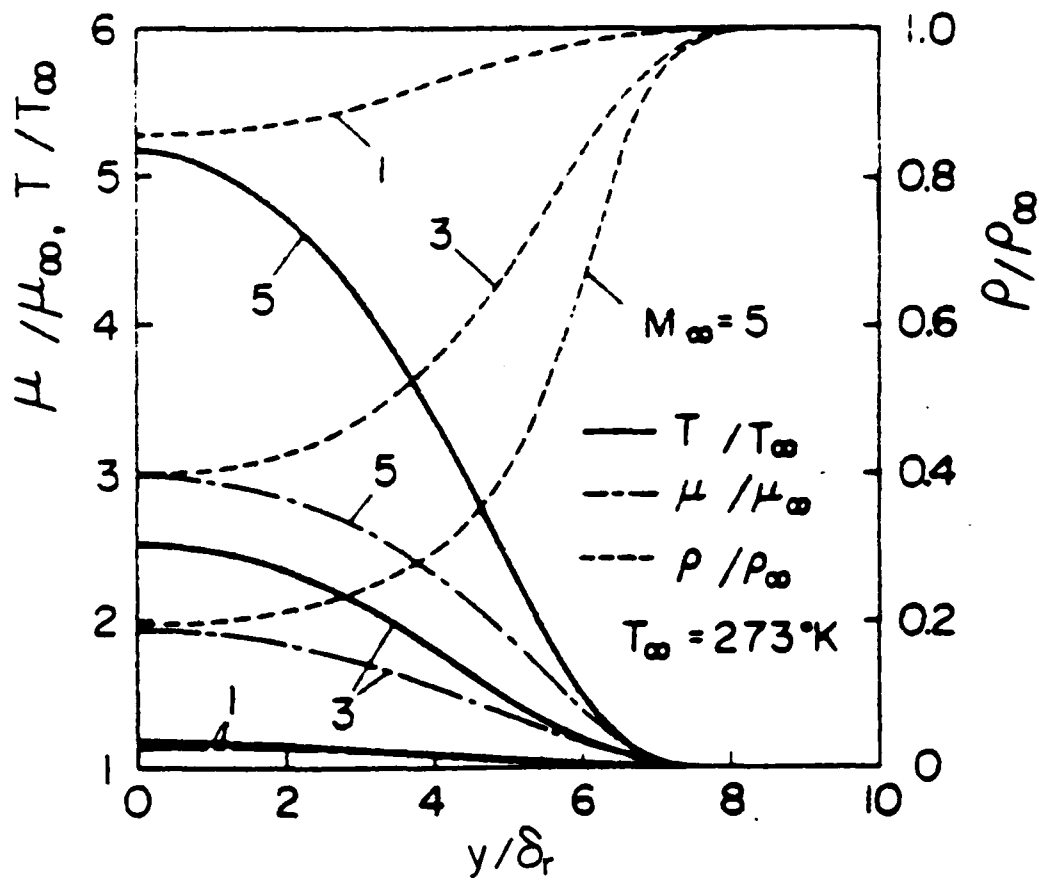


Figure 8. Distributions of temperature, density, and viscosity in compressible boundary layers on an insulated wall. [74]

previously. His results are shown in Figure 9. From these curves, the shift of amplification to lower frequencies as the Mach number increases can be seen. Concurrent with this effect is a decrease in minimum critical Reynolds numbers, with successive values, based on momentum thickness, being 150, 136, 126, 115, 104, and 92 as the Mach number increases from 0 to 1.3. However, as indicated by Mack [5], the rate of amplification of the most amplified frequency actually decreases with increasing Mach number in the subsonic flow regime.

The information in published literature on the effect of subsonic Mach number alone on transition is inconclusive. Evidently, other factors such as freestream disturbance level, heat transfer, and pressure gradients usually take precedence when there is not a significant amount of linear amplification (cf. [73] and [75]. Also, see [12, 42, 76]).

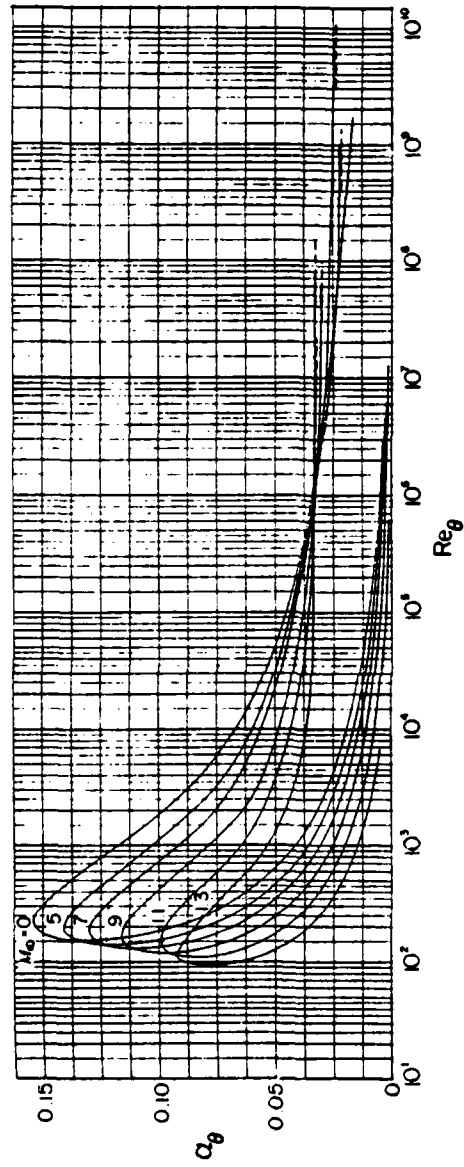


Figure 9. Effect of Mach number on the stability of flow over an insulated surface. [50]

V. TRANSITION ON STREAMWISE CURVED SURFACES AND THE GÖRTLER INSTABILITY

The behavior of the T-S type instability is not substantially affected by either convex or concave streamwise curvature, if the boundary layer thickness to local curvature ratio is small enough for the boundary layer approximation to be valid [77, 78]. Although, according to Schlichting [5], convex curvature tends to slightly stabilize and concave curvature to slightly destabilize the T-S modes. Also, it is known that convex curvature reduces and concave curvature increases the skin friction and heat transfer in turbulent boundary layers [77, 79, 80, 81, 82]. However, the centrifugal forces in the laminar boundary layer over a concave wall do induce a steady three-dimensional instability different from the T-S type. This instability appears as steady streamwise rows of contrarotating vortices which, provided the concavity is sufficient, can come into existence and amplify at Reynolds number much lower than that for the T-S disturbances. Figure 10 illustrates the configuration of these vortices, which result from the interaction of the centrifugal acceleration with the varying fluid momentum across the boundary layer. A general criterion for the existence of similar instabilities was deduced by Rayleigh (see Schlichting [5]) for inviscid flows. He determined that such flows become unstable when the tangential velocity decreases with distance outward along a flow turning radial more strongly than the reciprocal of the radius. Hence, similar vortex instabilities are observed, for example, in Couette flow between concentric cylinders, the inner one of which is rotating [83].

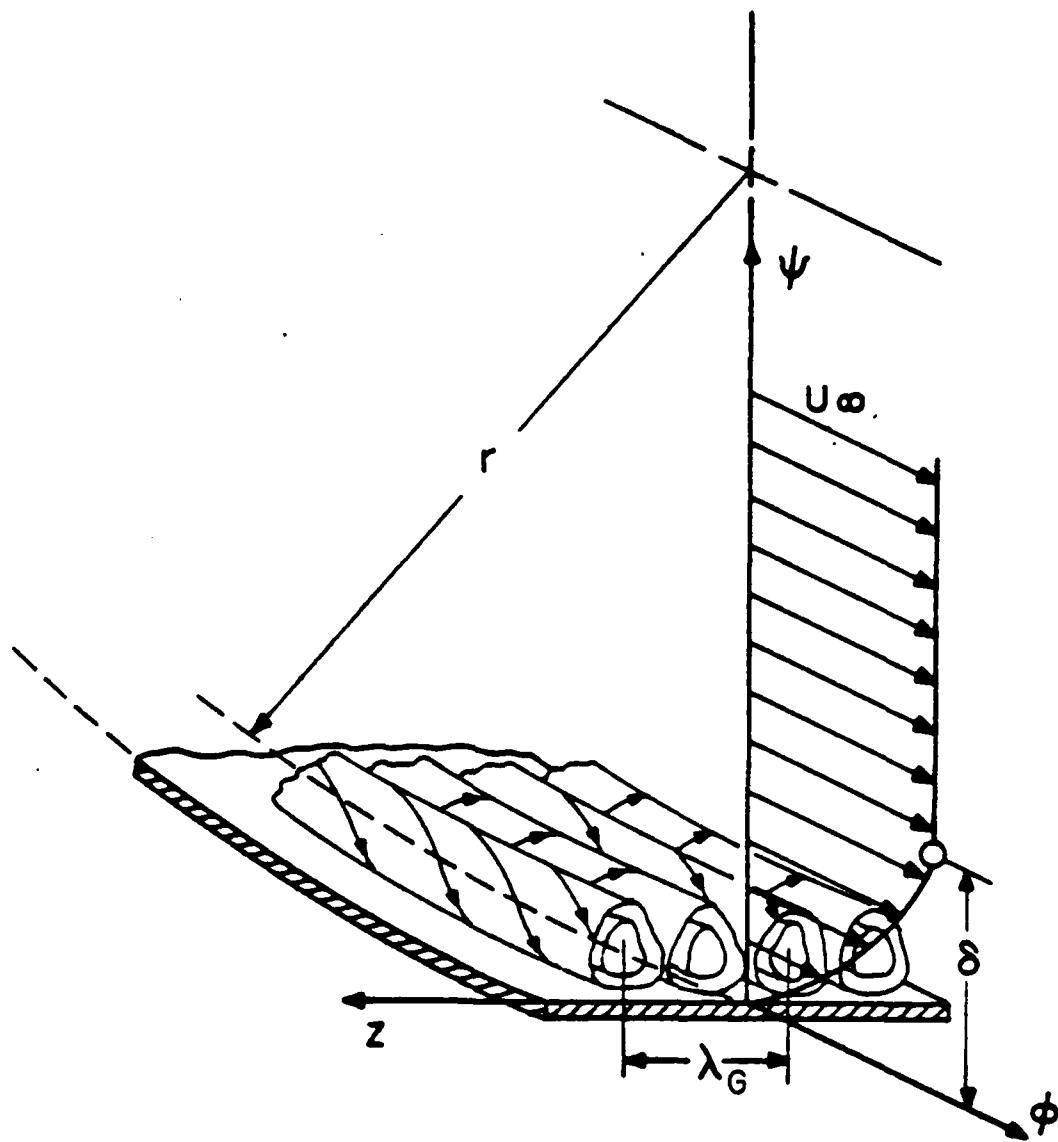


Figure 10. Görtler vortex instability in the boundary layer flow over a concave wall. [17]

Görtler [7] was the first to demonstrate analytically that the boundary layer flow over a streamwise concavely curved wall can be unstable to these vortical disturbances. Later, the physical existence of these vortices was verified, circumstantially in the experiments of investigators such as Tani [84], and visually by other investigators, most notably Wortmann [85], and Bippes and Görtler [86], both in water tunnels. From Tani's [84] investigations, it is known that the vortices can be produced in both laminar and turbulent boundary layers, although the laminar boundary layer seems to be considerably more unstable to them. Analogous instabilities and vortex formations can also be present in thermally (unstably) stratified boundary layers [84, 65]. In these cases, the buoyant force corresponds to the centrifugal force resulting from streamline curvature.

One reason for the importance of the Görtler phenomena, as Liepmann [57, 87] has shown, is that its occurrence can drastically lower the Reynolds number of transition onset as compared to boundary layer flows over flat or streamwise convex surfaces. Another, as McCormack, Welker, and Kelleher [88] have documented, is that the presence of the vortices in the laminar boundary layer can significantly increase the average heat transfer, and therefore, by Reynolds analogy, the skin friction.

Wortmann [85], Bippes and Görtler [86], and Tani and Aihara [78], and others, have examined experimentally the process by which transition occurs under the influence of Görtler vortices. From their investigations in constant freestream velocity, low disturbance level flows over constant radius concave plates, the following tentative description of the instability development is obtained:

- (1) Vortices (the primary instability) of wavelength λ_G amplify spatially with streamwise distance past the marginal stability location. In this small disturbance phase the amplification is described by linearized theory.
- (2) Amplification of the primary instability decreases as nonlinear finite amplitude development begins. The vortex cross-section distorts in reaction to the presence of adjacent vortices, although the spanwise periodicity is maintained. Concurrent with this stage, a gradual spanwise increase in wavelength sometimes seems to occur Ref. [85].
- (3) A tendency to finite amplitude is observed. Three-dimensional (obliquely oriented) unsteady "waves," which somewhat resemble three-dimensional T-S waves are generated in the thickest part of the boundary layer (the section of lowest streamwise velocity and least full velocity profile) between pairs of vortices. The obliqueness of the waves results from the spanwise variation of streamwise velocity. These waves are referred to as the secondary instability Ref. [86]. In connection with the secondary instability, the vortices exhibit a "corkscrew" motion, or unsteady spanwise movement also described as "meandering," "pulsating," or "oscillating" vortices. The motion is intensified as the waves become stronger, producing a collision and rebound action between adjacent vortices.
- (4) Transition begins when the oscillating vortex streets "tear-up" on a strongly curved surface or when they intermingle on a more weakly curved surface Ref. [86]. The first signs of turbulence (wave

breakdown) appear in the thickest part of the boundary layer between pairs of vortices. Breakdown is denoted by irregular high frequency fluctuations interspersed in the "wave." These fluctuations appear more frequently as breakdown proceeds Ref. [78], resulting in a rapid increase in mean boundary layer thickness.

The current interpretation of these events is that Görtler vortices are not directly responsible for transition, since the vortex amplification is moderate, even at transition onset, in most practical cases Ref. [78, 84, 89]. Rather, Tani and Aihara [78] have concluded, and others (e.g., Ref. [16, 90]) seem to concur that the effect is indirect, operating through the three-dimensional redistribution of streamwise momentum and the induced spanwise variation in boundary layer thickness, at least if the Görtler instability is sufficiently strong. The spanwise thickness variation, in turn, results in velocity profiles with spanwise varying stability characteristics, locally driving the amplification of three-dimensional unstable waves. This nonlinear coupling of the primary vortex and secondary wave instabilities thus appears to be a prerequisite for transition up to fairly high freestream disturbance levels Ref. [78, 85, 86]. Furthermore, Nayfeh [90] developed an analytical model for the vortex-wave interaction. His model indicates a strong tendency for the vortices to promote amplification of three-dimensional unsteady waves whose spanwise wavelength is twice the vortex wavelength. Additionally, it indicates that the presence of the vortices increases the range of amplifiable wave frequencies as well as significantly increasing the amplification rate at any frequency and spanwise wavenumber. Based on these results Nayfeh suggested that this resonance instability mechanism may dominate the transition process. In this context, it is interesting to recall that the local

streamline curvature resulting from the T-S wave front in a two-dimensional flat plate boundary layer leads to longitudinal and oblique vortex formations.

Due to the lack of experimental investigations of transition induced by the Görtler instability, linear stability analyses must serve as the primary qualitative guides for anticipating the importance and relative effects of various mean boundary layer modifiers. Nevertheless it must be re-emphasized that the relationship between any results of small disturbance theory and transition is, at best, weak. Moreover, if forcing disturbance levels in the freestream are high, unmodeled mean cross-flows are present, or wall irregularities such as roughness are prominent, the relationship may be non-existent. With this in mind, a few selected linear stability results will be referenced in the next subsection.

5.1 Linear Analyses of Görtler Instability

In the original linearized incompressible flow analysis, Görtler [7] made the assumptions that the boundary layer was parallel, pressure gradients were negligible, the small ($\theta/r \ll 1$) wall curvature was constant, the streamline curvature at any distance normal to the wall was constant and equal to the wall curvature, and that the vortices were restricted to the boundary layer. (In later analyses, it was shown that the vortices need not be confined to the boundary layer for the longer amplifiable wavelength [16]). His analysis revealed the characteristic parameter for the three-dimensional concave wall instability

$$G_{\theta} = Re_{\theta} \sqrt{\theta/r} \quad (6)$$

now known as the Görtler number. Also, it produced the result that the instability was relatively insensitive to the shape of the velocity profiles, so long as their momentum thicknesses were equal. (Contrast this to the sensitivity of the T-S instability to velocity profile shape.)

Smith [89] performed a more complex linearized analysis of the Blasius flow, which included some of the effects of nonparallelism of the base flow and variation of wall curvature. Also, he was the first to correctly model the vortex perturbation growth as spatial rather than temporal. His analysis verified the predominance of the Görtler number as a stability parameter, although other nondimensional parameters also appeared in his more general equations.

Smith's actual results will not be presented since his use of a body-oriented coordinate system resulted in approximate treatment of the streamline curvature variation away from the body. Also, his approximate solution technique (Galerkin's method) resulted in inaccurate solutions. The problems with his solutions and the propriety of his model are discussed in Hall [21], Floryan and Saric [17], and Ragab and Nayfeh [16].

More recently, Tobak [91] extended Görtler's parallel flow analysis with the objective of determining what effect a finite length of wall curvature would have on the Görtler instability. He assumed that the region of wall curvature was preceded and followed by a flat flow surface. The results indicated that for a given Reynolds number a smaller radius of concavity is needed to induce instability if the length of the curved region is finite. Also, for curvatures whose extent was of the order of the boundary layer thickness the analysis indicated that only the net flow turning angle is important in producing the instability, rather than the particular shape of

the concave surface. However, for curved regions longer than a few boundary layer thicknesses, the effect was small, except for some stabilization of the largest amplifiable wavelengths.

Herbert [92] did a comprehensive survey and evaluation, and computed accurate numerical solutions for the models of Görtler, Smith, Tobak, and others. He also showed that smaller streamwise extent of curvature, as well as decay of streamline curvature away from the wall, considerably stabilized the flow, especially to the longer wavelength vortex perturbations.

Ragab and Nayfeh [16] investigated the effects of more general streamwise curvature and nonsimilar pressure gradients on the Görtler instability in non-parallel incompressible boundary layer flows. As special cases, they considered the effects of displacement thickness and decay of streamline curvature away from the wall on the marginal Görtler stability of the Blasius flow. The results for the Blasius flow, with and without displacement thickness effects are shown in Figure 11. In this figure and the subsequent ones from their paper, the abscissa is the Görtler wavenumber nondimensionalized by the boundary layer reference length $\delta_p = \sqrt{vx/U_\infty}$ and the Görtler number in the ordinate is based on the same similarity variable. Curve 1 is the marginal stability curve for parallel flow (Görtler model), Curve 2 is the marginal curve for their nonparallel flow, and the dashed curves are for nonparallel flow computations including displacement thickness effects. Notice that the displacement effect is greater at the smaller Reynolds number because of the larger rate of growth in boundary layer thickness. Also note that the displacement thickness effects are most prominent for long disturbance wavelengths, becoming smaller as the disturbance recedes into the boundary layer.

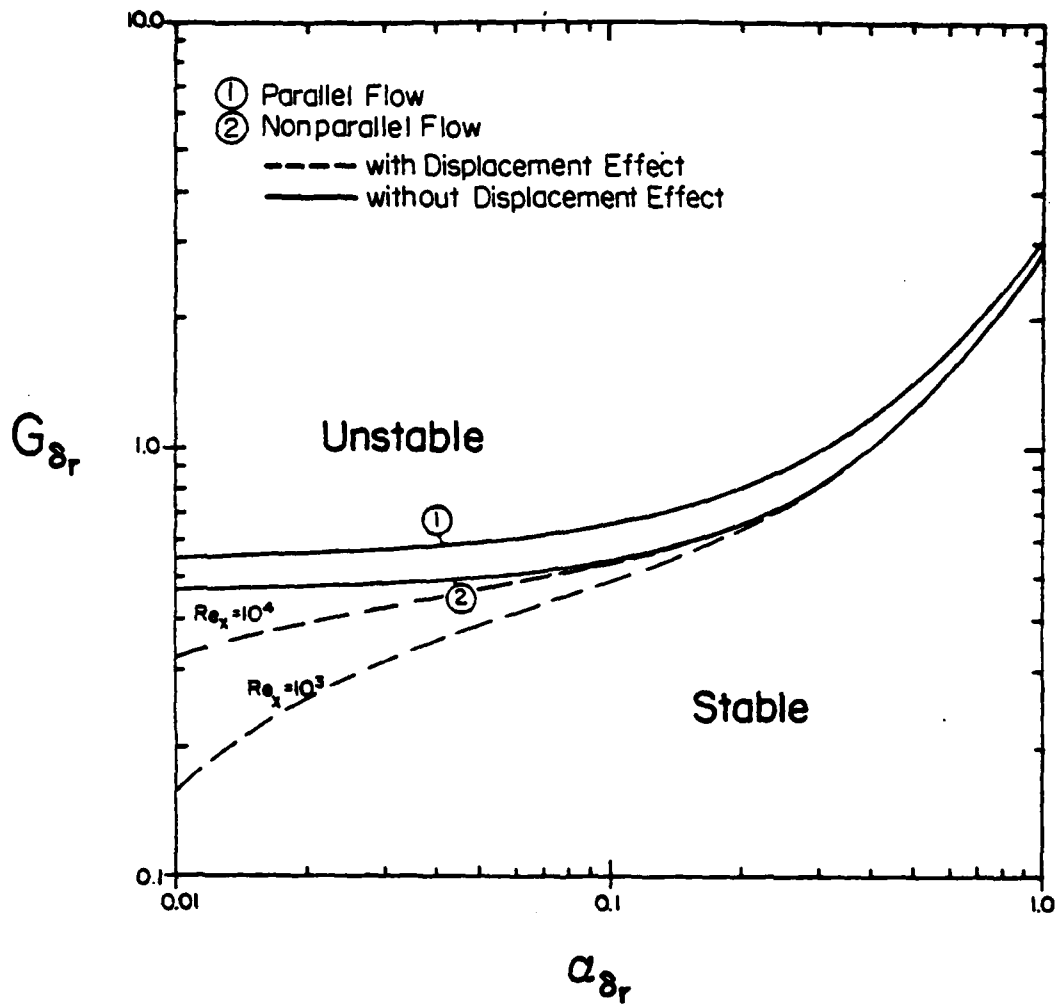


Figure 11. Marginal Görtler vortex instability on Blasius flow - displacement thickness effects. [16]

Figure 12 demonstrates the stabilization, especially evident at the longer wavelengths, afforded by exponential streamline curvature decay away from the wall. The dashed lines are the parallel flow marginal stability curves while the solid lines are for the nonparallel flow. Herbert [92] explained that this stabilizing effect is due to the reduction in local centrifugal force associated with the decreasing curvature. Thus, since the longer wavelength disturbances extend further outside the boundary layer, the reason for their increased stability is evident.

Figure 13 shows the influence of pressure gradient on marginal stability for some of the Falkner-Skan family of flows. The authors attribute the stability behavior to the increase or decrease in the wall normal velocity component of the boundary layer flow, corresponding to the degree by which the pressure gradient is adverse or favorable. However, the authors state that these results are an approximation since they "patched" the self-similar velocity profiles to their nonsimilar boundary layer for local values of the Falkner-Skan pressure gradient parameter. Therefore, the "history" of the boundary layer pressure gradient effects and the gradient at the local position are neglected.

From the analysis of their nonsimilar boundary layer, the authors determined that the linear amplification and damping rates of the Görtler disturbances are strongly dependent on both the local value of pressure gradient and the pressure gradient history. Thus, the results implied the uniqueness of linear amplification rate calculations for Görtler disturbances over generally curved walls.

Floryan and Saric [17] also analyzed the nonparallel stability of Blasius flow to the Görtler disturbances. They considered the case of a circular arc

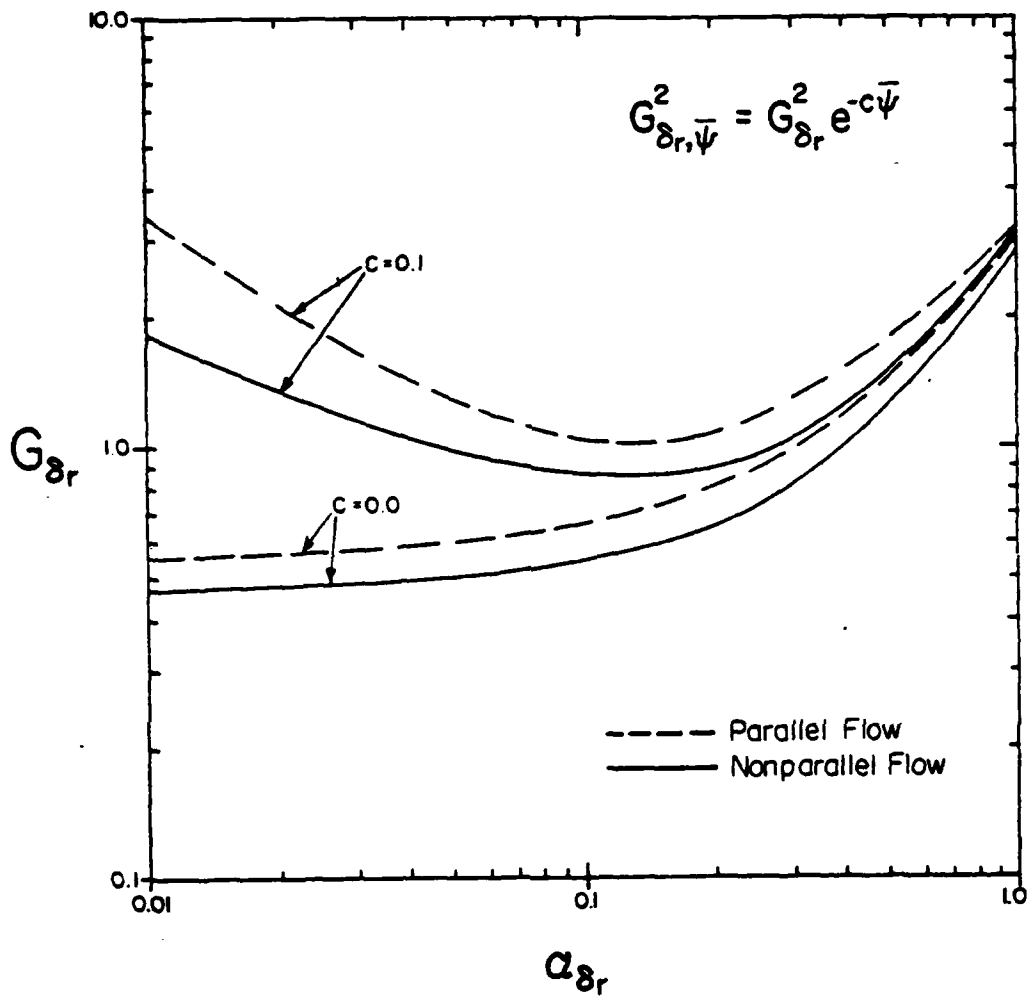


Figure 12. Marginal Görtler stability on Blasius flow - decaying streamline curvature effects. [16]

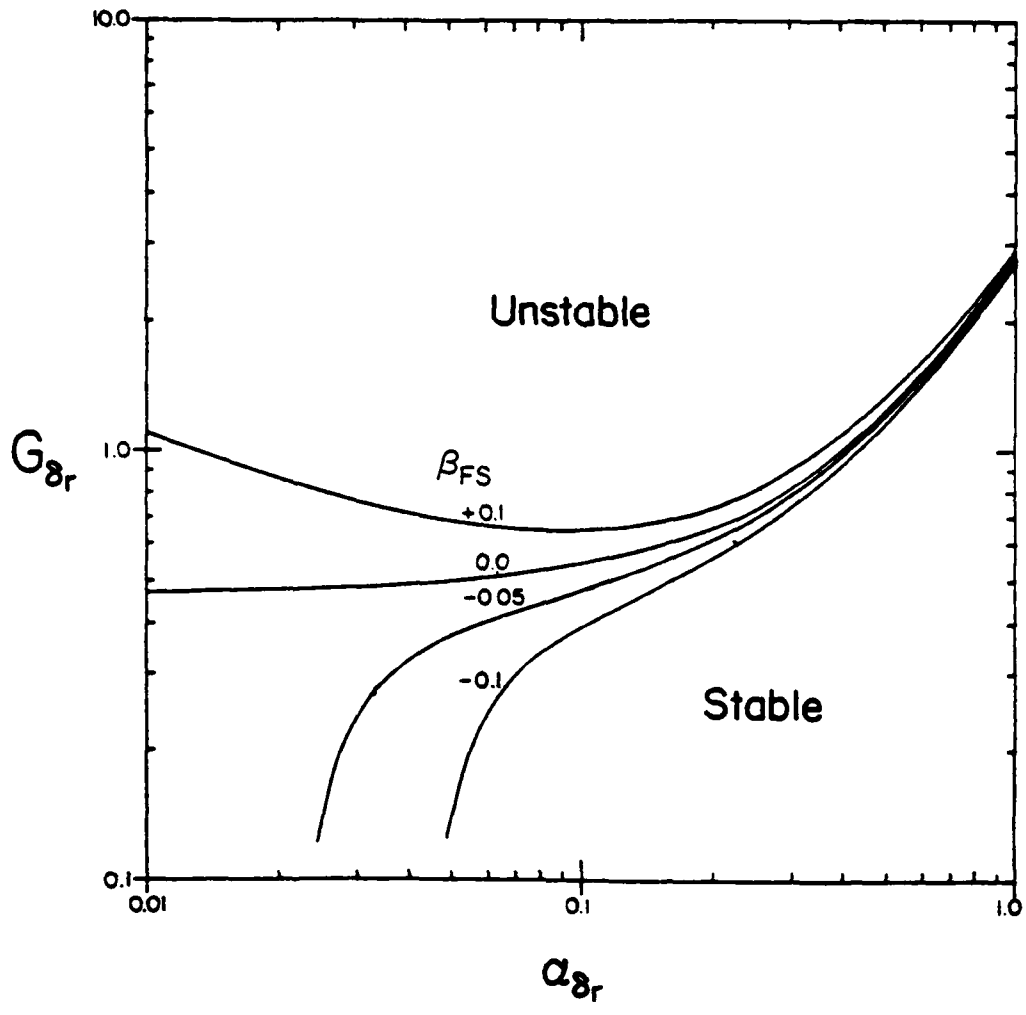


Figure 13. Marginal Görtler stability of some Falkner-Skan flows. [16]

shaped wall of small curvature and utilized an orthogonal coordinate system based on the inviscid flow streamlines and potential lines shown in Figure 14. For this analysis, "small curvature" indicates that

$$\frac{\delta_r}{r} \ll 0 \quad (1/Re_{\delta_r}) \quad (7)$$

which the authors state would make the assumptions of Blasius profile and momentum thickness approximately correct in a zero pressure gradient flow.

The curves they obtained for marginal stability and constant dimensionless spatial amplification rate, $\beta_a (= B\delta_r Re_{\delta_r})$, where B is the amplification per unit of distance along the streamwise coordinate are shown in Figure 15. In this plot the Görtler number is based on the boundary layer reference length, δ_r , and so is the nondimensional wavenumber. Since these results are for constant freestream velocity flow over a constant radius surface, the log-log plot of the amplification loci would result in curves of constant wavelength to fall on a straight line of slope 3/2. Although the authors determined a maximum amplification curve for their model, its slope in the flattened region is somewhat greater than 3/2, as can be seen by comparing it with the solid line of constant wavelength. It is worth noting that the relative flatness of the amplification rate loci about this maximum amplification curve would seem to indicate a range of amplifiable wavelengths. (Consider that amplification occurs at fairly small Reynolds numbers for which the displacement thickness effects are not negligible.) A discussion of how these curves compare with the available stability-amplification data is presented in the paper itself.

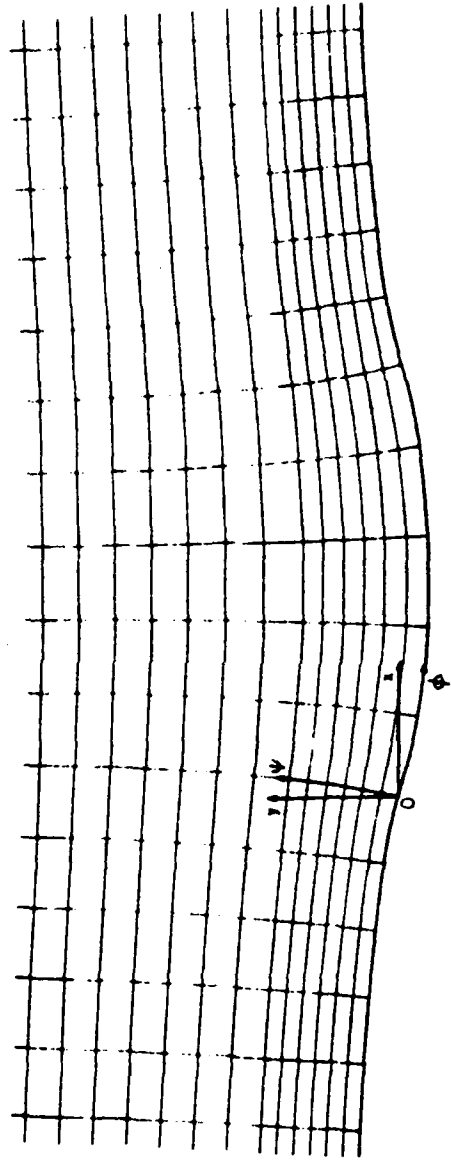


Figure 14. Potential flow net configuration for Floryan-Saric analysis. [17]

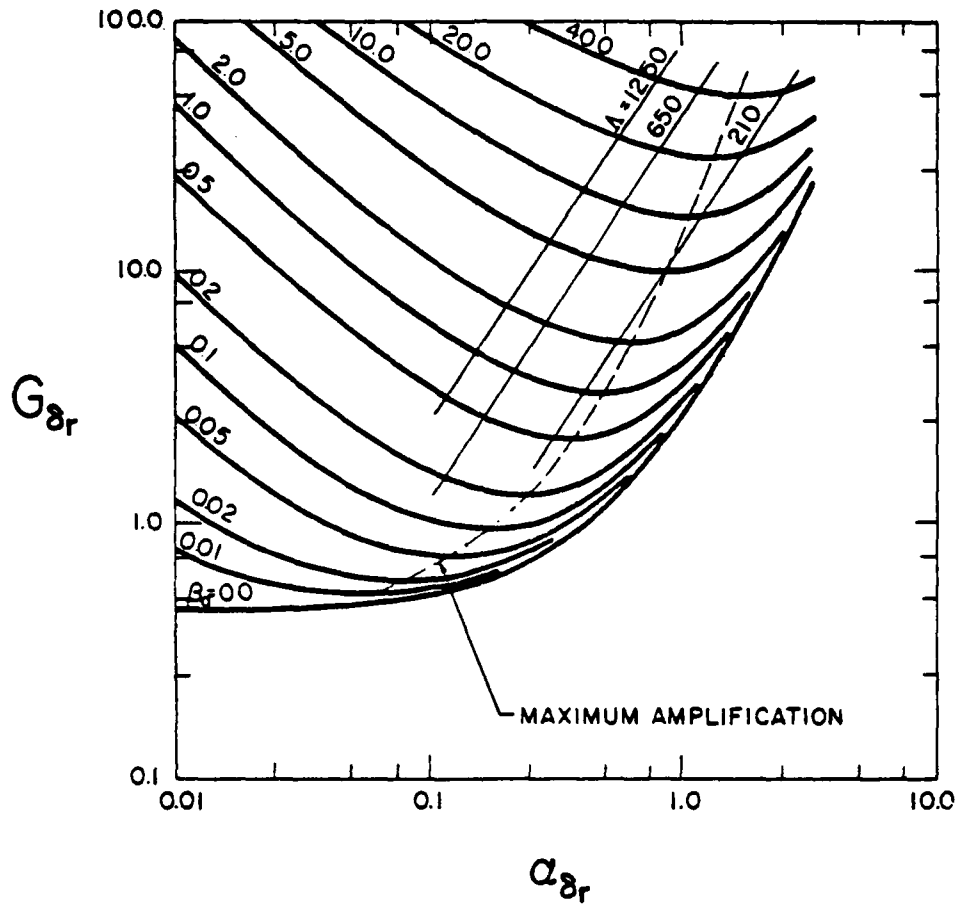


Figure 15. Curves of constant amplification rate for the Görtler instability in Blasius flow. [17]

The marginal stability curve Floryan and Saric obtained is identical to that calculated by Ragab and Nayfeh [16] for Blasius flow without displacement effects. In the small wavenumber limit, it is asymptotic to a Görtler number, based on δ_r , of approximately 0.4638 (see Figure 11), which is about 0.251 for the momentum thickness Görtler number. Also, an upper bound for amplifiable wavelengths can be described by a value of 44.29 for the wavelength parameter, $\Lambda = (U_\infty \lambda_G / D) \sqrt{\lambda_G / r}$. Nevertheless, Floryan and Saric emphatically point out that the stability curves, and therefore the minimum critical Görtler number, are dependent on both the configuration of the wall and the curvature of the streamlines away from the wall. In fact, since local centrifugal force drives the instability the role of wall curvature is of secondary importance compared to the role of flow field curvature away from the wall. Hence, stability-amplification curves such as those in Figure 15 are not universal.

The foregoing Görtler stability results are valid for constant property viscous flows without heat transfer. To complete the review of the linearized Görtler stability analyses, some results which include the effects of compressibility and wall-to-freestream temperature gradients will be examined.

Kobayashi and Kohama [74] analyzed the stability of compressible constant freestream velocity flows over slightly concave ($\theta/r \ll 1$) constant radius walls, with and without heat transfer. In the analysis, the temperature dependence of viscosity was included via Sutherland's formula. The Prandtl number and the specific heat were assumed constant. For the limiting case of $M \rightarrow 0$ and an adiabatic wall, their model was the same as that Görtler.

Figure 16 shows the marginal stability curves (solid lines) obtained from the calculations for flow over an insulated wall with Mach numbers ranging from 0 to 4. Also shown are the results of some stability calculations by

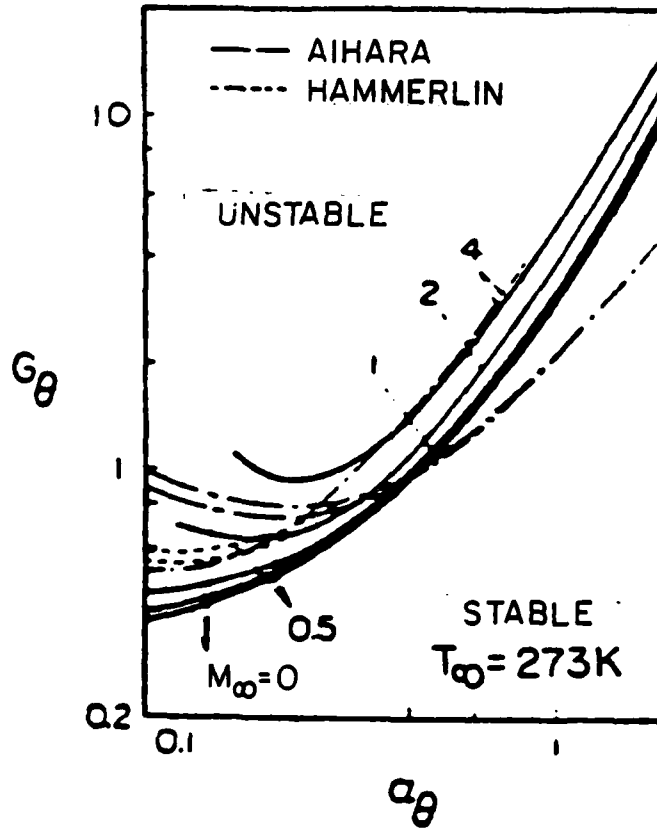


Figure 16. Effect of Mach number on Görtler stability in flow over an insulated wall. [74]

Aihara [93] and Hämmerlin [94]. Qualitatively, the results agree with those of Hämmerlin [94], who assumed a power law dependence of viscosity on temperature. For both analyses, the effect of increasing Mach number is stabilizing (albeit slightly in the subsonic regime) with increasing stabilization occurring for dimensionless wavenumbers, $\alpha_\theta (=2\pi\theta/\lambda)$, less than about 0.2. The primary differences between these results can be ascribed to Hämmerlin's assumption of exponentially decreasing streamline curvature away from the wall.

Based on an investigation of the density and viscosity variations in the boundary layer, Kobayashi and Kohama attributed the increased stabilization at the higher Mach numbers (adiabatic wall) to the fact that the stabilizing increase in viscosity near the wall overwhelms the destabilizing influence of the unstable density gradient. As a comparison, Aihara [93] assumed that the viscosity was constant and obtained a decrease in stability at the smaller wavenumbers.

In Figure 17 the influence of various wall-to-freestream temperature ratios (isothermal wall) is seen to be small in the subsonic, low supersonic range. However, the present results do indicate some destabilization for heat transfer to the wall in subsonic flows, with the larger and smaller wavelengths being influenced the most. Conversely, heat transfer from the wall is stabilizing, although either variation decreases with increasing Mach number. The results are presented in another perspective in Figure 18, which is plotted for three selected dimensionless wavenumbers.

Kahawita and Meroney [95] utilized a linearized, nonparallel, small concave curvature ($\theta/r \ll 1$) flow model to determine the influence of very slight heat transfer from the wall on the Görtler type instability in a zero

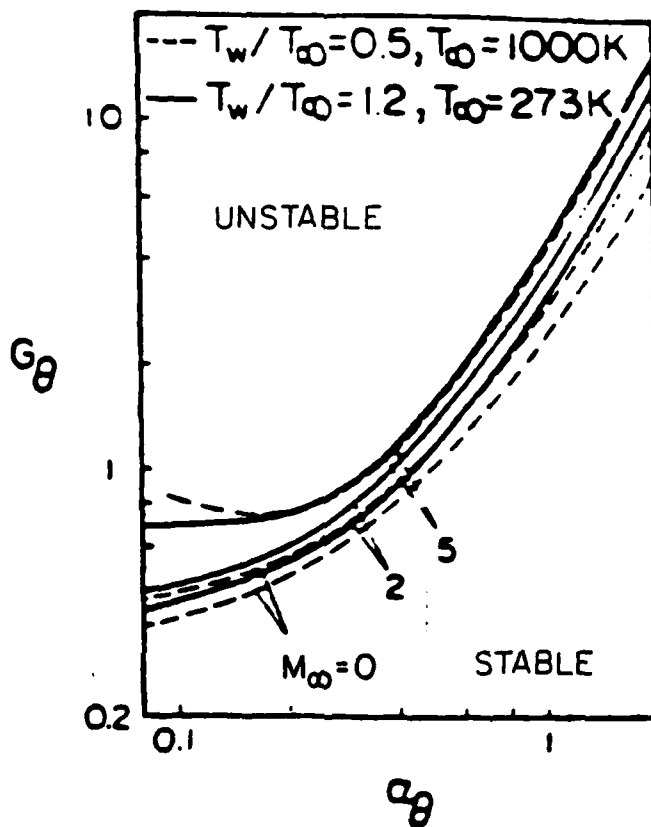


Figure 17. Effect of Mach number and heat transfer on Görtler stability in flow over an isothermal wall. [74]

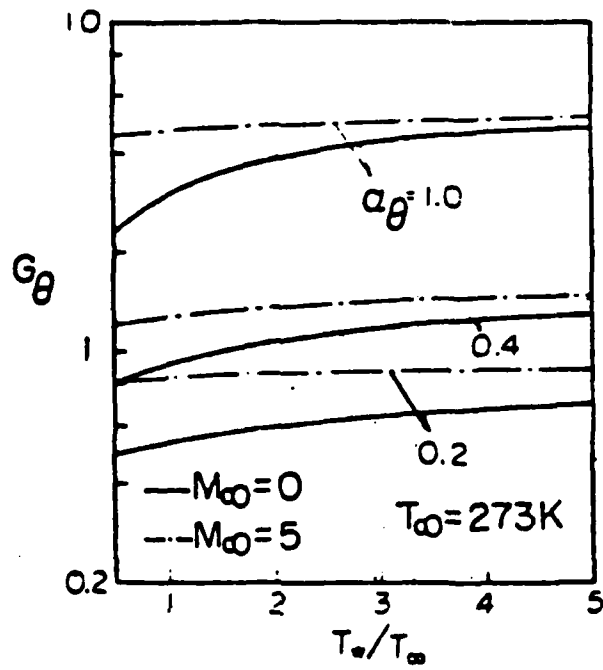


Figure 18. Variations of $G_{\theta c}$ with temperature ratio T_w/T_∞ under isothermal conditions. [74]

pressure gradient flow. Except for an additional term in one of the disturbance momentum equations and an extra equation obtained from the energy equation, their mathematical model was equivalent to that of Smith [89]. Since their objective was to obtain a Boussinesq approximation to buoyancy effects, the fluid properties were assumed to be constant and the gravity vector was assumed to be locally normal to the wall.

Figure 19 shows the results of their investigation for a Prandtl number (Pr) of 0.72. The Grashof number (Gr) in this plot has been calculated using $\sqrt{\frac{\nu x}{U_\infty}}$ as the length dimension. Therefore,

$$Gr = \frac{g\gamma\delta^3\Delta T}{\nu^2} \quad (8)$$

where

g = gravitational acceleration

γ = bulk expansion coefficient

$\Delta T = T_w - T_\infty$

As can be seen, the results indicate stabilization for α_0 less than about 0.3 (long wavelengths) and destabilization for higher values of α_0 . Kahawita and Meroney interpreted these results as meaning that the inertial and buoyancy mechanisms are favoring disturbances of different wavelengths at the lower wavenumbers, shifting to similar wavelengths above α_0 of 0.3. Recall, though, that the fluid properties were assumed to be constant so the applicability of the results is restricted to cases for which temperature differences are small, but not small enough that the buoyancy term from the Boussinesq approximation may be neglected. Alternately, it may be applied to fluids that exhibit only a minor dependence of viscosity and thermal diffusivity on temperature.

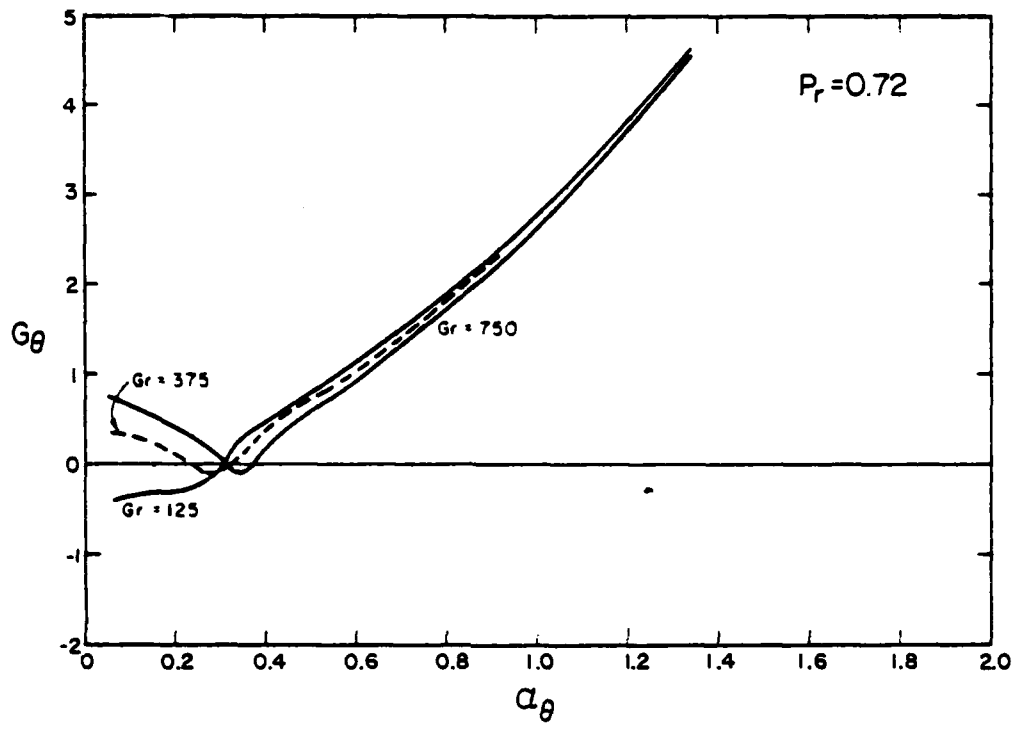


Figure 19. Marginal stability curves for combined Görtler and buoyancy instabilities. [95]

Pertaining to the validity of these curves, Floryan and Saric [17] suggested that their shape may be incorrect because of an approximate treatment of the mean flow and because of the approach used in numerical integration. However, the relative variation among the curves probably does provide qualitatively useful information.

In other results from [95] on Görtler instability, it was shown that if the normal (to the wall) component of velocity is toward the wall (e.g., as in a suction flow), the base flow is stabilizing; and if it is away from the wall, destabilizing. This concurs with previously reviewed stability results [16].

5.2 Nonlinear Analysis of Görtler Instability

Aihara [96] used an integral method of analysis employed by Stuart [23] to extend the investigations of Görtler instability into the nonlinear region. The basic equations in his model were obtained by applying the same assumptions used by Görtler. From the model, he obtained mathematical evidence of a finite vortex strength with the associated waveform distortion and a possible analytical explanation for the unsteady lateral movement observed in the amplified vortex region. Also, he demonstrated that at marginal stability for $\theta/r \ll 1$, the Görtler parameter is a physical rate parameter describing the product of the average of two ratios, as follows:

$$\frac{\text{Kinetic energy dissipation}}{\text{Kinetic energy production}} \times \frac{\text{vorticity energy dissipation}}{\text{vorticity energy production}}$$

Furthermore, Aihara showed mathematically that, subject to the assumptions noted above, the curvature of the flow field has no direct influence on the

vortex wavenumber. In connection with this, he cited the results of his own experimental (Blasius flow) investigations in which the vortex wavenumber was seemingly indifferent to wall curvature. Instead, it was apparently set by upstream irregularities in the flow stream of the experimental apparatus. He observed that the flatness of the marginal stability curve in the critical domain would seem to support this indication of low wavenumber selectivity for the instability. It is interesting to note that the experimental results of McCormack, Welker, and Kelleher [88] also manifest the insensitivity of the wavelength to either freestream velocity or wall radius.

Hall [21] analyzed the nonlinear development of Görtler vortices in nonparallel boundary layers. He demonstrated that there exists a critical value for rate of change of curvature in Blasius flow above which a finite amplitude solution can develop, and below which the disturbance will ultimately decay. However, he did not consider the oblique wave disturbances that appear and often lead to turbulence before the amplitude becomes finite, or the disturbance decays. If the results are valid, though, they provide analytical evidence that Görtler vortices are only indirectly responsible for transition.

5.3 Experimental Results on Transition Over Streamwise Curved Flow Surfaces

Before investigations of transition on streamwise curved flow surfaces are reviewed, some important experimental observations about the general nature and predictability of the vortex disturbances will be emphasized.

Tani's [84] experiments in an essentially Blasius flow over a constant radius concave surface revealed that the vortex wavenumber is independent of streamwise location and almost independent of freestream velocity. McCormack,

Welker, and Kelleher [88] obtained similar results. Tani and Aihara [78] surmised that the observed Görtler wavelength is "inherent" to a particular experimental flow arrangement, as long as it is predicted to be amplifiable by stability theory. To substantiate this conjecture, they artificially generated weak vortices in the boundary layer having a wavelength twice that of the "inherent" vortices. These artificial vortices were amplified without change in wavelength. Thus, at least for flow without a streamwise pressure gradient, the results implied the weak selectivity of the Görtler mechanism to wavelength. Referring again to the stability results of [16, 17], the relative flatness of the stability-amplification curves for Blasius flow would also seem to substantiate this viewpoint. Practically speaking, however, Tani and Aihara's [78] results also indicate that any streamwise vorticity which interacts with the boundary layer could influence the resultant Görtler wavelength.

As to the predictability of nonstimulated wavelengths, Tani [84] and Aihara [96] have concluded that stability theory cannot explicitly predict the wavenumber of the vortices which occur in the flow over a streamwise concavely curved surface. However, notice that the theory does indicate lower limits for the amplifiable wavelengths in self-similar boundary layers. Furthermore, it can be used to indicate a range for the wavelengths most susceptible to amplification.

Liepmann [57, 87] utilized a low speed wind tunnel to investigate transition on both concave and convex constant radius surfaces in the effective curvature range of $|\theta/r| \leq 10^{-3}$. For the higher effective concave curvatures [87], his test plate was smooth glass with a sharp leading edge and a 2.5 foot radius. His results are plotted in Figure 20 as Görtler number

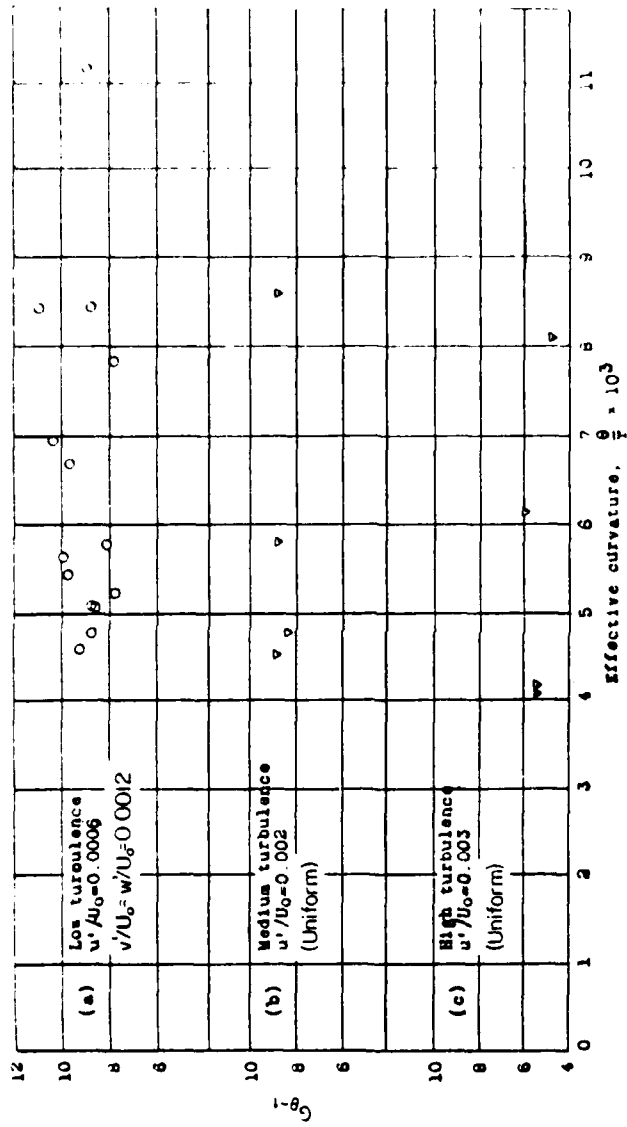


Figure 20. Transition measurements on 2.5-foot radius concave plate at three freestream turbulence levels. [87]

versus effective curvature for three freestream "turbulence" levels (no spectrum specified). Although there is considerable scatter in these data points, they do serve to support his conclusion that Görtler instability-dominated transition on constant-radius concave surfaces without a streamwise pressure gradient could be correlated with a constant value of the Görtler parameter. Additionally, Figure 20 illustrates that the effect of freestream disturbance on the Görtler instability dominated transition is of similar order to its effect on the T-S instability dominated transition. Liepmann judged that the average value of the transition Görtler number was 9.0 at the lowest freestream disturbance level and 6.0 at the highest. As to the scatter in the data points, Liepmann commented that detection of transition and boundary layer thickness measurements on the small (2.5 feet) radius plate were inherently difficult, particularly when transition occurred near the leading edge. In these experiments, transition was detected by moving a hot wire anemometer downstream in the boundary layer until high frequency turbulent bursts were first seen in an oscilloscope display.

For transition in Blasius flow over streamwise convex surfaces, Liepmann determined that the transition location was unaffected by curvature in the range of his experiments (see Figure 21). That is, within experimental scatter, the momentum thickness Reynolds numbers at transition were the same for both flat and convex plates in similar disturbance environments. In connection with these results, Liepmann found in stability experiments [57] that the unstable frequencies and amplification characteristics of the T-S waves on convex plates matched those obtained by Schubauer and Skramstad [6] in Blasius flow over a flat plate, within experimental accuracy. In contrast, his results for concave plates exhibited a systematic decrease in transition

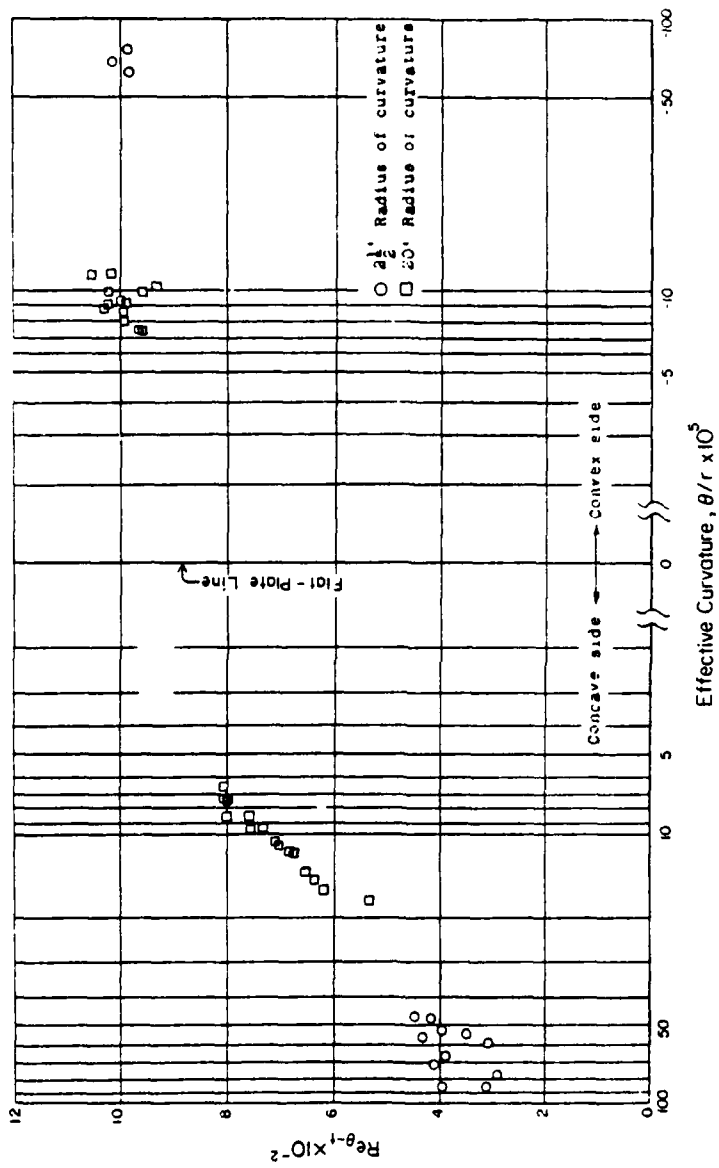


Figure 21. Effect of concave and convex streamwise wall curvature on transition. [87]

Reynolds number for increasing effective curvature, as shown in Figure 21. Points clustered at the smaller effective convex and concave radii were taken from a plate with a constant radius of 20 feet [57]. Liepmann notes that all the laminar boundary layer velocity profiles corresponding to these data points were fairly close to Blasius.

Although there has been at least one investigation designed to elucidate the mechanism of transition in the regime between the T-S instability dominated and Görtler instability dominated modes (i.e., [97]), the interaction is not yet clear. Nevertheless, as shown in Figure 22 from Liepmann [87], the changeover appears to be continuous as the effective concave curvature increases. The points in this plot are for nominally Blasius flow at Liepmann's lowest freestream disturbance level. The horizontal line $Re_{\theta-t} = 940$ represents the flat plate transition value for his wind tunnel disturbance environment, while $G_{\theta-t} = 9.0$ is the value for transition on the 2.5 foot radius concave plate in the effective curvature range of $4.5 \times 10^{-4} \leq \theta/r \leq 10.0 \times 10^{-4}$. From these results Liepmann concluded that there is a transfer of energy from one instability mode to the other in an intermediate effective curvature range. Dryden [42] in a later review of these results suggested that transition is definitely Görtler instability dominated for $\theta/r \leq 5 \times 10^{-4}$ in constant freestream velocity flows over a surface of fixed radius.

Figure 23 and 24 are Liepmann's results for the effects of small streamwise pressure gradients on transition over his convex 20-foot radius and concave 2.5-foot radius flow surfaces, respectively. All of the data points were taken at his lowest freestream disturbance level. A comparison of these two plots led him to believe that the effect of either adverse or favorable

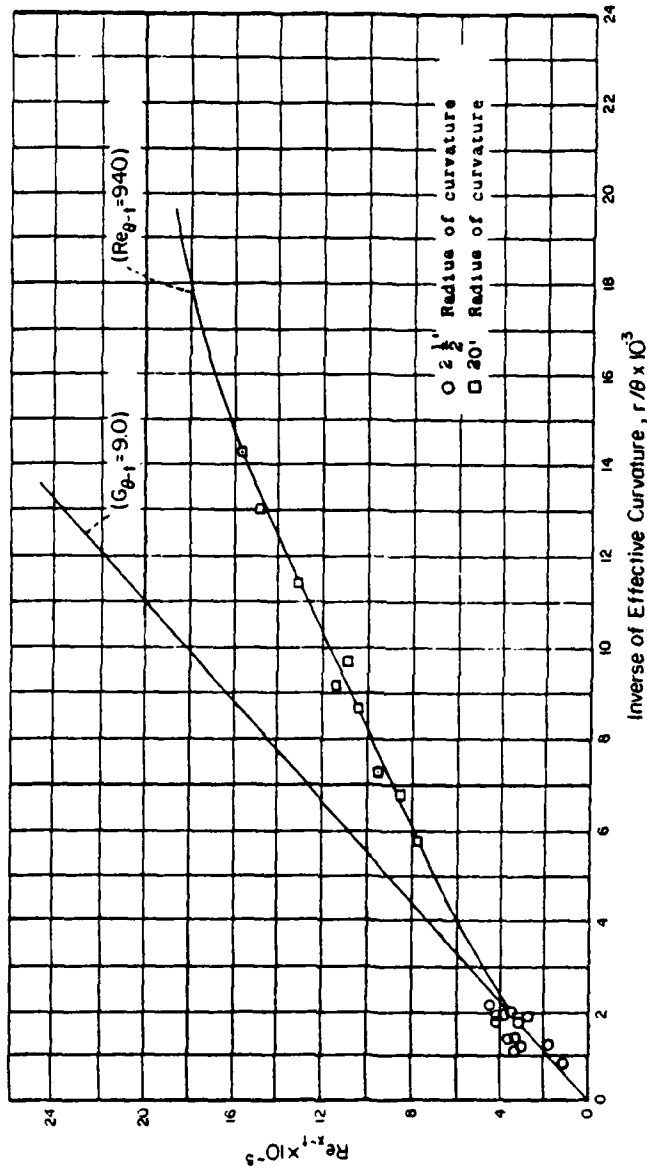


Figure 22. Transition measurements at various effective concave curvatures. [87]

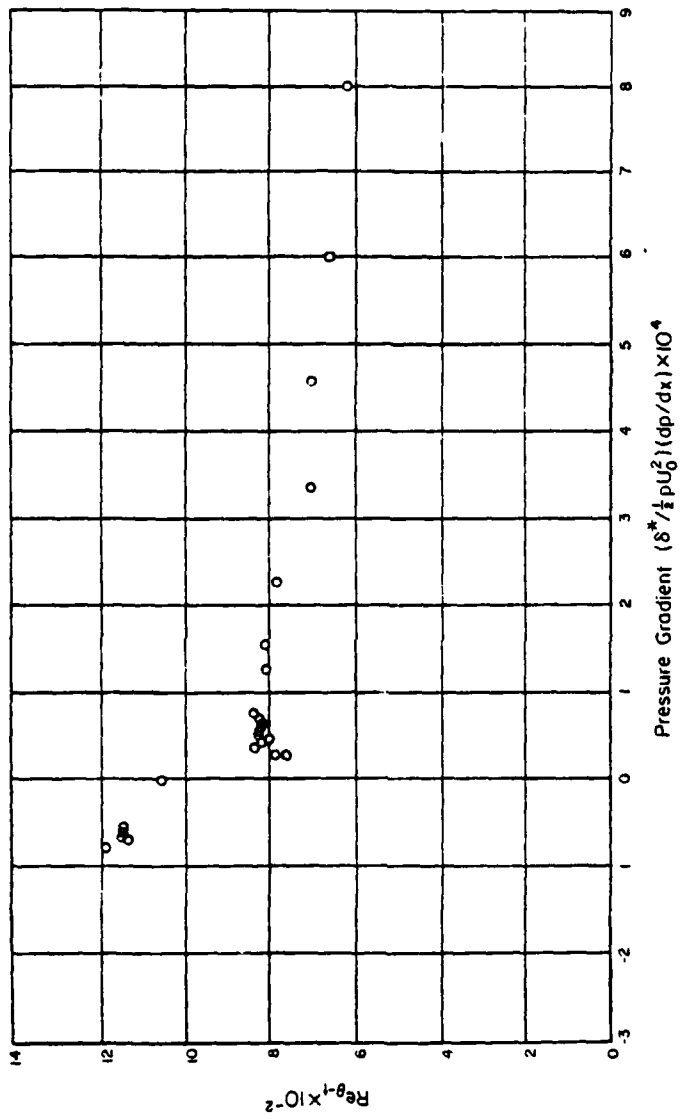


Figure 23. Effects of pressure gradient on transition over a 20-foot radius convex surface. [87]

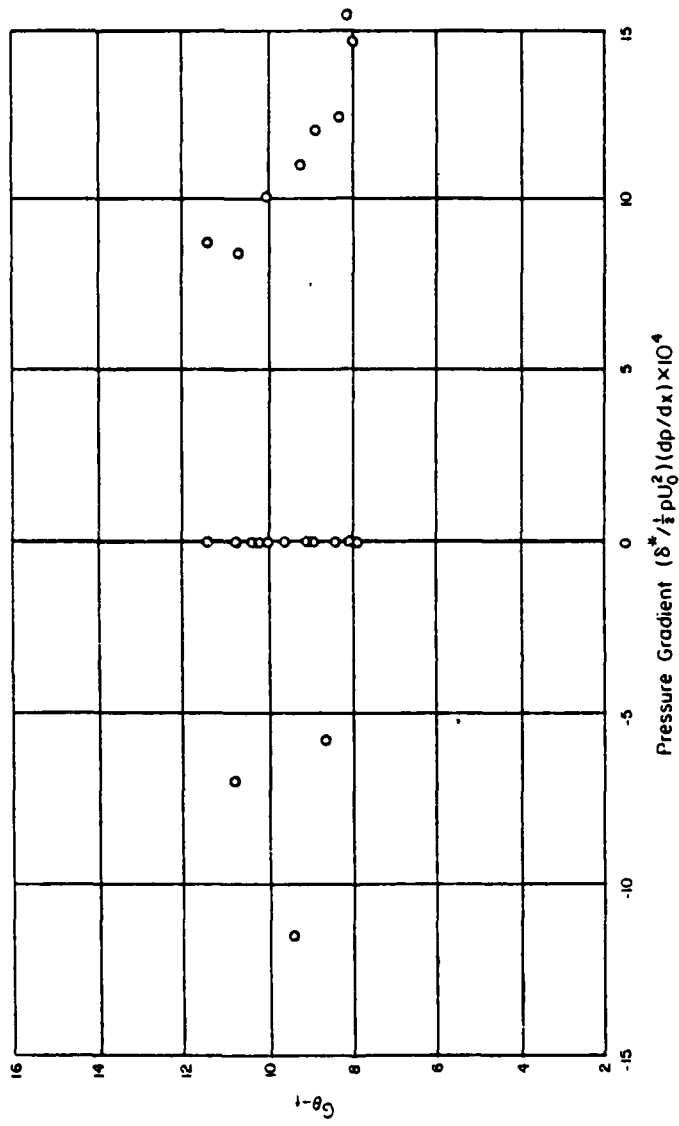


Figure 24. Effect of pressure gradient on transition over a 2.5-foot radius concave surface. [87]

pressure gradients on Görtler vortex induced transition is, at most, small when the correlating parameter is the momentum thickness Görtler number. Although there appears to be a downward trend in the data for the adverse pressure gradient on the concave plate (Figure 24), Liepmann concluded that it was not systematic, since the values fell within the (considerable) range of scatter for the zero pressure gradient case. In the flow over the convex surface, though, the change of $Re_{\theta-t}$ with pressure gradient was systematic: increasing with a favorable and decreasing with an adverse pressure gradient (Figure 23). Furthermore, he observed that the largest rate of change of $Re_{\theta-t}$ with pressure gradient occurred for small deviations from the zero pressure gradient, at least if the gradient was adverse. The finite length of the plate prohibited him from determining if the decreasing rate trend also held for favorable pressure gradients.

Concerning these results, Liepmann pointed out that the Blasius solution is a singular solution in the sense that $\partial^2 u / \partial y^2 = 0$ at $y = 0$ (the wall). Therefore, knowing the sensitivity of the T-S instability to velocity profile shape, one might suspect that small deviations from the Blasius profile would result in significant changes in transition behavior. Conversely, Görtler's parallel flow result indicating insensitivity of the vortical instability to velocity profile shape seemed to support his opinion concerning the influence of pressure gradients on the vortex induced transition. Nevertheless, Liepmann was aware that transition depended on the level and spectrum of freestream disturbances, and the integrated effect of instability development. Thus, he cautioned that these results are not universally applicable based on disturbance level, but suggested that the trends observed for pressure gradient influence would be quite general. Interestingly enough,

there have apparently been no experiments comparable to those of Spangler and Wells [41] that examine the effect of disturbance spectrum on transition induced by Görtler vortices. As will be seen later, though, Abu-Ghannam and Shaw [48] obtained results very comparable to Figure 23 for pressure gradient influence on flat plate transition at low freestream disturbance levels. However, Liepmann's conclusion about the insensitivity of Görtler vortex induced transition to streamwise pressure gradient influence has not yet been verified.

Tani and Aihara [78] were less conclusive than Liepmann about the coreliability of the data with a constant Görtler number, even for the case of supposed predominance of the Görtler instability ($\theta/r \geq 5 \times 10^{-4}$). They did suggest, however, that transition in zero pressure gradient boundary layer flows over constant curvature concave walls could be correlated as a function of the Görtler parameter, the value of which increased with increasing effective curvatures.

Smith [89] disagreed with Liepmann's conjecture that a correlation of Görtler instability-dominated transition over a constant radius surface is virtually independent of streamwise pressure gradient when the correlating Görtler parameter is based on momentum thickness. He maintained that the vortices must achieve a certain strength relative to a characteristic velocity before transition can occur, and stated that the Görtler (rate) parameter provided such a measure of vortex strength only under conditions of constant curvature and constant freestream velocity for a boundary layer beginning at the edge of a curved plate. Pippes and Görtler's [86] measurements of vortex growth under essentially these conditions do lend credence to this statement. They indicate that the vortex growth is a linear function of the

momentum thickness Görtler number for a region of development after the disturbances become measurable, but before the onset of the meandering motion. Nevertheless, Liepmann's conclusions are not totally implausible for constant radius surfaces when one recalls that momentum thickness growth is retarded in accelerating flows and advanced in decelerating flows relative to its growth in a Blasius layer. Also, the radial force driving the vortex development would vary with freestream velocity. Therefore, it may well be that moderate pressure gradient effects on the Görtler instability induced transition over a constant radius surface could be fairly well accounted for by a Görtler number criteria.

However, Smith was influenced by consideration of more general and practical applications in nonsimilar boundary layers over varyingly curved walls. In such cases, a local criterion probably would be untenable, because it cannot adequately account for the cumulative influence of boundary layer history on the instability development. In addition, one has to deal with the nonidealistic aspects of flows over strongly curved surfaces. These may include violations of the boundary layer assumptions or flow divergence and other three-dimensionality leading to net cross-flows.

From the analytical and experimental investigations reviewed in this section, some qualitative inferences may be made about the effects of some of the mean boundary layer modifiers on the Görtler instability, and thus, possibly, the relative significance of their effects on transition. The stability results of Ragab and Nayfeh [16] indicate that pressure gradients have a substantial influence on the longer amplifiable wavelengths. From these results and the experimental data of Liepmann, it would seem that pressure gradients should influence Görtler dominated transition, but the

effect is not nearly so great as for transition on flat or convexly curved surfaces. Furthermore, as with transition on nonconcavely curved surfaces, increasing levels of freestream disturbance may reduce even further the effects of moderate pressure gradients on transition.

As to the effects of heat transfer, the stability results of Kobayashi and Kohama [74] indicate no substantial changes if the Reynolds numbers are fairly large and buoyancy effects are negligible. However, if the boundary layer is unstably stratified, the results of Kahawita and Meroney [95] indicate destabilization. Both of these results have been qualitatively confirmed in other analyses (see Rosenhead [98], Chapter IX). Finally, Kobayashi and Kohama's [74] results might also lead one to speculate that compressibility effects are small in subsonic flows.

VI. INSTABILITY AND TRANSITION IN PERIODICALLY UNSTEADY NONREVERSING BOUNDARY LAYERS

Prominent investigations of stability and transition in oscillating boundary layer flows include those of Obremski and Fejer [99], Miller and Fejer [100], and the review of Loehrke, Morkovin, and Fejer [9]. Other experimental results on stability and transition in unsteady boundary layer flows are available in Kobashi, Kayakawa, and Nakagawa [101], Walker [102], Cousteix, Houdeville, and Desopper [103], and Pfeil, Herbst, and Schröder [104].

The review of Loehrke, Morkovin, and Fejer [9], which is current to 1975, dealt with nominally two-dimensional incompressible flows with freestream velocities described by

$$U(t) = U_0 (1 + N_A \sin \omega t) \quad . \quad (9)$$

Here, U_0 is the average velocity of the freestream, N_A [$= \Delta U_0 / U_0$] is the amplitude of the unsteady component, and ω is the circular frequency of oscillation. From their investigations, the authors found no evidence of new types of instabilities in nonreversing oscillating boundary layers, even with mean pressure gradients imposed. Instead, instability waves of the T-S type were found to precede transition onset, so long as the freestream disturbances were small and flow separation or other bypasses did not occur. For dominant instability waves with a frequency (β) greater than approximately 10 times the

base flow oscillation frequency (ω), the instabilities were viewed in a quasi-steady approximation. That is, as the instability waves propagated downstream in the boundary layer (at roughly $0.3 U_0$ for the "Blasius mean" flow), they were assumed to be amplified and dampened in response to the local instantaneously "frozen" instability characteristics of the boundary layer, producing transition onset during the most unstable portion of the first freestream oscillation cycle. To further clarify this concept, it is helpful to refer to the Saric-Nayfeh linear stability results for the Falkner-Skan profiles (Figure 5) and visualize an infinite progression of marginal stability curves ranging between those for a moderately negative and a moderately positive pressure gradient. Each of these would, successively, correspond to an infinitesimal time increment and a particular velocity profile in a half-cycle of flow oscillation, with the mean for the flows on which the paper was primarily focused, being that for Blasius flow. (Saric and Nayfeh [18] verified that the average of their "Blasius mean" boundary layer was still a solution of the steady Navier-Stokes equations.) Assuming that the frequency of the dominant instability wave is preserved, the instantaneous (spatial) rate of amplification or damping would depend on the relation of that frequency and the displacement thickness Reynolds number (both spatially and temporally dependent) to the curve instantaneously in effect.

For instability to freestream frequency ratios less than 10 but somewhat greater than unity, i.e. $1 < (\delta/\omega) < 10$, no persistent behavior patterns emerged. However, less instability was anticipated, since the T-S waves have less time to react to the rapidly changing amplification characteristics of the boundary layer. For frequency ratios approaching unity, the instability waves appeared to "lock onto" the freestream oscillation frequency, making the

frequency ratio unity. Nevertheless, it was not anticipated that this occurrence would produce transition earlier than the quasisteady first cycle mode.

According to Loehrke, Morkovin, and Fejer [9], the effects of freestream unsteadiness in the quasisteady regime would most easily fit into the "OPERATION MODIFIERS" box of Morkovin's diagram (Figure 1). With oscillation amplitudes, N_A , less than about 0.01, though, the appropriate box would be "DISTURBANCES" since the randomness and three-dimensionality of the oscillation increases in response to the relatively larger disturbances and flow irregularity. An intermediate amplitude range would result in a "multiple responsibility" transition.

At least in the quasisteady regime, the effect of increasing amplitude modulation is destabilizing because of the tendency to greater periodic velocity profile inflections. In particular, such flows are susceptible to periodic local separations leading to "bypasses." More generally, the widely varying stability characteristics increase their sensitivity to disturbances and flow nonuniformities. At any rate, in the transition regime, the rate of growth of the turbulent patches and the quiescent laminar region following the wake of the turbulent patches are comparable, over a wide range of the governing parameters, to that observed for steady flows [9]. The Obrenski-Fejer [99] measurements produced average speeds for the turbulent "patch" leading and trailing edges of approximately $0.88 U_0$, respectively, in a Blasius mean quasisteady boundary layer. Recall that the corresponding speeds for the Schubauer-Klebanoff [31] turbulent "wedge" in a Blasius boundary layer were approximately $0.88 U_0$ and $0.50 U_0$. However, the turbulent patches are described in Loehrke, Morkovin, and Fejer [9] as "slightly sinuous two-dimensional ribbons" extending transversely across the flow surface, when the

oscillating pressure gradient amplitude is large and uniform enough to assure essentially two-dimensional unsteadiness. As further evidence of the similarity of transition in steady and unsteady flows, Loehrke, Morkovin, and Fejer [9] note that the lateral propagation of turbulence in unsteady flows from the transverse-contamination bypass of Charters [10] appears to be like that observed for steady flows, with the exception of possible periodic emphasis caused by local separation.

The Obremski-Fejer [99] wind tunnel transition results for "quasi-steady" flat plate boundary layers are shown in Figure 25, along with locus C-C' from the Miller-Fejer [100] experiments. Parameter ranges for the former results are $0.014 < N_A < 0.29$, $4.5 < f < 62$ Hz ($28 < \omega < 390$ rad/s) and $50 < U_0 < 115$ ft/s ($15 < U_0 < 35$ m/s). The wind tunnel freestream disturbances are described as having an amplitude of "approximately 0.2 percent" (based on the streamwise component of disturbance velocity with the spectrum unspecified) which probably included acoustic contributions. Note the radical differences between loci A-A' ($0.014 < N_A < 0.092$, $12.6 < f < 62$ Hz) and B-B' ($0.039 < N_A < 0.27$, $4.5 < f < 14.7$ Hz), which are both for zero mean pressure gradients. The visual distinction in transition occurrences for the data of locus B-B' was that turbulent ribbons appeared close to the location of the velocity minimum in essentially every cycle (i.e., periodically) with the turbulent formations being exceptionally regular and uniform for nonsteady Reynolds numbers, $Re_{ns} = [U_0 \Delta U / \omega \nu]$, greater than 40,000. In contrast, the appearance of turbulent patches for locus A-A' was usually delayed and more irregular ("aperiodic"). For the latter case, the length Reynolds number of transition onset was approximately constant at 1.6×10^6 , being somewhat less than the steady flow transition Reynolds number expected for their disturbance environment.

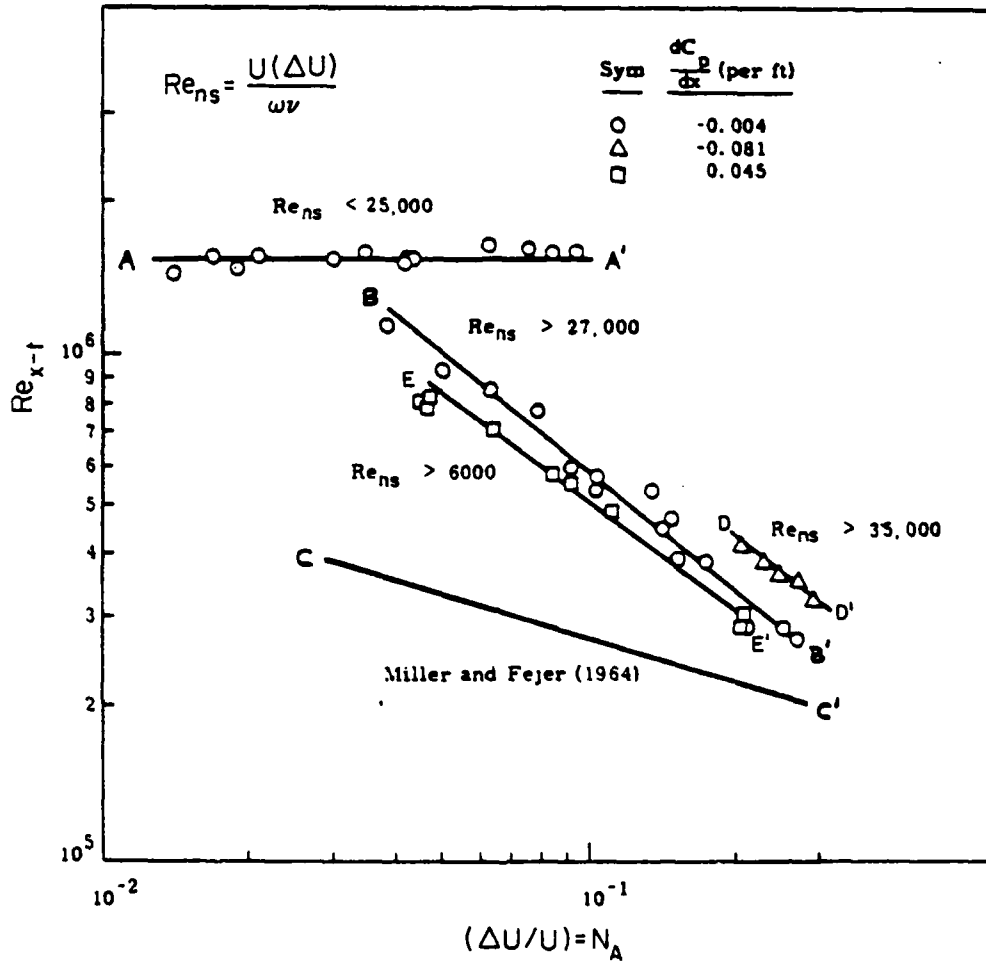
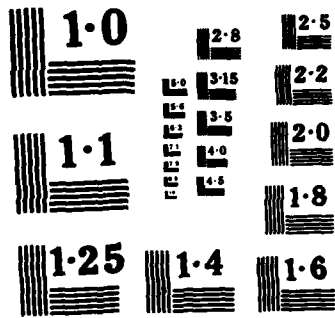


Figure 25. Transition Reynolds number as function of amplitude and mean pressure gradient in periodically unsteady boundary layer flows. [99]

Obremski and Fejer [100] attributed this discontinuous variation to the differences in nonsteady Reynolds number ranges for the data. Later, however, Obremski and Morkovin [105] suggested and Loehrke, Morkovin, and Fejer [9] substantiated that the more fundamental underlying reason for the shift to locus B-B' was a "wider opening of the 'pulsating gate' to instability" corresponding to a larger β/ω ratio in the quasisteady regime ($\beta/\omega > 10$). Thus, according to [105], those instabilities that exceeded the "turbulent threshold" in the decelerating (more unstable) portion of the first cycle were expected to correlate along the periodic transition locus, B-B'. Whereas, locus A-A' corresponded to those instabilities which did not exceed the breakdown threshold during the first cycle and were dampened by the acceleration portion of the cycle, as well as the red-shift in amplification bandwidth with increasing Reynolds number (note the variation of amplified frequencies with Reynolds number in the Saric-Nayfeh stability curves). As reported by Loehrke, Morkovin, and Fejer [9] demonstrated that the Re_{ns} shift point between the two curves was not unique, since it also depended on the disturbance environment. They were able to produce "first-cycle" transition at a nonsteady Reynolds number of 7500 by artificially stimulating the initial boundary layer instabilities.

From Figure 25, it is also obvious that imposed mean pressure gradients have qualitatively the expected effects on "quasisteady" transition. For both D-D' ($0.21 \leq N_A \leq 0.29$, f in the range of 12 Hz) and E-E' ($0.04 \leq N_A \leq 0.21$, $4.5 \leq f \leq 37$ Hz) the observed transitions were periodic [99]. Loehrke, Morkovin, and Fejer [9] have indicated that such results are expected from theoretical considerations, since ". . . functionally, the amplification rates remain dependent primarily on the mean flow parameters, at least for



NATIONAL BUREAU OF STANDARDS
MICROCOPY RESOLUTION TEST CHART

small and moderate oscillatory amplitudes." Therefore, it is reasonable to anticipate that the effect of heat transfer on "quasisteady" transition would be qualitatively similar to its effects on steady transition.

Apparently, the further skewed locus C-C' resulted from the two separate "bypass" mechanisms of periodic leading edge separation and periodic static pressure tap venting in response to the oscillating pressure gradients [9, 99]. Otherwise, the flow conditions from which this zero mean pressure gradient data of Miller and Fejer [100] was obtained were nearly identical to those in the Obremski-Fejer experiments.

Concerning parameters for correlating transition onset in unsteady boundary layers, it is already evident that a partial list would include the steady flow parameters, such as Reynolds number and some measure of pressure gradient to describe the mean flow conditions. In addition, the unsteady flow parameters of amplitude, N_A , and nonsteady Reynolds number, Re_{ns} , would be required, as well as an appropriate description of the disturbance environment. Loehrke, Morkovin, and Fejer [9] note that Re_{ns} appears explicitly in the equations for a quasi-steady normal modes amplification analysis based on linearized theory, but that other independent parameters also appear. They suggest that Re_{ns} provides a qualitative parameter link for the effects of N_A and the length of the unstable half-cycle $U_o/2f$. Nevertheless, even for a zero mean pressure gradient, it incorporated aspects of three separate effects as shown in Figure 26. In this parametric plot, X_w [$= X_w/U_o$] describes the unsteady boundary layer (Stokes) thickness to mean boundary layer (Blasius) thickness in the functional form

$$\delta_{Stokes} / \delta_{Blasius} = \text{const} / \sqrt{x_w / U_o} \quad (10)$$

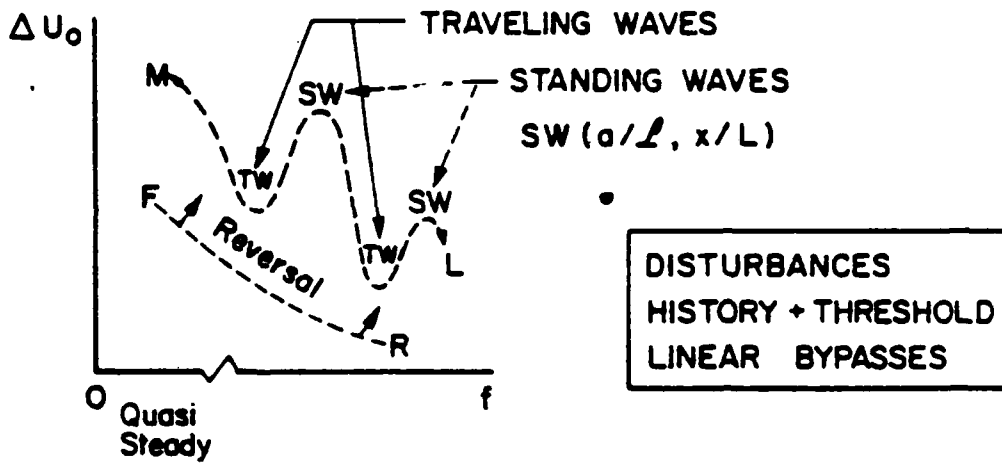
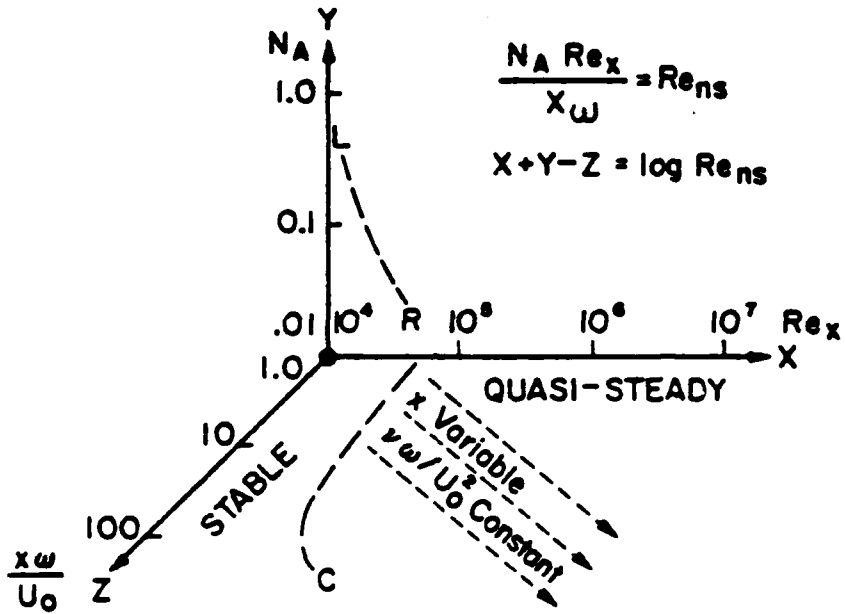


Figure 26. Overview of flow and instability regimes expected in the presence of zero mean pressure gradient flow oscillations. [9]

Based upon their information, the authors [9] anticipated that the critical range for this parameter would be approximately $(1-2) < X_w < (25-30)$. The lower limit represented boundary layers whose stability characteristics are either essentially uninfluenced by unsteadiness (ω small), or flow lengths so short that stability could be expected. The upper limit was chosen based on the assumption of a smooth flow surface and the discovery [106] that the quasisteady boundary layer stability characteristics are insensitive to velocity profile changes which occur suitably close to the wall. These expectations for the variation in stability limits are reflected in the curving of the dashed line marked "C" in the upper part of Figure 26. The dashed curve L-R denotes the expectation of increasing destabilization in the quasisteady regime for larger unsteady component amplitudes. In connection with this, the authors [9] emphasize that ΔU_0 is strongly dependent on the amount of pressure wave (acoustic) resonance which may develop in a closed flow structure, making the speed of sound, a , and any number of resonance lengths, L , important. At higher frequencies, for which the wavelength of the pressure wave is equal to or less than the flow surface length, L , standing waves may have a strong influence. These aspects are denoted in lower Figure 26. Also, in lower Figure 26, the curve M-L indicates "mechanical limitations," which result in generally decreasing unsteadiness amplitude for increasing frequency. Finally, the possible occurrence of periodic flow reversal at the wall for the combination of large f and ΔU_0 is depicted schematically by the curve marked F-R and the arrows extending from it. The influence of flow reversal on either transition or separation of the mean flow is essentially unexplored, although it is expected that roughness and surface nonuniformity would cause earlier

transition as this condition is approached [9]. However, experimental investigations of the possible bypasses resulting from roughness or high-level freestream disturbances (turbulence) are lacking.

Therefore, the limits on instability caused by unsteadiness as defined in Loehrke, Morkovin, and Fejer [9] are expected to be bounded by an imaginary curved surface passing through the N_A - Re_x plane along "L-R" and cutting the X_w - Re_x plane along "C." Note, though, that these tentative schematic limits are only applicable to zero mean pressure gradient unsteady flows without bypasses or cross-flows. The question of what influence combined unsteadiness and streamwise vorticity have on instability and transition is still open.

Miller and Fejer [100] were able to correlate the transition length for their Blasius mean oscillating flows in terms of the viscously nondimensionalized flow oscillation frequency. The functional form of the relation was

$$\frac{Re_T - Re_t}{Re_t} = f(\omega v / U_0^2) \quad (11)$$

in which Re_t and Re_T are the flow length Reynolds numbers for transition onset and transition completion, respectively. As mentioned earlier, though, transitions in their experiments were bypass-dominated. A preliminary check of the data of Obremski and Fejer [99] produced no similar correspondence.

Apparently, no data yet exists in open literature for intermittency distribution in nonbypass quasisteady transition. Although, judging by the increasing periodicity and uniformity of the turbulent ribbons for increasing ΔU_0 and β/ω , one could speculate that the distribution becomes more linear. Whereas, by comparison, the "irregular" appearance of turbulent spots in

steady flows seems to be correlated well in a Gaussian integral intermittency distribution.

Pfeil, Herbst, and Schröder [104] documented their more recent investigations of unsteady flow transition in a nominally zero pressure gradient boundary layer. As opposed to the previously discussed experiments, the boundary layer on their flat plate was disturbed by cross-flow wakes from the cylinders inserted around the circumference of a rotating cage. For these investigations, the circumferential cage speed (12.6 m/s) and wind tunnel speed (20 m/s) were maintained constant while wake passage frequency was varied by changing the number of cylinders in the cage.

Pfeil, Herbst, and Schröder [104] found that the cylinder wakes periodically forced transition onset at the passage frequency. The initiation of this forced transition occurred significantly upstream of the location of random turbulent bursts in undisturbed flow, but downstream of the marginal stability location. At the lowest passage frequencies, the combination of the large time spacing between the forced turbulent regions and the subsequent becalmed laminar flow following these regions resulted in a transition length extending further downstream than that for the undisturbed flow. The appearance and growth of random turbulence bursts was also noted interspersed between the periodic forced turbulence. Although the onset location remained constant, the transition length decreased with increasing wake passage frequency until the closeness of the periodic turbulence regions precluded the formation of random turbulent bursts. Further frequency increases resulted in wake merge until the transition length tended to zero.

Experiments in a mildly favorable pressure gradient produced even more dramatic results, apparently forcing transition in a laminar boundary layer

which was linearly stable to T-S disturbances. However, in all cases, the authors were unsure of the role of either the stochastic or the periodic wake velocity fluctuations in producing transition. Also, the nature of the experiments elicits questions about the possibility of periodic flow separation on the sharp leading edge of their plate.

VII. PREDICTING TRANSITION

From Morkovin's reviews [2, 3] and his consolidated schematic of the transition processes, a checklist may be established of the physical phenomena that transition prediction methods must deal with in order to be generally applicable. This list is as follows:

- (1) Disturbance environment - character and spectrum
- (2) Receptivity
- (3) Linear amplification processes
- (4) Three-dimensional, nonlinear growth and secondary instability development
- (5) Localized breakdowns into turbulence
- (6) Growth and coalescence of turbulent regions to form fully turbulent flow

Beside these items, a physically sound method must be able to handle bypasses, resulting from the rapid forced nonlinear response of the boundary layer to high intensity disturbances, large distributed roughness, and flow separations.

To date, the only facet of the instability-transition process that has been extensively and effectively modeled is linear amplification. As for the other items on the list, there are formidable experimental and theoretical difficulties in ascertaining, quantifying, and modeling these features of the flow, even in the simplest cases. In order not to ignore the achievements of

some of the turbulence models, it can be said that they may eventually be able to provide some useful results in bypass transitions (e.g., see [107]). However, this, of necessity, must be accomplished through simplified, semi-empirical models for the effects of the boundary layer disturbers. Otherwise, our ability to quantify transition rests on empirical data from judiciously planned and executed experiments that model the salient features of the flow. Even then, a consistently thorough approach inspiring confidence in the results dictates that any anticipated contingencies to which the outcome may be sensitive (surface roughness and cross-flows) must be introduced as "spoiling" features to those carefully planned experiments [9]. Nevertheless, because of the singular nature of transition, most of this data will be pertinent only for a specific application or for testing the abilities of empirically embellished theoretical methods as they are developed.

7.1 Linear Theory Approaches

Methods of transition "prediction" employing damping/amplification rate information from linear stability theories obtained their most substantial start in the works of Smith [89, 108] and Van Ingen [109]. Primarily, the concept originated from Liepmann [87], who proposed that transition occurs when the Reynolds stress in the boundary layer becomes of the same order of magnitude as the laminar viscous stress. He suggested, as a practical approach, that this location could be approximated adequately by computing instability amplification until the oscillation is sufficiently strong to alter the mean flow. Therefore, it may be deduced that any usefulness of such methods is conditional to the leading contributions of linear instability damping and amplification mechanisms which sometimes precede the nonlinear

stages and breakdown in occurrences of transition. Strictly speaking, though, even if the assumptions used in linearizing the perturbation equations are appropriate, they account rationally only for item 3 on the checklist in the preceding section.

The benefits of linear theory methods stem from the fact that they are based on linearized approximations of exact solutions to the Navier-Stokes equations. Thus, they provide a unified means for incorporating the influence of some boundary layer modifiers, such as steady [110] and (by further assumptions) quasisteady [9, 106] pressure gradients and wall normal temperature gradients on the T-S instability development. The linearity of the methods makes easier their extension to compressible boundary layers with oblique (three-dimensional) T-S waves (see Mack's review in Chapter 15 of Schlichting [5]). Mack [14] expounds on the various approaches for T-S type disturbances in steady, incompressible "quasiparallel" boundary layer flows including the differences between, the suitability of, and the difficulties with, spatial and temporal amplification assumptions. Also, he outlines his own thoughtful approach for including the effects of the freestream disturbance spectra and orientations.

Since Görtler vortices are, in the initial development stage in a low disturbance environment, a linear instability mechanism, analogous approaches have been applied [89], which can include steady pressure gradients [16] and temperature gradients. It may be said that this is probably the only viable method now available for estimating the strength of the vortices and therefore the nearness to transition in nonsimilar boundary layers over surfaces of varying curvature. Nevertheless, it cannot be used to predict, in advance the vortex wavelength, which in turn determines the influence of varying

streamline curvature and boundary layer modifiers, such as pressure gradients. This shortcoming can be circumvented somewhat by assuming the worst case and computing the strength of the most amplified wavelength as suggested by Smith [89].

For the aforementioned reasons and lack of a better approach, the linear theory based methods have been applied, primarily for low freestream disturbance environments, in calculating the assumed linear growth of boundary layer disturbances to some amplitude presumed to be indicative of incipient breakdown. However, beside the obvious fact that linear theories cannot account for nonlinear developments, such methods have other intrinsic weaknesses. One is that they are dependent on the suitability of the assumptions made in the linear theory from which the damping-amplification rate information is obtained. For boundary layers with pressure gradients, especially nonsimilar flows, this information from any of the linear theories apparently is quantitatively unverified [9]. Secondly, the quasiparallel theories, in particular, are expected to be in error near the marginal stability location, since the spatial boundary layer growth rate is greater than the spatial instability growth rate, violating the assumption of locally parallel flow [9]. Although the quasiparallel approximation seems to be acceptable for T-S type disturbances in negative and zero pressure gradient flows [1], the more rapid boundary layer growth in decelerating flows leads to increasing error as the pressure gradient becomes more positive. This may, in part, explain the error in the Smith-Van Ingen " e^n " method as applied to the T-S instability in flows with adverse pressure gradients [111]. Furthermore, Donaldson [112] has indicated that the results from linear T-S stability theory may be inaccurate for boundary layers with large favorable pressure gradients. He suggested

that the stream tube stretching tends to increase the relative magnitude of the boundary layer disturbance components normal to the streamwise direction, offsetting the stabilization afforded by a more full velocity profile. A third shortcoming of linear theory approaches is that, as mentioned earlier, they do not within themselves, account for the disturbance environment effects on the boundary layer response. As Reshotko [1] points out, linear stability theory is a problem dealing in homogeneous equations and boundary conditions, whereas with the addition of receptivity considerations, either or both are nonhomogeneous. Thus, the inclusion of freestream disturbance effects has necessitated empiricisms which, with the exception of a few approaches such as Mack's [14], are usually applied as though all freestream disturbances were alike in the spectral and orientational distribution of their energy. Finally, if the total disturbance environment, including wall vibrations, has sufficient energy to cause three-dimensional, nonlinear distortion and possible driving of the initial boundary layer instability, the region of action of amplification mechanisms identified by linear theory will be shortened severely. At very high disturbance levels, it may even be eliminated (a bypass), thereby nullifying the reasons for any applicability of the methods. Also, the linear theory predictions are threatened whenever wall roughness, flow irregularities, or cross-flows cause deviation from the presumed two-dimensional laminar velocity profiles, particularly with the T-S type instability.

7.2 Turbulence Models

Reynolds [113] reviews the hydrodynamic aspects of partial differential equation turbulence models and some of their limitation in application to

turbulent flows. He classifies them in order of increasing complexity and generality, as follows:

- (1) Zero-equation models - Models using the partial differential equations describing only the mean velocity field.
- (2) One-equation models - Models including additional partial differential equations for the turbulence velocity scale.
- (3) Two-equation models - Models with the equations of (2) plus additional partial differential equations for describing the turbulence length scale.
- (4) Stress-equation models - Models incorporating partial differential equations for all nonzero components of the turbulent stress tensor.
- (5) Large-eddy simulations - Models of the three-dimensional, time-dependent, large-eddy structure that include a low-level model for the small-scale turbulence.

The turbulence models most commonly used for engineering applications (1, 2 and very recently 3 and 4) require a variety of empiricisms if one intends to apply them only to fully turbulent boundary layer flows. When they are extended for "general" computations of all three flow regimes, the degree of empiricism increases greatly. In the transition regime, the results are an attempt to describe an averaged flow condition for the purposes of providing an acceptable evaluation of heat transfer and skin friction variation. No attempt is made at describing the physics of the intermittency development. The transition regime is simply and smoothly bridged over an "appropriate" range of Reynolds numbers. For the zero-equation models (e.g., Forest [114]), simplicity usually dictates the use of overall empirical data for transition onset, completion, and intermittency distribution. Multiequation models

(e.g., the mixed partial differential-integral equation approach of McDonald and Fish [115]) usually provide for gradual activation of turbulence production terms through the inclusion of simple smaller scale models for the effects of freestream turbulence and surface roughness. To preclude misconceptions, it must be understood that these multiequation models do not describe the physics of receptivity phenomena in producing laminar boundary layer instability, nor do they model the subsequent unsteady instability developments. Wilcox [116], however, has a notable approach that synthesizes linear stability theory and a two-equation model.

As could be suspected, turbulence model transition predictions are substantially limited by the generality of their empirical data base. Their function, primarily, is one of mimicking the data, with the understandable result that transition evaluations are somewhat ad hoc.

Daniels and Browne [117] compare some presently available examples of the first three types of models, all of which have been adapted for general boundary layer computations. Their experimental data was obtained from a model turbine cascade in a compressible flow, transient operation wind tunnel. It was representative of actual gas turbine conditions in Mach number, Reynolds number, and wall-to-freestream temperature ratio, but not in freestream turbulence level (or its make-up), which was 4 percent or less. None of the model's transition predictions agreed impressively with the data for the higher chord Reynolds numbers, particularly for the concavely curved pressure surface. Presumably, this was attributable to the presence of Görtler vortices and the lack of flow deceleration past about 10 percent of chord on the pressure surface.

7.3 Empirical Correlations

Since correct modeling of the physics of the instability-transition process is presently and may perhaps always be an unattainable goal, estimates for the transition location are often derived either from ad hoc data or "generic" empirical correlations. The focus of most of the correlations has been on major transition influencers, such as freestream turbulence and pressure gradients, and their effects in flat plate transitions. Parametric correlations also have been devised for the effects of distributed roughness (see Tani [12] and Morkovin [3]) and attempted for the effects of heat transfer. However, the former are not explicitly considered in this report because of its limited scope in the available literature, and any of the latter are not prominent. With the exception of curve fits [114, 118] based primarily on Liepmann's [57, 87] data, quantitative information on transition preceded by Görtler vortices is also sparse. Similarly, the most significant data on transition in unsteady flows is that reviewed by Loehrke, Morkovin, and Fejer [9], although there undoubtedly is ongoing research on both of these latter topics.

Quantitatively, the indications of the correlations for pressure gradient and freestream turbulence effects on flat plate transitions vary, especially at high and low turbulence levels and for large favorable pressure gradients. Much of the disagreement at low turbulence levels (below about 0.5 percent) can be ascribed to the differences in spectral distribution of disturbance energy in the various experimental environments. Also, some of the differences are attributable to the variety of techniques used to detect transition. Among these are hotwire transverses, Pitot tube surveys near the wall, surface thin film measurements (heat transfer), and visual information

from Schlieren photographs. Harris [119] and Hall and Gibbings [111] note that the sensitivity of these methods vary, and each detects a different aspect of the flow process. Consequently, each can provide a different indication of the location of transition onset or completion, even in the same boundary layer. Probably, though, most of the overall differences are due to the very nature of the transition process itself, and its sensitivity to many influences. Hall and Gibbings [111] observed, "These experimental difficulties result in an undesirably large degree of scatter in the results, even when collected on a single apparatus. This makes prediction an uncertain matter under accurately specified flow conditions, and the use of results from one system for prediction on another reduces accuracy even further."

Besides the difficulties in modeling transitional flows and obtaining suitable transition data, there is the problem of selecting or determining measurable and calculatable parameters that are sufficiently strong, general, and unambiguous reflections of the various effects to be correlated. Nonsimilar, nonadiabatic boundary layers are especially a problem, since transition is nonlinearly dependent on the unique cumulative effect (history) of the boundary layer modifiers, receptivity and amplification mechanisms, and the stochastic disturbances. The result is that local boundary layer parameters are usually inadequate, except for use in ad hoc correlations.

Of the empirical correlations in published literature, the most tenable in accounting for freestream turbulence and pressure gradient effects on transition onset seem to be those of Van Driest and Blumer [120], Seyb (see [121, 122, 123]), and Abu-Ghannam and Shaw [48]. Brown and Martin [118, 121, 122, 124] and Brown and Burton [123] favor the use of the Seyb correlation for transition onset estimation on their model cascade turbine blade suction

surfaces, although they acknowledge [125] that it is unconfirmed for large favorable pressure gradients and high freestream turbulence levels. Blair [126] obtained good agreement with the correlation of Van Driest and Blumer [120] and the data of Abu-Ghannam and Shaw [48] in his experimental Blasius and laminar sink-flow boundary layers. The other well-known correlations of Hall and Gibbings [111] and Dunham [56] have not worked well when applied to favorable pressure gradient flows [122, 126]. Both of these incorrectly predicted rapid increases in the transition onset momentum thickness Reynolds number for increased strength of favorable pressure gradients (based on the momentum thickness Pohlhausen parameter).

Since the work of Emmons [37] in which the random appearance of turbulent "spots" was noted and their growth analyzed, various attempts have been made at defining a transition region intermittency distribution function to account for the apparent statistical similarity of turbulent spot formation and growth in many transitions (e.g., [8, 31, 48, 127]). Dhawan and Narasimha [8] found that a normally distributed turbulence source-rate function with standard deviation approaching zero and maximum at the location of transition onset, combined with the a posteriori spot growth theory of Emmons, described their zero pressure gradient intermittency data. Preliminary comparisons with data obtained from nonzero pressure gradient boundary layers indicated that this distribution would match the data, except near transition onset. Intermittency data obtained by Owen [128] in zero pressure gradient boundary layers, and Sharma, et al., [129] and Debruge [130] in adverse pressure gradients (the Debruge data was taken from the suction surface of a model turbine blade in cascade) agreed well with the Dhawan-Narasimha intermittency distribution. Chen and Thyson [127] utilized a more general approach

applicable to flow over axisymmetric bodies at a zero angle of attack, and also suggested that their approach might be useful in three-dimensional flows. Their more general expression reduced to the form of that of Dhawan and Narasimha for the flat plate case. Lessmann [131] proposed a more fundamental approach, which utilized the boundary layer equations of motion.

Empirical correlations for the transition length as a function of the start of transition have been proposed by Dhawan and Narasimha [8] for flows over flat plates, by Debruge [130] for flows over the suction surface of a model turbine blade in cascade, and by Chen and Thyson [127]. The latter correlation included the effects of Mach number for adiabatic flows, although in the subsonic regime the correction fell approximately within the experimental scatter. All of these are essentially of the same form and the scatter of experimental data around them is substantial, even for zero pressure gradient data (see [122, 123]).

7.4 Abu-Ghannum and Shaw's Correlation

The correlations acknowledged in the preceding paragraphs are those that figure prominently in published literature. They were mentioned primarily to provide a vehicle for outlining supporting or vitiating information. However, the only correlations which will be given in this report are those of Abu-Ghannam and Shaw [48]. These represent both the latest and, in the opinion of the authors of this report, most comprehensive attempts to account for the effects of freestream turbulence and pressure gradients on transition and to correlate the statistically averaged variation of integral flow properties during transition. In application, they will probably be as useful as any of the other empirical correlations which are for low-speed adiabatic two-dimensional boundary layers over smooth surfaces.

The experimental data on which the correlations of Abu-Ghannam and Shaw [48] are based was obtained from a low-speed, ambient temperature wind tunnel. Turbulence, which ranged from about 0.5 to 5 percent at the test surface leading edge, was generated by various grids placed far enough upstream to insure that the disturbances were homogeneous and isotropic at the entrance to the test section. The relative influence of turbulence length scale on the experimental data was determined to be negligible. Following the suggestion of Dunham [56], the turbulence levels used in the correlations were the average of the values at the leading edge and the point under consideration. (Here, it is worth reemphasizing that transition is dependent on the cumulative effect of disturbances. Not only do viscous dissipation and acceleration or deceleration change its relative level, but they also tend to make it anisotropic [5].) Pressure gradient distributions were "typical" of those on gas turbine blades without flow separation, and were adjusted by changing the contour of the tunnel wall opposite the test plate. The actual test plate was flat aluminum with a smooth surface and a rounded leading edge. (Note here that the introduction of a definite leading edge stagnation region can render the boundary layer less stable than one beginning on a sharp edge [37]). Hot wire anemometry, supplemented by a boundary layer Pitot probe, was used in detecting transition onset and completion. Measurements were made by placing the transducer close to the surface and increasing the tunnel wind speed until the appropriate part of the transition region coincided with it or moving the transducer.

Transition onset in the zero pressure gradient boundary layer at various turbulence levels was found to be represented well by the relation

$$Re_{\theta-t} = 163 + \exp(6.91 - \tau) \quad (12)$$

as shown in Figure 27. In equation (12), τ is the freestream turbulence level in percent. The asymptotic high turbulence value of $Re_{\theta} = 163$ was chosen to agree with the Blasius flow minimum critical Reynolds number calculated by Tollmien and Schlichting. Recall, however, that this value has been revised to be 200 by Jordinson for parallel stability and 154 by Saric and Nayfeh for nonparallel stability. Therefore, it has no particular significance except that it seems to fit the data. The transition end in the zero pressure gradient case was fairly well represented by

$$Re_{\theta-T} = 2.667 Re_{\theta-t} \quad (13)$$

As can be seen in Figure 27, there is more scatter in the data for transition completion than for transition onset.

A modification of the correlation for $Re_{\theta-t}$ to include the effects of pressure gradients produced

$$Re_{\theta-t} = 163 + \exp \{F (1 - \tau/6.91)\} \quad (14)$$

$$F(\lambda_{\theta}) = \begin{cases} 6.91 + 12.75 \lambda_{\theta} + 63.34 \lambda_{\theta}^2 & (\lambda_{\theta} < 0) \\ 6.91 + 2.48 \lambda_{\theta} - 12.27 \lambda_{\theta}^2 & (\lambda_{\theta} > 0) \end{cases} \quad (15)$$

These functions are plotted in Figure 28, along with the experimental data of Abu-Ghannam and Shaw and other investigators. At low turbulence levels, the curves accord qualitatively with Liepmann's [87] observation that the greatest changes in $Re_{\theta-t}$ occur for small changes in λ_{θ} about zero. There is a noticeable lack of data points at high turbulence levels and large adverse pressure

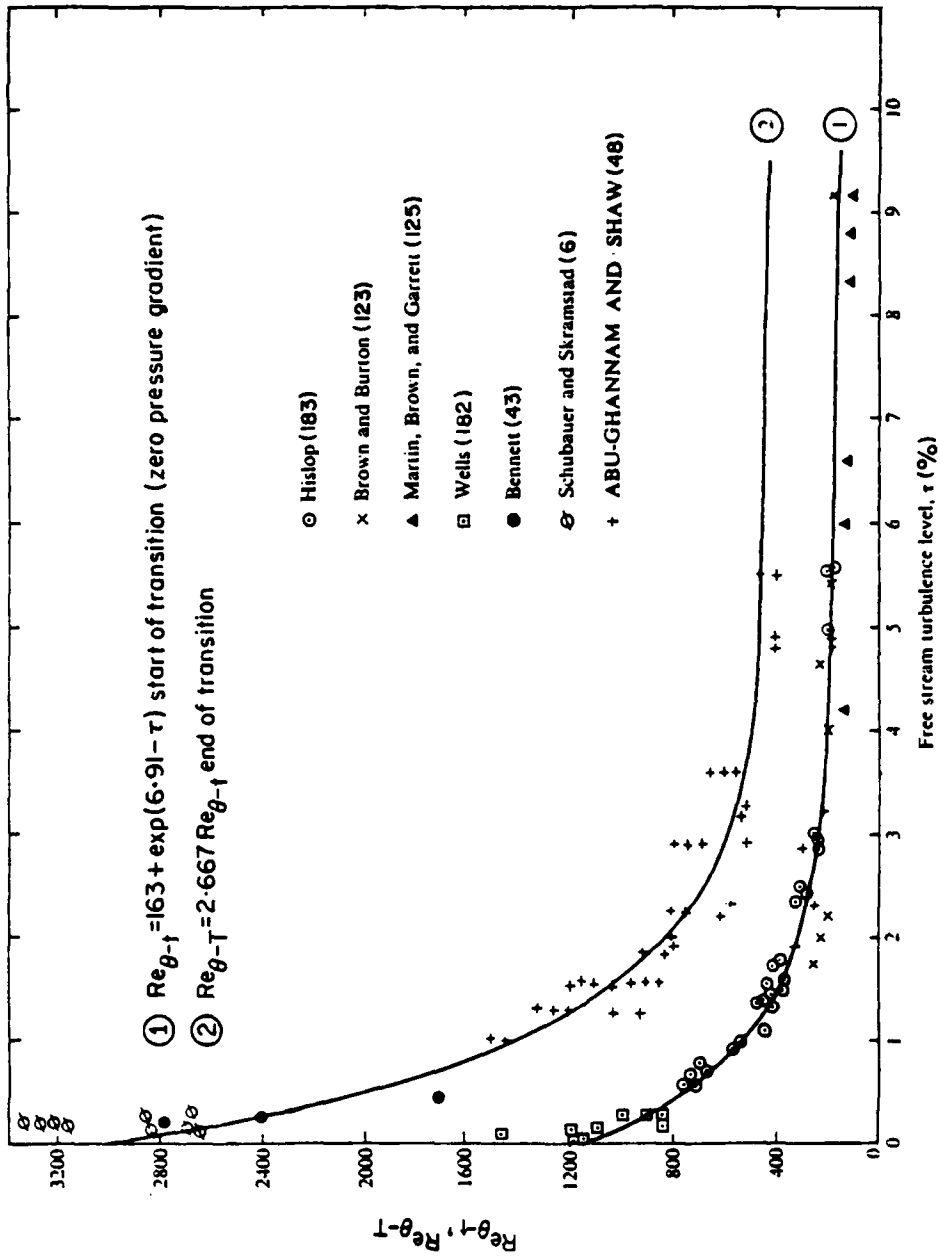


Figure 27. Effect of freestream turbulence level on the momentum thickness Reynolds numbers for transition onset and completion. [48]

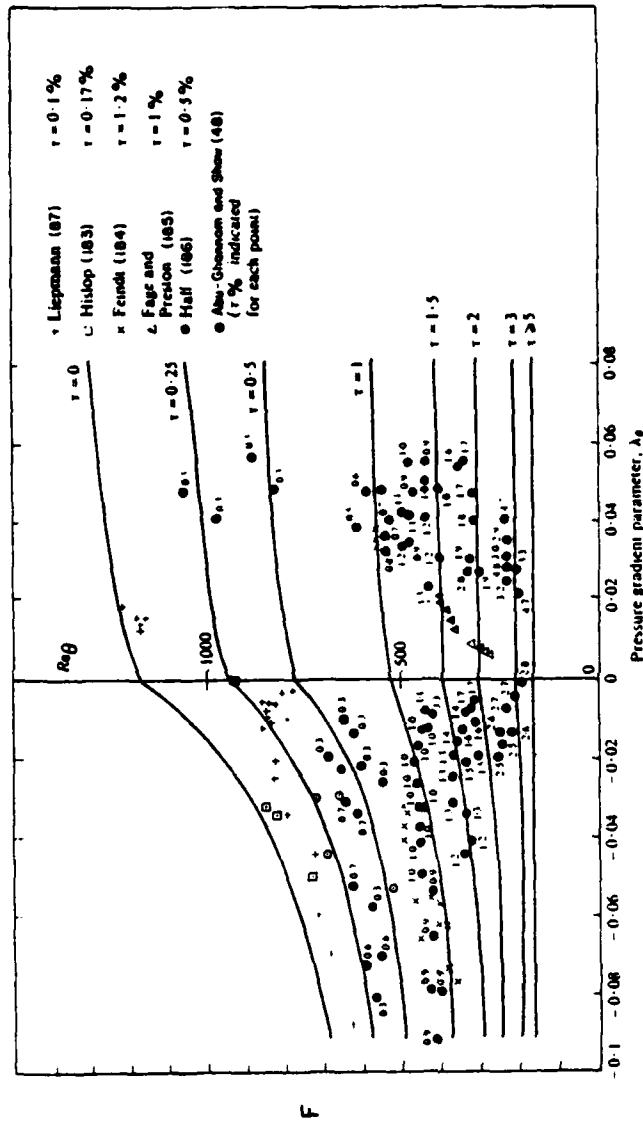


Figure 28. Influence of freestream turbulence level and pressure gradient on the transition onset momentum thickness Reynolds number. [48]

gradients because of the rapid occurrence and completion of transition. Also, for low turbulence levels and large favorable pressure gradients the data points were few and scattered because the flow tended to remain laminar over the full length of the plate. $Re_{\theta-t} = 163$ was ascribed as the lower limit for transition onset, regardless of pressure gradient. Keep in mind, though, that favorable pressure gradients inhibit boundary layer growth (in very strong favorable pressure gradients the momentum thickness Reynolds number can actually decrease [132]), while adverse pressure gradients promote it. Thus, the flow must travel further in a favorable pressure gradient than in an adverse pressure gradient to achieve the same momentum thickness Reynolds number.

The pressure coefficient distributions for the flows from which this data was taken are shown as the first favorable and first adverse gradients in Figure 29. Pressure gradient histories were relatively unimportant because an extreme value of λ_{θ} corresponded to $Re_{\theta-t}$.

Correlation of the transition length was accomplished through a modification of Dhawan and Narasimha's [8] relation for zero pressure gradient boundary layers. The results, which are shown in Figure 30, were

$$R_L = 16.8 (Re_{x-t})^{0.8} \quad (16)$$

$$R_L = Re_{x-T} - Re_{x-t} \quad (17)$$

$$Re_{x-T} = \frac{X_T U_{\infty t}}{\nu}, \quad Re_{x-t} = \frac{X_t U_{\infty t}}{\nu} \quad (18)$$

and applied to both zero and nonzero pressure gradients.

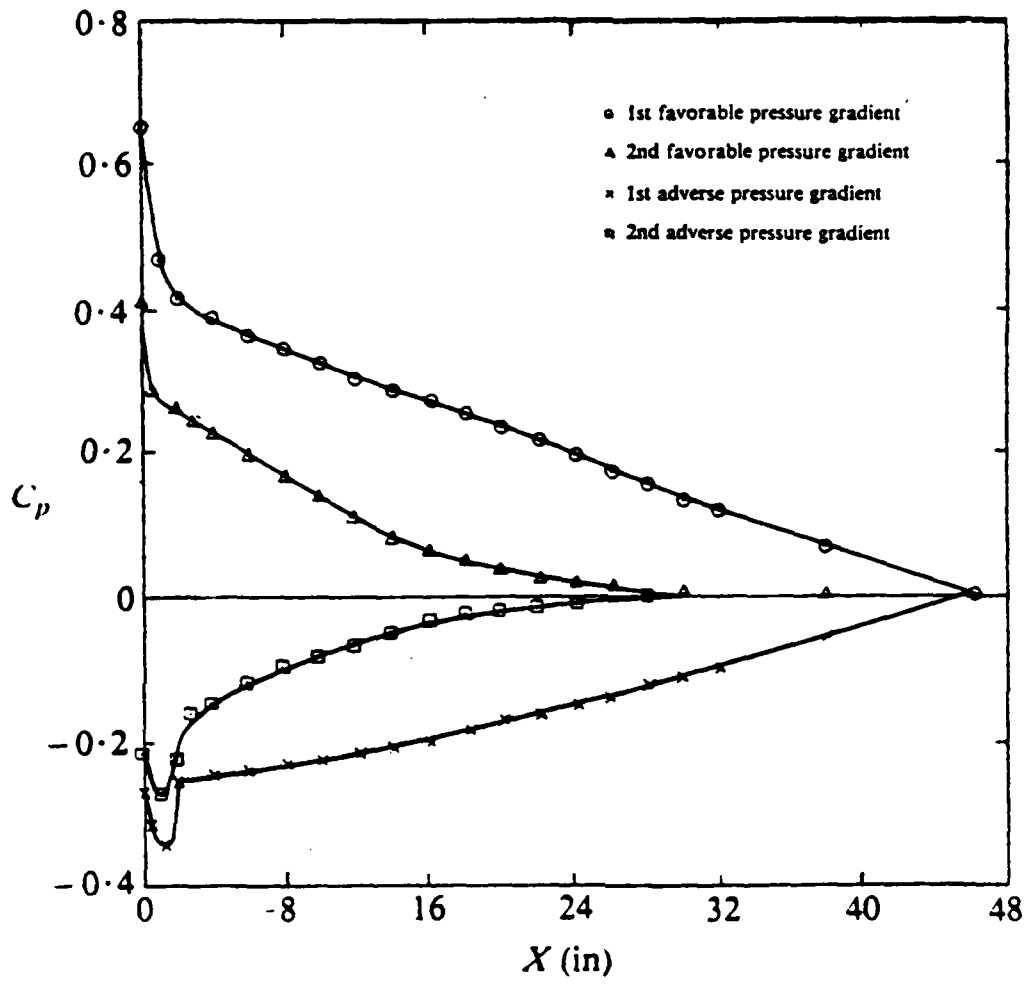


Figure 29. Pressure distributions for the Abu-Ghannam and Shaw experiments.
[48]

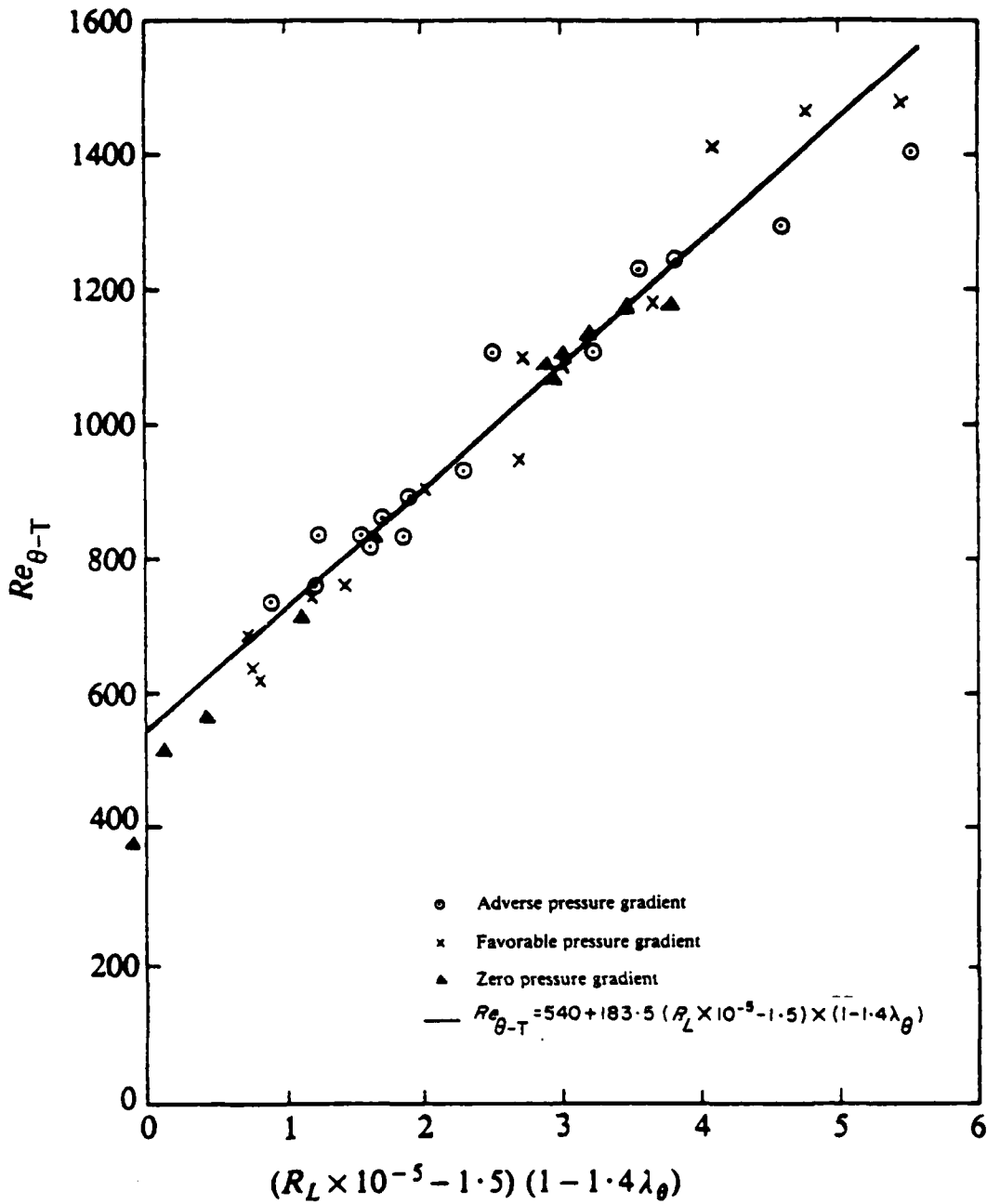


Figure 30. Relation between length Reynolds numbers for onset and completion of transition. [48]

The momentum thickness Reynolds number for the end of transition was fitted functionally as

$$Re_{\theta-T} = 540 + 183.5 (R_L \times 10^{-5} - 1.5)(1 - 1.4 \lambda_{\theta}) \quad (19)$$

which can be solved as a quadratic in θ_T if x_t , x_T , $U_{\infty t}$, $U_{\infty T}$, and $(dU_{\infty}/dx)_T$ are known. In the relation, the constant, 1.5, reflects the fact that the authors found no influence of pressure gradient on transition extent at high (~ 5 percent) turbulence levels. Therefore, for R_L less than 1.5×10^5 the pressure gradient term is ignored. The quality of fit for this relationship is shown in Figure 31.

Another approach was required for correlating transition onset influenced by the second adverse (decreasing adverse) and second favorable (decreasing favorable) pressure gradient distributions shown in Figure 29. For these distributions, the use of a local or average value of λ_{θ} did not yield acceptable correlation. However, utilization of an extreme value of λ_{θ} (either greatest positive or greatest negative) in the relation for transition onset resulted in good agreement with the data. Flow histories for these pressure gradients were found to affect the length of the transition only indirectly, through their influence on the start of transition.

Transition Properties. Flow parameter distributions in the transition regime were correlated as function of the normalized dimensionless parameter η , defined by

$$\eta = \frac{Re_x - Re_{x_t}}{Re_{x_T} - Re_{x_t}} \quad (20)$$

In terms of this parameter, the expressions for momentum thickness and shape factor were

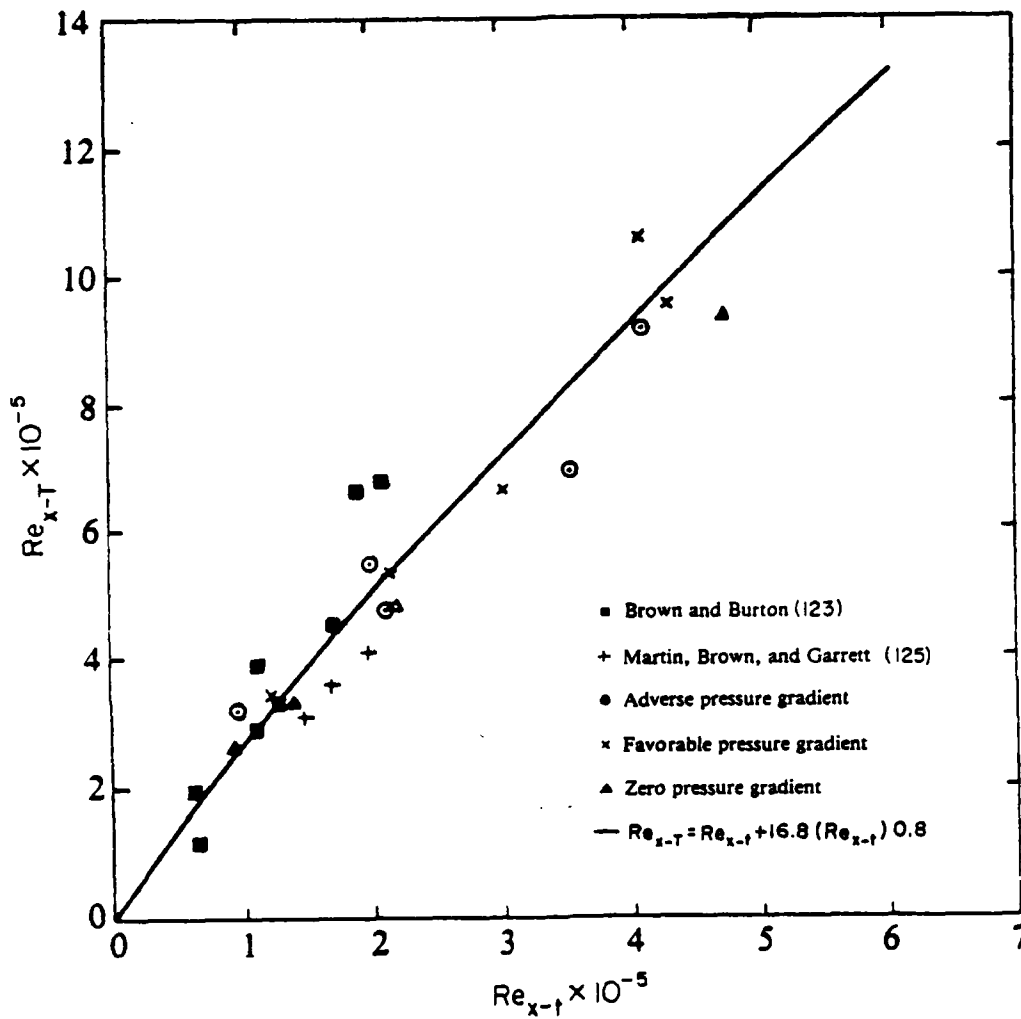


Figure 31. Influence of pressure gradient on transition completion momentum thickness Reynolds number. [48]

$$\theta' = \frac{\theta - \theta_t}{\theta_T - \theta_t} = n^{1.35} \quad (21)$$

$$H' = \frac{H_t - H}{H_t - H_t} = \sin \left(\frac{\pi}{2} \cdot n \right) \quad (22)$$

Plots of these are shown in Figures 32 and 33, respectively. Abu-Ghannum and Shaw [48] attributed the larger data scatter about the shape factor function to their inability to determine displacement thickness, δ^* , as accurately as the momentum thickness, θ .

Intermittency data for the various turbulence levels and pressure gradients was correlated by

$$\gamma = 1 - \exp(-5 n^3) \quad (23)$$

This function and the data are shown in Figure 34, along with the intermittency curves of Dhawan and Narasimha [8] and Schubauer and Klebanoff [31]. Abu-Ghannam and Shaw [48] suggested that the differences among the curves were partially because of the different sampling times used. Their sampling intervals were up to 5 seconds long, whereas the other investigators sampling intervals were around one-sixth of a second.

Employing a modification of another of Dhawan and Narasimha's [8] relationships, Abu-Ghannam and Shaw [48] expressed the normalized skin friction variation during transition as

$$C_f' = \frac{C_f - C_{f_t}}{C_{f_T} - C_{f_t}} = 1 - \exp(-5.645 n^2) \quad (24)$$

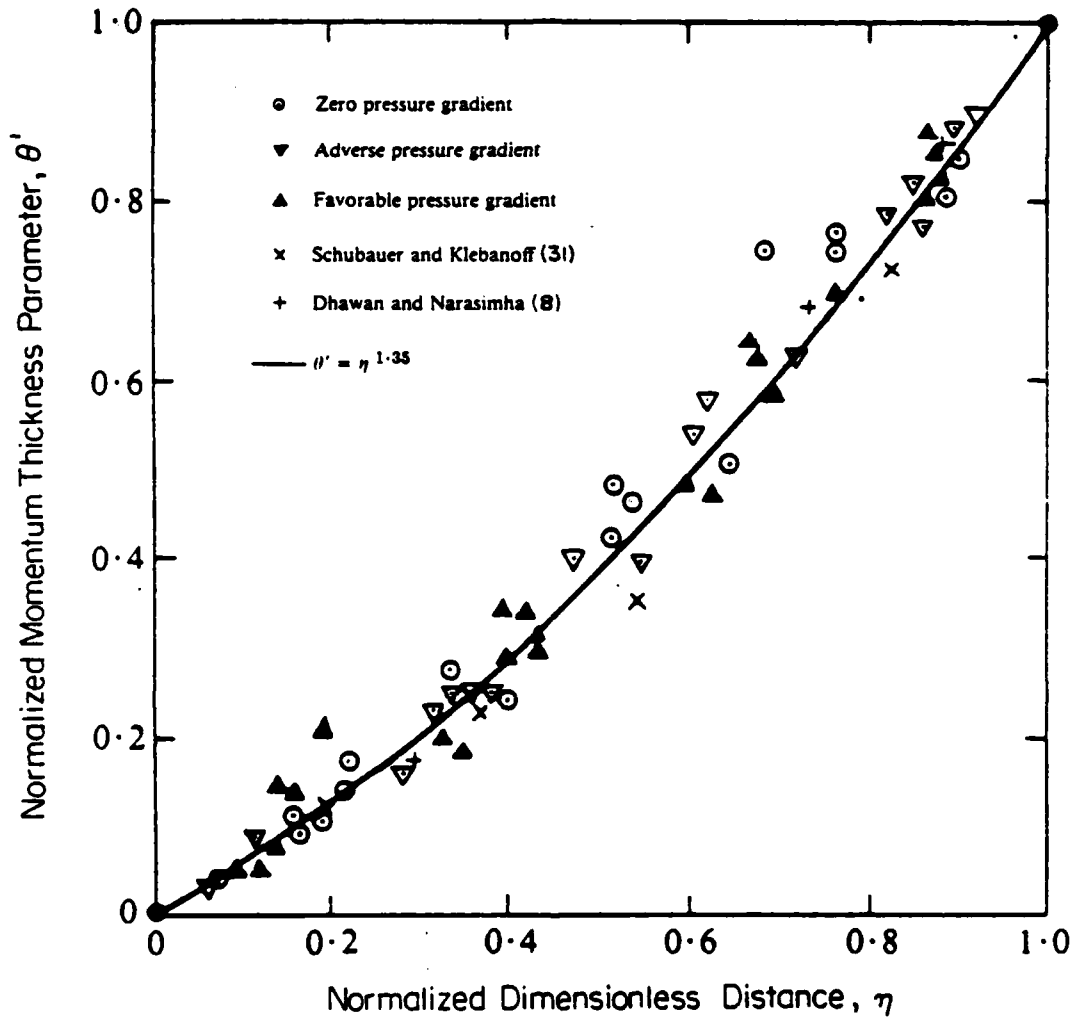


Figure 32. Distribution of the normalized momentum thickness parameter in the transition regime. [48]

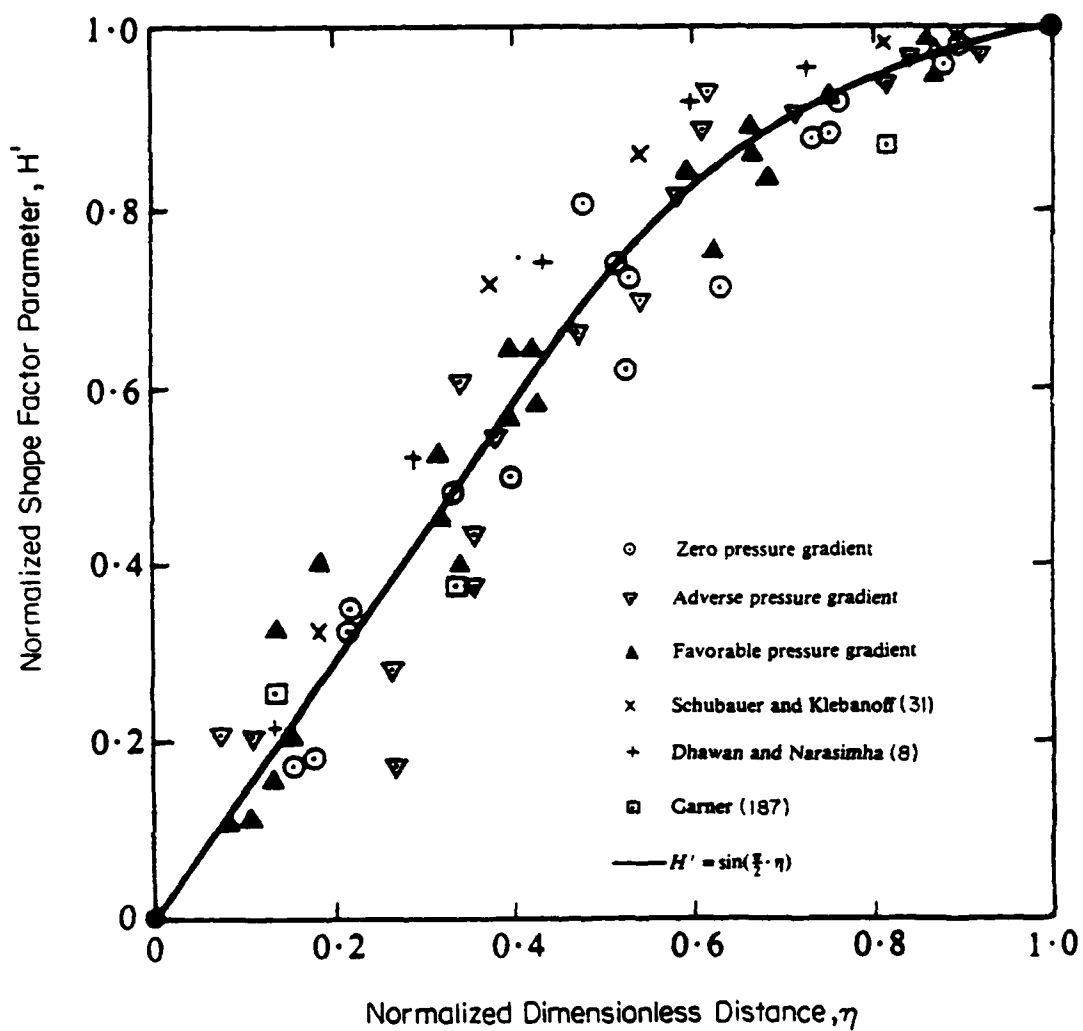


Figure 33. Distribution of the normalized shape factor parameter in the transition regime. [48]

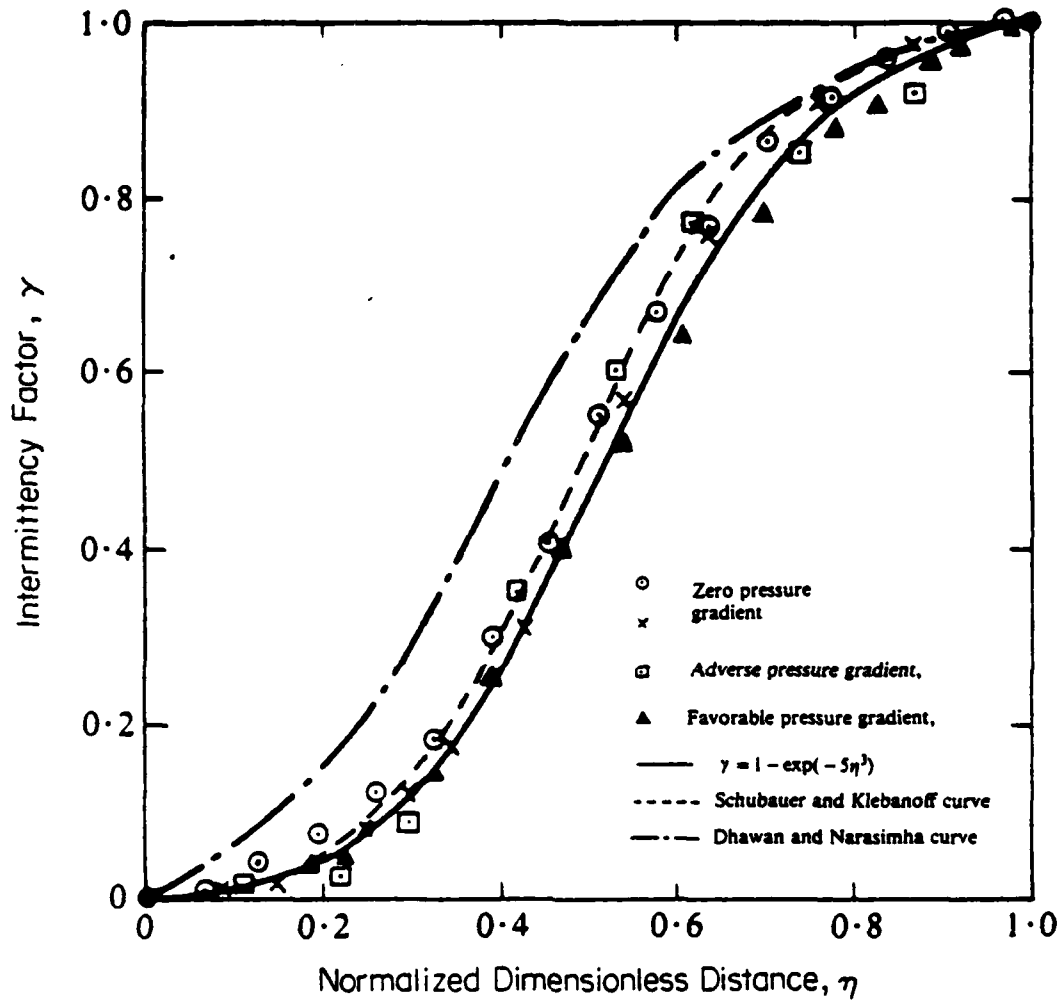


Figure 34. Intermittency distribution in the transition regime. [48]

In conclusion, these correlations apply to two-dimensional incompressible flows over smooth adiabatic surfaces. There is reason to believe, though, that they would not be quantitatively valid at the lower (<0.5 percent) turbulence levels. In this range, acoustic and vibration disturbances tend to be relatively larger contributors. Depending on whether or not they fall in the Tollmien-Schlichting susceptibility spectrum, they may cause a substantially different variation in $Re_{\theta-t}$. Also, the authors' selection of asymptotic limits for momentum thickness Reynolds numbers of transition onset and end must be regarded with caution, especially since turbulence levels were 5 percent or less in their experiments. Notice in Figure 31 at the shorter transition lengths that the data did deviate to momentum thickness Reynolds number substantially lower than given by their correlation for transition end. Finally, the use of an extreme value of λ_{θ} may not be acceptable for other pressure gradient distributions, particularly if the gradients are larger, or do not exhibit a similar variation.

7.5 Abu-Ghannam and Shaw's Method and Its Operational Features

The method outlined by Abu-Ghannam and Shaw [48] incorporates only two influencing factors in transition initiation--freestream turbulence and pressure gradient. For flows over flat surfaces, i.e. without curvature, the authors demonstrated, by a number of examples, satisfactory agreement between predicted properties of transition and experimental ones. This is due, of course, to the data base used in formulating their methodology and is therefore not unexpected.

In their presentation, the surface friction coefficients preceding transition initiation and following its completion are given respectively by

the integral-method applied separately to these two flow regimes of complete laminar and turbulent flows. In the transition zone, the friction coefficients are taken to be composed of two parts: a turbulent contribution whose magnitude is due to turbulent flow only were it to prevail by itself, modified by λ , the intermittency factor; and a laminar part that is the pure laminar friction coefficient modified by $(1 - \lambda)$. Such a combination results in the following:

$$C_f = (1 - \gamma) C_{f-l} + \gamma C_{f-tb} \quad (25)$$

where subscripts "l" and "tb" refer to laminar and turbulent respectively.

In order to ascertain how the method works when used in conjunction with a finite-difference numerical integration procedure, calculations were performed first for flat-plate flows without pressure gradients but with freestream turbulence levels of 0.2 and 4 percent. Starting from a uniform velocity profile at the leading edge, local momentum Reynolds numbers along the surface locations were calculated until it reached a critical value determined by equation (14) for transition initiation. The transition region parameters were then calculated, which included transition length from equation (16) and the transition completion position from equation (17).

Downstream from the transition initiation point, turbulent viscosity is activated by the intermittency factor calculated from equation (23); a total viscosity comprising the laminar and turbulent contributions follows the mixture rule:

$$\mu_o = \mu_l + \gamma \mu_{tb} \quad (26)$$

Prandtl's mixing length theory was used in obtaining turbulent viscosity μ_{tb} via the formulation

$$\mu_{tb} = \rho l^2 du/dy \quad (27)$$

where l is the mixing length, while other symbols are those conventionally understood.

Two forms for the mixing length were used in the computations reported herein; one is the commonly used Van Driest modification and the other is an exponential model developed in this research program. They are:

$$l^+ = K_1 y^+ [1 - \exp(-y^+/26)] \quad (28)$$

and

$$l^+ = (K_1/K_2) [\exp(K_1 u^+) - \exp(-K_1 u^+)] \quad (29)$$

In the preceding expressions, conventionally used plus coordinates are understood and the dimensionless mixing length l^+ is given by

$$l^+ = l u_\tau / \nu \quad (30)$$

Constants K_1 and K_2 have values of 0.41 (Von Karman) and 9.025 respectively.

Results of Computation. Using the Van Driest form for mixing length, the resulting C_f variations with Re_x are shown in Figure 35 and Re_θ vs Re_x variations in Figure 36. While C_f in the transition zone does bridge the gap between the calculated laminar and turbulent curves, there are significant differences between the positions of C_f -minimum and C_f -maximum according to the finite-difference calculations on the one hand and those positions of

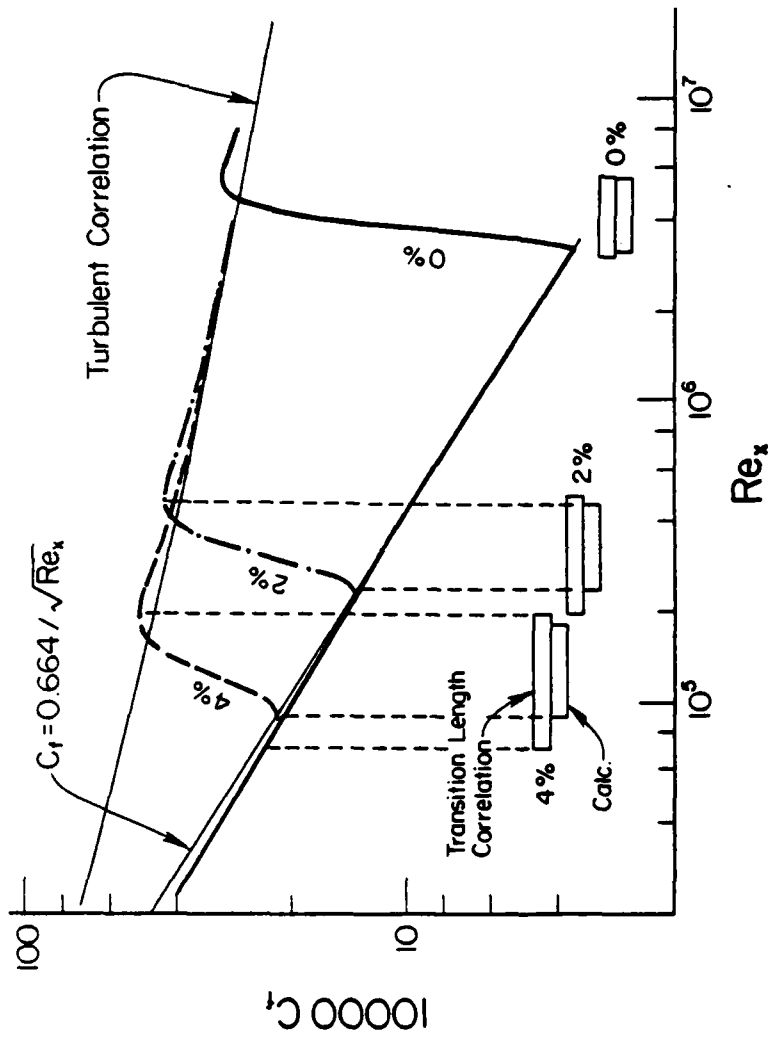


Figure 35. Friction coefficient variations by finite-difference calculations, van Driest model, flat plate

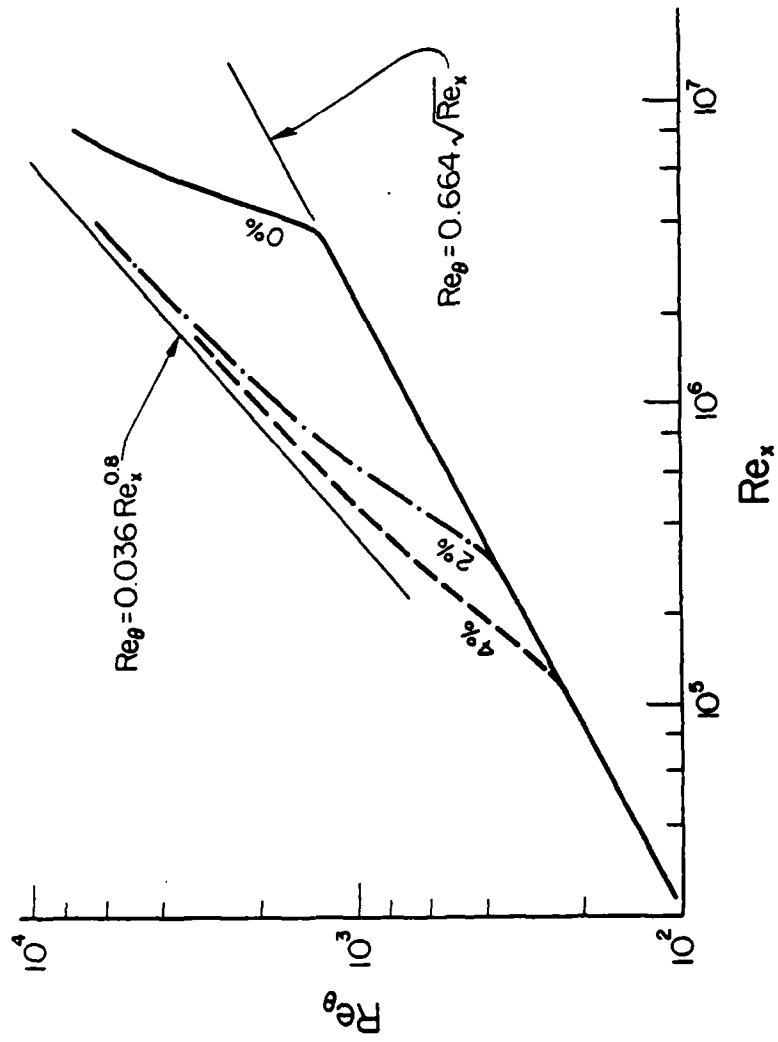


Figure 36. Momentum thickness variations by finite-difference calculations, van Driest model, flat plate

transition start and end predicted by the method on the other. This is to say that while C_f -minimum and -maximum do coincide with the predicted transition initiation and completion when integral correlations for the two leading and trailing regions connected by an intermittency-modified transition region are used; the same cannot be expected when numerical integration of the boundary layer equations is employed to obtain the C_f -variation on the surface. From a computational viewpoint, merely activating the intermittency factor of turbulence $\gamma > 0$ does not result in an immediate upturn of C_f ; nor does setting $\gamma = 1$ produce an automatic maximum for C_f . Indeed, from a physical ground, such an observation is a plausible one, and lends further credence to the various criteria used in defining transition initiation and termination by various researchers. Thus, on a same configuration under identical flow conditions, it is entirely possible to have different transition points observed experimentally, depending on the method and the criterion used in delineating transition.

The discrepancy described previously appears progressively larger as the turbulence level increases and the calculated results are characterized by a marked overshoot of the C_f -values near transition termination. Momentum Reynolds number variations shown in Figure 36 indicate a smooth cross-over from a laminar to turbulent relation without overshoot, because the momentum thickness is an integral of the local friction coefficient.

Corresponding to Figures 35 and 36 based on van Driest's model, Figures 37 and 38 show results when the exponential model for turbulent mixing length, equation (27), is used instead. These two sets of results based on two different mixing length formulations are nearly identical and hardly distinguishable from one another.

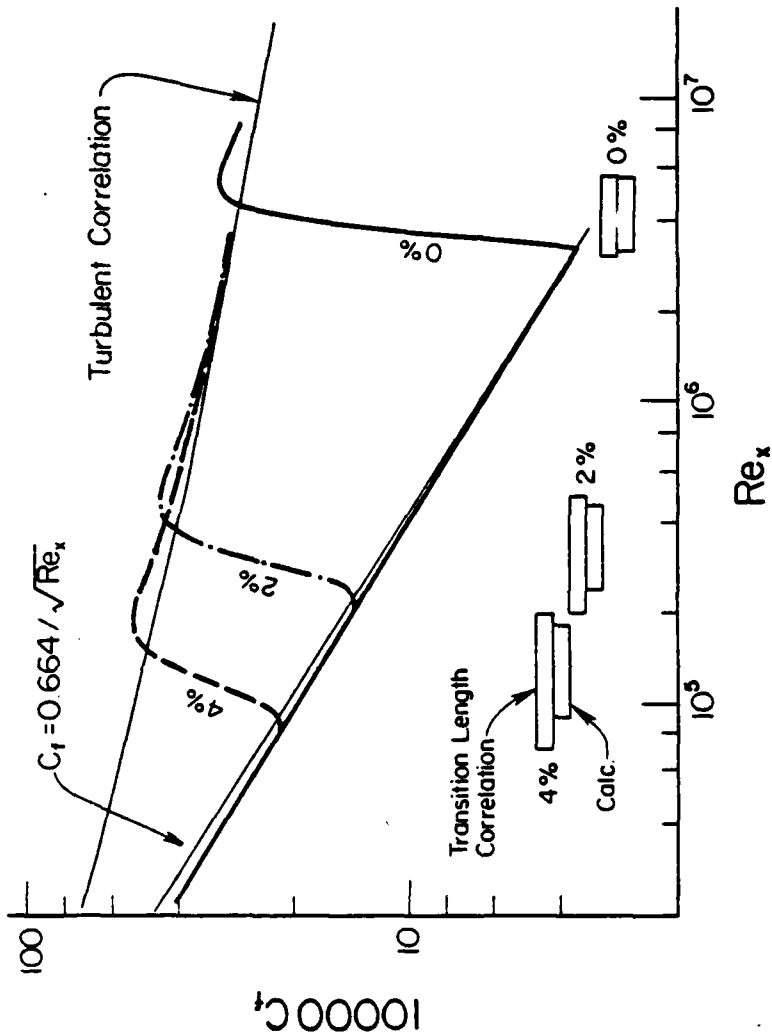


Figure 37. Friction coefficient variations by finite-difference calculations, exponential model, flat plate

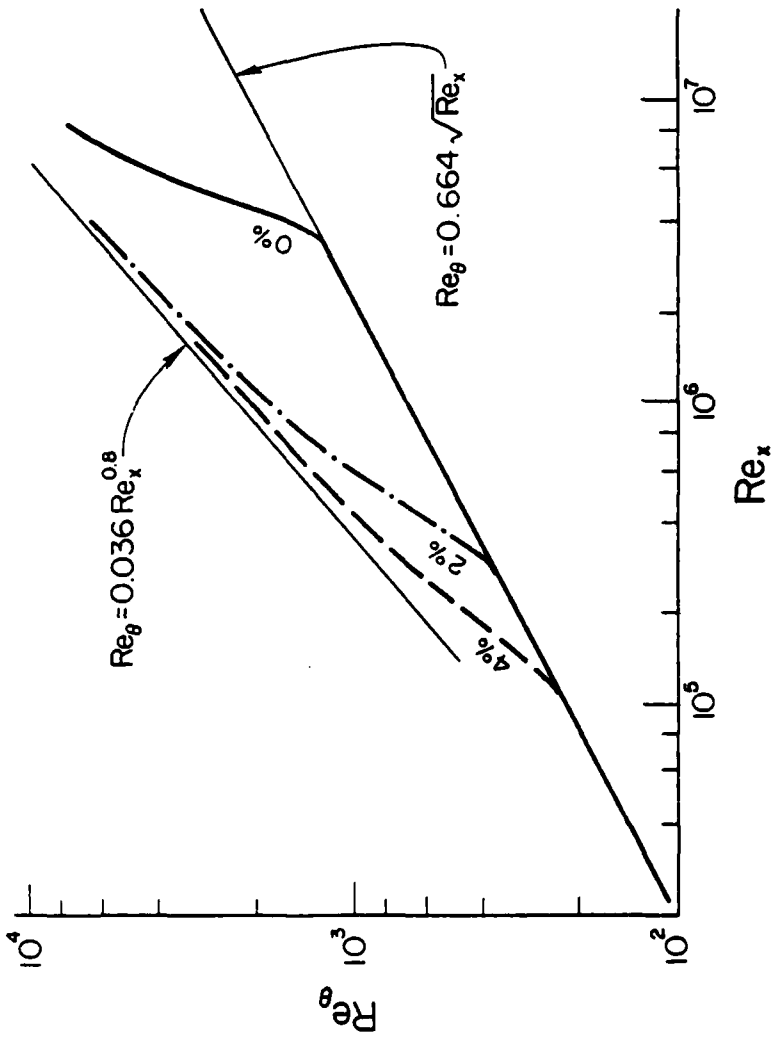


Figure 38. Momentum thickness variations by finite-difference calculations, exponential model, flat plate

Transition Prediction on Turbine Airfoil. Flow around turbine vanes and airfoils is compounded by a round nose region and curvature, which are known to hasten instability of laminar flow and are therefore promoters for transition onset. Even though the transition prediction method by Abu-Ghannam and Shaw [48] is admittedly unsuited to turbine airfoil applications, it is of interest to establish how inadequate is the flat-plate prediction scheme when applied to a turbine airfoil for which there are experimental data available. Evaluated in this light, it is possible to judge the presence of the nose region and curvature in rendering ineffective the prediction scheme and, in fact, all other schemes as well.

Selected for this purpose was the Blade A of Han, Cox, and Chait [148], which has, on its suction side of the surface, a velocity distribution and measured heat transfer variation shown in Figure 39. In the first 60 percent of the surface, the velocity is accelerating and in the remaining portion, mildly decelerating. Barring curvature and nose region effects, the flow velocity distribution would be stabilizing in the frontal portion and only mildly destabilizing in the rear. Examination of the heat transfer distribution indicates a very pronounced jump at the 60 percent chord position and strongly suggests transition onset and completion over a short surface length.

On the calculation side, Faulkner-Skan's flow was used to start the stagnation point laminar boundary layer and numerical integration of the boundary layer equations allowed downstream marching in evaluating all relevant parameters. To detect transition onset, three criteria were used: $Re_{\theta-t} = 200$, $Re_{\theta-t} = 380$, and the third is the critical momentum Reynolds number according to the Abu-Ghannam and Shaw's [48] method. The first criterion has been suggested as an average value for all flows regardless of

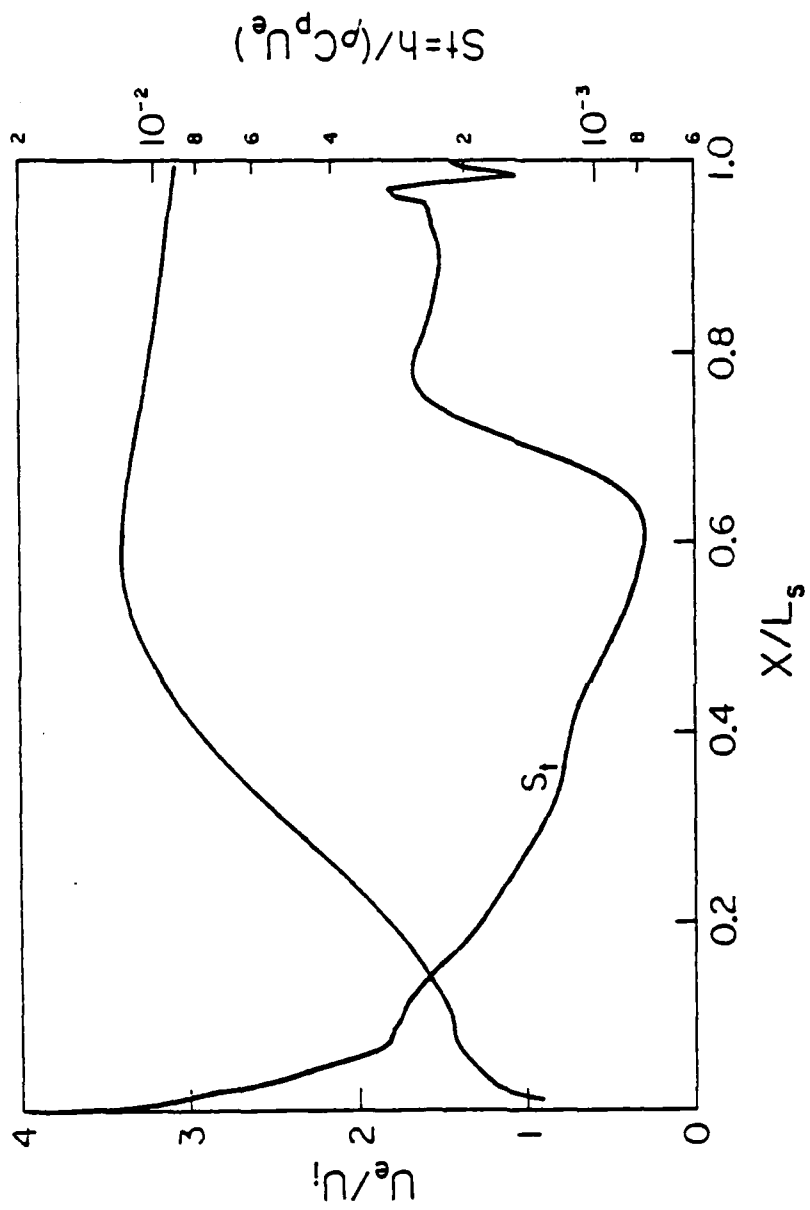


Figure 39. Blade-A suction surface velocity and heat transfer data,
 $U_1 = 22$ fps.

other flow conditions and is, obviously, meant to be substituted by a more rational criterion; the second criterion of a transition momentum Reynolds number of 380 was found to be more representative of this particular flow environment since the resulting friction coefficient shows a jump at $x/L_s = 0.60$ approximately, where the heat transfer coefficient exhibits a steep rise. The use of Abu-Ghannam and Shaw's criterion, however, did not indicate any transition probability; in the first portion of the surface, transition was not found because of local flow acceleration; and in the rear portion of the surface, flow deceleration caused the still laminar boundary layer to separate at the $x/L_s = 0.8$ position before transition onset was induced. The calculated variations of the friction coefficient for $Re_\theta = 200$ and 380 are graphically shown in Figure 40. By following the distribution for $Re_{\theta-t} = 380$, the general contour of C_f follows that of the experimental Stanton number curve quite closely. Thus, it appears that the presence of a nose region and curvature has a significant impact on the transition prediction. More on this point is discussed in Section XI.

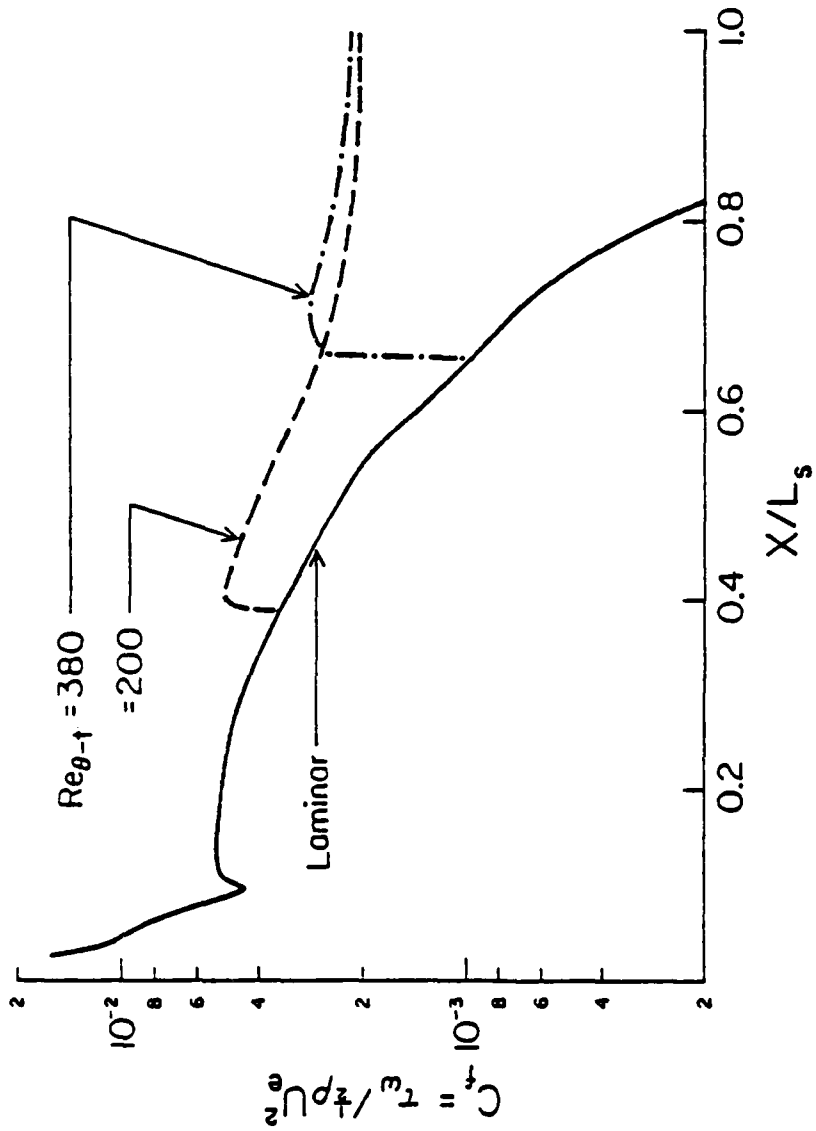


Figure 40. Calculated friction coefficient, blade-A suction surface, $U_i + 22$ fps.

VIII. HEAT TRANSFER IN THE TRANSITION REGIME

Two of the earliest investigations of heat transfer in the transition regime are those of Reynolds, Kays, and Kline [133] and Dhawan and Narasimha [8]. Both applied a heat transfer correlation with the intermittency factor γ of the form

$$\dot{q}_t = \dot{q}_l (1 - \gamma) + \dot{q}_T \gamma \quad (31)$$

and an analogous expression for local skin friction in describing these statistically averaged properties of the transitioning boundary layer. However, the former paper also dealt with application of the expressions to abruptly induced transition. This would suggest possible usefulness in bypass transitions, such as induced by surface roughness and/or high intensity freestream disturbances, which do not necessarily exhibit any intrinsic intermittency.

Use of these expressions presupposes either the ability to calculate the growth and spread of turbulence in the transition regime or a predefined intermittency distribution function. Both require an assumption as to the "virtual origin" of the turbulent boundary layer, plus methods for computing suitably general turbulent boundary layers, particularly at low Reynolds numbers. Pertaining to the location of the virtual length, Dhawan and Narasimha [8] proposed that it would be most appropriately taken as the location of transition onset. Primarily this suggestion was based on information obtained

from extrapolation of zero pressure gradient turbulent boundary layer growth into the transition regime. Further evidence supporting this proposal was their observation that transition onset, although random in time, occurred very nearly on a discontinuous line in the flow. The experimental data of Coles [134] and Charnay, Comte-Bellot, and Mathieu [135] for turbulent boundary layers concurs with the virtual origin selection of Dhawan and Narasimha [8] at least for zero pressure gradient sub- and supersonic boundary layers.

If a predefined intermittency distribution function is used, the greater problem is one of lack of generality. Although a representative distribution, such as that of Abu-Ghannam and Shaw [48] in the previous section, may have utility in many two-dimensional boundary layers, this is not the case in general. (A similar comment would apply to the use of their skin friction distribution function along with some form of Reynolds analogy.) Any rapid variation in strength of the more influential boundary layer modifiers (e.g., pressure gradient) during transition would be likely to influence the distribution. As an example, delay, arrest, or reversal of the transition process, as might result when rapid acceleration occurs midway through transition, would not be anticipated or accounted for in such a distribution. Furthermore, Blair [126] has observed in transition experiments that the establishment of fully turbulent wall heat transfer rates falls progressively further downstream of the establishment of fully turbulent mean velocity profiles as the degree of acceleration in boundary layers increases.

Other complications are introduced by the fact that, so far, published literature about the influence of Görtler vortices or unsteadiness on intermittency development is either scarce or nonexistent. Those which do exist

for unsteady flows [9, 104] seem to indicate that turbulence initiation is less random (more periodic) in time, leading to a more nearly linear spatial intermittency distribution.

IX. THE GAS TURBINE ENVIRONMENT

In this section, the salient features of the flow within the axial gas turbine cascade will be briefed. Also, typical blade geometry and surface conditions will be outlined. A more complete summary of the flow characteristics within the turbine engine is available in the compendium of Graham [136].

9.1 Basic Cascade Flow Conditions

As noted by Graham [136], the average total turbine inlet temperatures and pressures are about 2000°F (1094°C) and 20 to 25 atmospheres, respectively, for most modern commercial transport aircraft. In new generations of commercial aircraft and present engines for military applications, the inlet temperatures and pressures are about 2500°F (1371°C) and 25 to 30 atmospheres. Future designs will call for temperatures near 2800°F (1538°C) and pressures up to 40 atmospheres.

Typically, surface temperatures on a modern high-pressure stage rotor blade are at or below 1610°F (877°C) [114] for the alloy blades, although higher temperatures are permissible for those with ceramic thermal barrier coatings. Flow turning angles are around 75 to 100° or so, over blades with chord lengths in the range of 2 to 4 inches. Entrance flow speeds are about Mach 0.3, accelerating to Mach 0.8 [114], even through there are usually regions of acceleration and deceleration on both the concave (pressure) and convex (suction) surfaces of the blades.

As is well known, though, the flow fields in turbomachinery are not two-dimensional. Rather, they are three-dimensional, spatially nonuniform, and highly unsteady with complex viscous secondary flow patterns, particularly at the hub and tip sections of the blades or vanes. However, if the flow only at midspan is considered, the secondary flow effects are less prominent. Figure 41 depicts just such a section. There, the boundary layer begins its development from a stagnation line created by flow impingement on the rounded leading edge. This developing boundary layer is probably laminar near the stagnation zone because of the rapid flow acceleration but it becomes transitional along both the concave and convex surfaces of the blade as its growth continues. The location of the transition region is nonlinearly dependent on the combined cumulative influences of all the boundary layer modifiers and disturbers addressed in previous sections, plus others, which are chiefly surface roughness, secondary flows, stagnation line induced flow phenomena, and possibly shock wave-boundary layer interaction. The flow may remain transitional, become turbulent, or relaminarize and retransition, depending on the relative strengths of these influences.

9.2 Flow Disturbances

The flow through the turbine cascade is both macroscopically unsteady and highly turbulized [137]. Flow disturbance levels caused by the upstream compressor and combustor are probably well over 10 percent with the combustor turbulization being the much greater contributor. Graham [136] cited some measurement results that indicated that velocity fluctuations at a combustor exit could exceed 50 percent. However, this level would be reduced through stream tube stretching and viscous dissipation as the flow accelerates through the blade row.

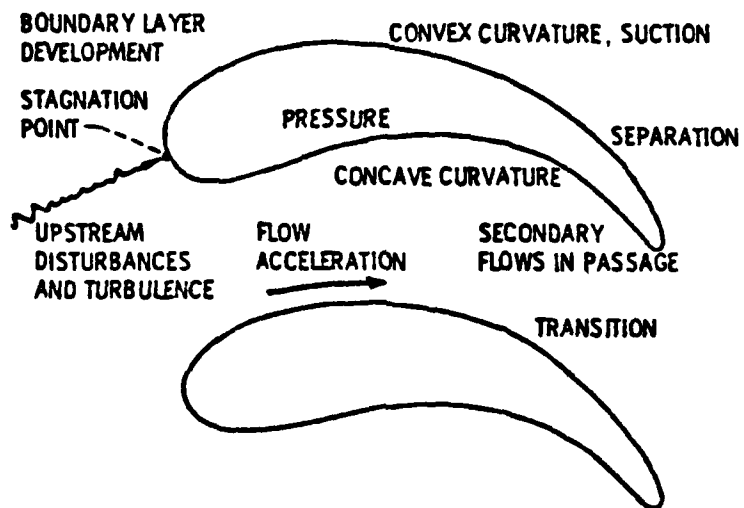


Figure 41. Schematic of a section of a turbine blade row and associated convective phenomena. [136]

The disturbances encountered as the flow progresses through the turbine section cannot be considered as turbulence in the classical sense. Rather, they are a complicated combination of potential flow unsteadiness caused by upstream and downstream blade-vane interactions, secondary flow formations, and wake disturbances, in addition to the smaller scale high intensity turbulization from the combustion process [137, 138]. Forest [114] has suggested that any immediate upstream blade-vane interactions alone could produce pulsating velocity fluctuations of around 20 percent at frequencies of the order of 10^4 Hz. (blade pass frequency).

One means of describing the flow disturbances has been proposed by Evans [139] in the following definitions.

$$T_{U_D} = \frac{(v'_D)^2}{\bar{U}} \quad \text{Overall Disturbance Level}$$

$$\hat{T}_U = \frac{(v')^2}{\bar{U}} \quad \text{Freestream Turbulence Level}$$

$$\tilde{T}_U = \frac{[\bar{u}(t) - \bar{U}]^2}{\bar{U}} \quad \text{Unsteadiness Level}$$

where the parameters are related by

$$T_{U_D}^2 = \hat{T}_U^2 + \tilde{T}_U^2$$

Figure 42 depicts the velocity fluctuations to which these definitions relate.

The disturbance levels represented by these definitions will vary continuously as the flow moves through the cascade. Also, the combination of

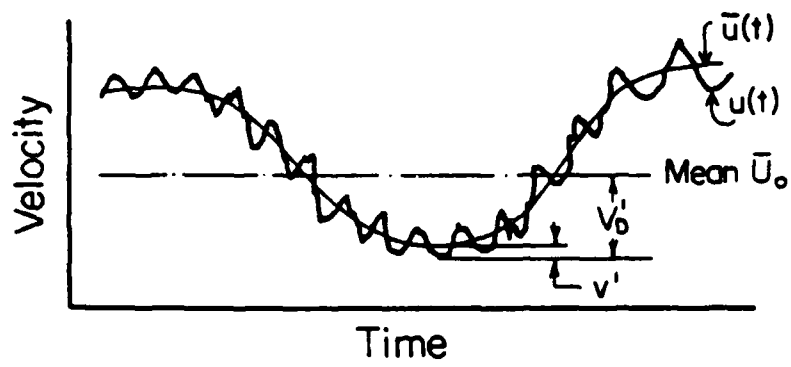


Figure 42. Hot wire trace of unsteady flow. [139]

potential flow unsteadiness and enclosed flow environment is likely to produce traveling wave resonance and standing waves.

9.3 Leading Edge Flow Stagnation

Stagnation line incidence on turbomachinery blading changes, oscillating primarily with passage by blades or vanes in the row immediately upstream [138]. Both the unsteady incidence and the stagnation line boundary layer initialization affect the subsequent boundary layer development. To be stressed here, though, is the fact that stagnation incidence leads to flow phenomena not encountered in boundary layers beginning on a sharp leading edge.

Generally, leading edge bluntness is destabilizing to the boundary layer. One reason for this is that the flow field around a stagnation line is not two-dimensional, but has an organized vortical structure. The vortices, which apparently result from a non-Görtler type, inviscid instability, are observed in parallel, uniformly spaced rows wrapped around the upstream side of the stagnation body [40]. As a consequence of their presence, the local rates of heat and mass transfer, as well as the local shearing stresses at the wall, vary periodically along the stagnation zone, with the average values being significantly greater than that for Hiemenz flow. The vortex spacing depends on $Re^{-1/2}$ and the freestream turbulence level, decreasing with increased turbulence. The net effect is reduced spacing and increased heat transfer ($Nu \sim Re^{1/2}$) with increases in Reynolds number and turbulence [140, 141]. Also, Gorla [142] acknowledges that, in the case of unsteady flows, the frequency of the unsteadiness significantly influences skin friction and heat transfer.

Sadeh, Brauer, and Garrison [143] did a visual study of these vortices in stagnation line cross-flow around a cylinder. From their observations, the vortices appeared to stretch, reduce in scale, and increase in rotational velocity as they approached the cylinder. Additionally, the vortices turned such that their axes aligned closely with the flow streamlines around the cylinder. Finally, when the vortices were close enough to interact with the laminar boundary layer on the cylinder, a noticeable scale increase occurred.

Stagnation zones also greatly augment the local turbulence intensity [144]. This increased intensity must also be boundary layer destabilizing when compared to the development of boundary layers originating on a sharp edge.

9.4 Secondary Flows

Many aspects of the turbine geometry promote viscous secondary flows, and three-dimensionalize the main flow field through a blade or vane passage. Besides stagnation line phenomena, some predominant influences are the centripetal and coriolis components of acceleration in flow over rotor blades, the interactions of hub and outer casing boundary layers with passage flow and blade boundary layers, flow around the tips of rotor blades, pressure differentials between adjacent blade surfaces in a row, blade twist, taper and curvature, and the lack of parallel flow resulting from having a finite number of blades in a row.

Hansen and Herzig [145] summarized, in a series of NACA reports, various techniques used to visualize the more readily identifiable secondary flow patterns. These reports also indicate a strong tendency for secondary flow vortex formations to collect at the hub in vane passages and at the blade tips

in rotor passages. Additionally, multistaging leads to accumulation of these flows in the downstream passages. From the evidence in the reports, it is surmised that secondary flows, especially in combination with flow unsteadiness, can result in leading edge separation of the boundary layers at the blade endwalls (horseshoe vortex).

9.5 Flow Surface Roughness

The influence of surface roughness on the flow regime over actual turbine blades is particularly nondeterministic, since the amount, size, and distribution of roughness varies with operation time and environment. Even in the practical absence of foreign matter, roughness is produced by high temperature flow erosion of the blade surface and by combustion product deposition [147].

In general, no reasonable assessment of the transition location can be effected without considering roughness. Particularly, the combined effects of acceleration and thermal boundary layer thinning in the presence of otherwise small roughness may be synergistic in promoting transition [148]. This would have stronger implications for the ceramic coated blades because of the greater as-produced roughness [149] and susceptibility to flow erosion, although the problem may be mitigated somewhat by the proposed use of a vitreous overcoat/binder on the ceramic.

9.6 Film Cooling

In meeting blade cooling requirements, present generations of aircraft gas turbines utilize leading edge blowing of compressor bled air (film cooling) on at least the first turbine stage vanes and blades. This added

surface normal velocity component acts to trip the boundary layer or to cause local separations. Often, then, the question about the flow regime centers on the strength of the relaminarization promoting flow acceleration and thermal gradients relative to other influences which favor a continued turbulent boundary layer. A summary of NASA studies on film cooling is given in [149].

As a final comment, a major drive in reducing the uncertainty in the hot gas side heat transfer coefficient distribution is warranted, at least based on Stepka's analysis [150]. His results indicated that the uncertainty in local hot gas side heat transfer constitutes a greater barrier to predicting blade temperature distributions (and thus blade life) than does coolant side heat transfer uncertainty.

X. TURBINE CASCADE MODEL TRANSITION INVESTIGATIONS

The inclement environment and small flow surface dimensions inside a gas turbine inhibit proper instrumentation for passage flow and boundary layer studies. As a result, few details are known about the actual flow, not to mention simulation under laboratory conditions [122]. In attempts to bridge this knowledge gap, many investigators have resorted to upscaled blade models for flow visualization and heat transfer evaluation. Simulations using these large scale models are representative of their turbine counterparts in chord Reynolds number, but neglect compressibility. More significantly, the cascades are often static, with nominally two-dimensional, steady flow and reversed heat flux, and the disturbance levels are usually low. The objectives in such flow model studies have been to promote understanding of some of the basic phenomena occurring in flow over a gas turbine blade. Too often, however, the results of such investigations are implicitly assumed to be sufficiently representative of the gas turbine environment for transition studies, and for testing the abilities of transition "prediction" methods to be used in design. Although dynamic similarity is required, prerequisite for transition studies related to turbine blading are much more stringent than those for stagnation, blade wake, and even secondary flow visualization. This becomes especially evident when one recalls the nonlinear nature of the boundary layer oscillator, the irregular and statistically nonuniform nature of the disturbances, plus the multitude of concurrently acting boundary layer

modifiers that are also irregular, and, consequently, the ultimately non-deterministic character of transition.

From the essentially parametric examination of transition influencers in previous sections, it is evident that such simulations must include Reynolds numbers, wall-to-freestream temperature ratios, freestream disturbances and unsteadiness, and wall roughness. These factors constitute minimum considerations in transition and heat transfer investigations over idealized "2-D" static cascades. Secondly, Mach number (compressibility) effects would need to be included. Tertiary considerations might involve nonideal gas and nonNewtonian fluid effects resulting from the high fluid temperatures and pressures. These secondary and tertiary factors, though, will undoubtedly pale to a host of three-dimensional and secondary flow influences, the latter of which are engendered primarily at the hub and tip sections. Other factors would include upstream wake vorticity, resonance of traveling waves, standing waves, and vibrations with the turbine structure. Additionally, for turbine rotor blades, the centrifugal and coriolis flow accelerations are important [151].

More recently, secondary flows in turbomachinery have been the topic of an AGARD conference [152] and papers by Binder and Romey [153], Sharma and Graziani [154], and Walker and Markland [155, 156]. The investigations were directed toward identifying and calculating secondary flows [152, 153, 154] and their effects on boundary layer development and heat transfer [155, 156], without explicitly considering transition. These and other investigations, in particular [137], have verified that secondary flows can influence boundary layer development, even over the blade midsection. The character of this influence changes with, among other things, aspect (span-to-chord) ratio,

hub-to-tip ratio, and blade loading, with the result being that transition is also affected.

Some turbomachinery flow unsteadiness considerations are addressed in an AGARD conference report [157], and in papers by Dring, et al., [138] and Joslyn, Dring, and Sharma [137]. These analytical and experimental investigations seek to characterize the unsteadiness resulting from rotor blade-vane interactions and to evaluate its aerodynamic and laminar or turbulent boundary layer heat transfer effects. All of the investigations, and particularly Joslyn, Dring, and Sharma [137] and Dring, et. al., [138] indicate a strong dependence of potential flow unsteadiness on stator-rotor spacing. Especially of interest, though, are the experiments of Dring, et al., [138] in a large scale one and one-half stage rotating cascade rig with low speed flow. On their stator blade suction surfaces, the authors observed laminar, transitional, and turbulent flows, with the demarcation between the flow regimes oscillating periodically with rotor blade passage downstream. Transition was preceded by Tollmien-Schlichting waves. The (downstream) rotor suction surface boundary layer varied periodically between laminar and turbulent flow with passage into and out of the stator wakes. In these investigations, though, the blade surfaces were smooth and, apparently, freestream "turbulence" was relatively low. No flow separations were observed, however.

Static cascade rigs with representative flow Mach numbers and wall-to-freestream temperature ratios have also become more prevalent. Investigations utilizing such rigs are typical. [See 72, 125, 158-167].

Without belaboring the point, it suffices to say that none of the present transition "prediction" methods work well even for the static cascades. This

conclusion is supported by the findings of Daniels and Browne [117], Brown and Martin [121, 122, 124], Consigny and Richards [165], and Litchfield and Norton [166]. Generally, transition region predictions on the pressure surface are poorest because of the combined Görtler instability, changing blade curvature and continued flow acceleration which results in extended transition regions. Although suction surface predictions are often not satisfactory, the occurrence of a distinct static pressure minimum followed by flow deceleration can precipitate transition and render the predictions more acceptable. Nevertheless, most of the boundary layer transition studies are conducted with freestream turbulence levels substantially below those encountered in an operating turbine. Probably the most representative static cascade results with regard to turbulence levels are those of Lander [158], Bayley and Milligan [161], Bayley and Priddy [168], and Krishnamoorthy [169].

Regardless of the effects of the various flow phenomena on transition itself, it is evident from these and other investigations (e.g., [55, 72, 88, 118, 121-124, 169, 170, 171]) that Görtler vortices, surface roughness, secondary flows, unsteadiness (both frequency and intensity), and turbulence all play an important role in determining laminar boundary layer heat transfer. Also, the turbulent boundary layer heat transfer may be influenced, particularly by surface curvature [77], roughness [136], and acceleration [136]. Further consideration of these effects, especially on the laminar boundary layer, would most likely help mitigate the consequences of the seemingly inevitable misprediction of the transition region location.

XI. CONCLUDING REMARKS

Transition prediction for gas turbine blade and vane boundary layers is exceedingly difficult because the occurrence of transition depends on the cumulative effect of many nonlinearly interacting influences as well as the nonuniform disturbances. The unavoidable result is that an already singular process assumes highly nondeterministic characteristics, in effect, making the term "prediction" a particularly strong misnomer. Compounding this problem is the lack of understanding of the phenomena and the fact that much of the transition data is parametric and is substantially limited to two-dimensional flows. Therefore, for the near future, estimates for the location of the transition region will remain both highly uncertain and experiential. The experimental data from which the information for these estimates is obtained will probably be ad hoc, and will be based on modeling of influences that appear parametrically to be dominant, combined with the introduction to the model environment of any anticipated contingent conditions.

Nevertheless, defining a usable criterion for evaluating transition is still a problem, and indeed a pressing one, since the combination of a highly driven nonlinear boundary layer response and augmentation or suppression of this effect by boundary layer modifiers can evoke questions as to when "true" turbulence may be considered to exist. For example, defining transition as the region for which turbulence production exceeds dissipation does not provide an unambiguous criterion in a transitioning, relaminarizing, or

retransitioning boundary layer that might be viewed also as highly excited laminar or strongly repressed turbulent flow. At least from a heat transfer perspective, the latter two can, in some instances, be quite similar. However, it would seem that the repercussions of this problem and the inevitable misprediction of the transition region location could be mitigated somewhat by considering the manifestations of disturbers and modifiers in the heat transfer through both the laminar and turbulent boundary layers. In particular, the augmentation or suppression of laminar or turbulent boundary layer heat transfer by freestream disturbances, unsteadiness, Görtler vortices, secondary flows, surface roughness, flow acceleration or deceleration, surface curvature, and combinations of these would also need to be adequately accounted for.

BIBLIOGRAPHY

(The references listed are publications pertinent to this study and are those consulted. Not all of them have been specifically cited, however.)

1. Reshotko, E.: "Boundary-layer Stability and Transition," Annual Review of Fluid Mechanics, Vol. 8, 1976, pp. 311-349.
2. Morkovin, M.V.: "On the Many Faces of Transition," Viscous Drag Reduction (Wells, C.S., ed.), Plenum Press, 1969, pp. 1-31.
3. Morkovin, M.V.: "Instability, Transition to Turbulence and Predictability," AGARDograph No. 236, 1978.
4. Meyer, R.E. (ed.): Transition and Turbulence, Academic Press, 1981.
5. Schlichting, H.: Boundary-Layer Theory, 7th ed., McGraw-Hill, 1979.
6. Schubauer, G.B. and H.K. Skramstad: "Laminar Boundary-Layer Oscillations and Transition on a Flat Plate," NACA Technical Report No. 909, 1948.
7. Görtler, H.: "On the Three-Dimensional Instability of Laminar Boundary Layers on Concave Walls," NACA Technical Memorandum No. 1375, 1954.
8. Dhawan, S. and R. Narasimha: "Some Properties of Boundary Layer Flow During the Transition from Laminar to Turbulent Motion," Journal of Fluid Mechanics, Vol. 3, Part 4, 1958, pp. 418-436.
9. Loehrke, R.I.; M.V. Morkovin; and A.A. Fejer: "REVIEW - Transition in Nonreversing Oscillating Boundary Layers," ASME Journal of Fluids Engineering, Vol. 97, No. 4, Decm. 1975, pp. 534-549.
10. Charters, A.: "Transition Between Laminar and Turbulent Flow By Transverse Contamination," NACA Technical Note No. 891, 1943.
11. Morkovin, M.V.: "Transition from Laminar to Turbulent Shear Flow - A Review of Some Recent Advances in Its Understanding," Trans. ASME, Vol. 80, No. 5, July 1958, pp. 1121-1128.
12. Tani, I.: "Boundary Layer Transition," Annual Review of Fluid Mechanics, Vol. 1, 1969, pp. 169-196.
13. Tani, I.: "Review of Some Experimental Results on Boundary Layer Transition," The Physics of Fluids, Part II, Vol. 10, No. 9, Sept. 1967, pp. S11-S16.

14. Mack, L.M.: "Transition Prediction and Linear Stability Theory," AGARD Conference Proceedings No. 224 on Laminar-Turbulent Transition, 1977, Paper No. 1.
15. White, F.M.: *Viscous Fluid Flow*, McGraw-Hill, 1974.
16. Ragab, S.A. and A.H. Nayfeh: "Gortler Instability," *The Physics of Fluids*, Vol. 24, No. 8, Aug. 1981, pp. 1405-1417.
17. Floryan, J.M. and W.S. Saric: "Stability of Gortler Vortices in Boundary Layers," *AIAA Journal*, Vol. 20, No. 3, Mar. 1982, pp. 316-324.
18. Saric, W.S. and A.H. Nayfeh: "Nonparallel Stability of Boundary Layer Flows," *The Physics of Fluids*, Vol. 18, No. 8, Aug. 1975, pp. 945-950.
19. Saric, W.S. and A.H. Nayfeh: "Nonparallel Stability of Boundary Layers With Pressure Gradients and Suction," AGARD Conference Proceedings No. 224 on Laminar-Turbulent Transition, 1977, Paper No. 6.
20. Gaster, M.: "On the Effects of Boundary-Layer Growth on Flow Stability," *Journal of Fluid Mechanics*, Vol. 66, Part 3, 1974, pp. 465-480.
21. Hall, P.: "On the Non-linear Evolution of Gortler Vortices in Non-parallel Boundary Layers," *IMA Journal of Applied Mathematics*, Vol. 29, No. 2, Sept. 1982, pp. 173-196.
22. Stuart, J.T.: "On the Non-linear Mechanics of Wave Disturbances in Stable and Unstable Parallel Flows. Part I. The Basic Behavior in Plane Poiseuille Flow," *Journal of Fluid Mechanics*, Vol. 9, Part 3, 1960, pp. 353-370.
23. Stuart, J.T.: "On the Nonlinear Mechanics of Hydrodynamic Stability," *Journal of Fluid Mechanics*, Vol. 4, Part 1, 1958, pp. 1-21.
24. Watson, J.: "On the Non-linear Mechanics of Wave Disturbances in Stable and Unstable Parallel Flows. Part 2. The Development of a Solution for Plane Poiseuille Flow and for Plane Couette Flow," *Journal of Fluid Mechanics*, Vol. 9, Part 3, 1960, pp. 371-389.
25. Stuart, J.T.: "Nonlinear Stability Theory," *Annual Review of Fluid Mechanics*, Vol. 3, 1973, pp. 347-370.
26. Murdock, J.W.: "A Numerical Study of Nonlinear Effects of Boundary-Layer Stability," *AIAA Journal*, Vol. 15, No. 8, Aug. 1977, pp. 1167-1173.
27. Fasel, H.F.: "Investigation of the Stability of Boundary Layers By a Finite-Difference Model of the Navier-Stokes Equations," *Journal of Fluid Mechanics*, Vol. 78, Part 2, 1976, pp. 355-383.

28. Fasel, H.; H. Bestek; and R. Schefenacker: "Numerical Simulation Studies of Transition Phenomena in Incompressible Two-Dimensional Flows," AGARD Conference Proceedings No. 224 on Laminar-Turbulent Transition, 1977, Paper No. 14.
29. Murdock, J.W. and T.D. Taylor: "Numerical Investigation of Non-linear Wave Interaction in a Two-Dimensional Boundary Layer," AGARD Conference Proceedings No. 224 on Laminar-Turbulent Transition, 1977, Paper No. 4.
30. Rogler, H.L.: "The Coupling Between Freestream Disturbances, Driver Oscillations, Forced Oscillations, and Stability Waves in a Spatial Analysis of a Boundary Layer," AGARD Conference Proceedings No. 224 on Laminar-Turbulent Transition, 1977, Paper No. 16.
31. Schubauer, G.B. and P.S. Klebanoff: "Contributions on the Mechanics of Boundary-Layer Transition," NACA Technical Report No. 1289, 1956.
32. Klebanoff, P.S. and K.D. Tidstrom: "Evolution of Amplified Waves Leading to Transition in a Boundary Layer with Zero Pressure Gradient," NASA Technical Note D-195, 1959.
33. Klebanoff, P.S.; K.D. Tidstrom; and L.M. Sargent: "The Three-Dimensional Nature of Boundary-Layer Instability," Journal of Fluid Mechanics, Vol. 12, Part 1, 1962, pp. 1-39.
34. Kovaszny, L.S.G.; H. Komoda; and B.R. Vasudeva: "Detailed Flow Field in Transition," Proceedings of the 1962 Heat Transfer and Fluid Mechanics Institute, Stanford University Press, 1962, pp. 1-26.
35. Hama, F.R.; J.D. Long; and J.C. Hegarty: "On Transition from Laminar to Turbulent Flow," Journal of Applied Physics, Vol. 28, No. 4, April 1957, pp. 388-394.
36. Hama, F. and J. Nutant: "Detailed Flow-field Observations in the Transition Process in a Thick Boundary Layer," Proceedings of the 1963 Heat Transfer and Fluid Mechanics Institution, Stanford University Press, 1963, pp. 77-93.
37. Emmons, H.W.: "The Laminar-Turbulent Transition in a Boundary Layer - Part I," Journal of the Aeronautical Sciences, Vol. 18, No. 7, July 1951, pp. 490-498.
38. Elder, J.W.: "An Experimental Investigation of Turbulent Spots and Breakdown to Turbulence," Journal of Fluid Mechanics, Vol. 9, Part 2, 1960, pp. 235-246.
39. McCormick, M.E.: "An Analysis of the Formation of Turbulent Patches in the Transition Boundary Layer," ASME Journal of Applied Mechanics, Vol. 35, No. 2, June 1968, pp. 216-219.
40. Wyganski, I.; M. Sokolov and D. Friedman: "On a Turbulent Spot in a Laminar Boundary Layer," Journal of Fluid Mechanics, Vol. 78, Part 4, 1976, pp. 785-819.

41. Spangler, J.G. and C.S. Wells, Jr.: "Effect of Freestream Disturbances on Boundary-Layer Transition," AIAA Journal, Vol. 6, No. 3, March 1968, pp. 543-545.
42. Dryden, H.L.: "Transition from Laminar to Turbulent Flow" in Turbulent Flows and Heat Transfer (C.C. Lin, ed.), 1959, Princeton University Press, pp. 1-74.
43. Bennett, H.W.: "An Experimental Study of Boundary Layer Transition," Kimberly-Clark Corp. Report, Neenah, Wisconsin, 1953.
44. Mitchner, M.: "Propagation of Turbulence From an Instantaneous Point Disturbance," Journal of the Aeronautical Sciences, Vol. 21, No. 5, May 1954, pp. 350, 351.
45. Kelbanoff, P.S.; G.B. Schubauer and K.D. Tidstrom: "Measurements of the Effect of Two-Dimensional and Three-Dimensional Roughness Elements on Boundary-Layer Transition," Journal of the Aeronautical Sciences, Vol. 22, No. 11, Nov. 1955, pp. 803, 804.
46. Coles, D.: "The Turbulent Boundary Layer in a Compressible Fluid," The Physics of Fluids, Vol. 7, No. 9, Sept. 1964, pp. 1403-1423.
47. Poll, D.I.A.: "Leading Edge Transition on Swept Wings," AGARD Conference Proceedings No. 224 on Laminar-Turbulent Transition, 1977, Paper No. 21.
48. Abu-Ghannam, B.J. and R. Shaw: "Natural Transition of Boundary Layers - The Effects of Turbulence, Pressure Gradient, and Flow History," Journal of Mechanical Engineering Science, Vol. 22, No. 5, 1980, pp. 213-228.
49. Donaldson, C. DuP.: "A Computer Study of an Analytical Model of Boundary Layer Transition," AIAA Paper No. 68-38, 1968.
50. Lees, L.: "The Stability of the Laminar Boundary Layer in a Compressible Fluid," NACA Report No. 876, 1947.
51. Narasimha, R. and K.R. Sreenivasan: "Relaminarization in Highly Accelerated Turbulent Boundary Layers," Journal of Fluid Mechanics, Vol. 61, Part 3, 1973, pp. 417-447.
52. Brown, A. and B.W. Martin: "The Use of Velocity Gradient Factor as a Pressure Gradient Parameter," Proceedings of the Institution of Mechanical Engineers, Vol. 190, No. 14, 1976, pp. 227-285.
53. Jones, W.P. and B.E. Launder: "Some Properties of Sink-Flow Turbulent Boundary Layers," Journal of Fluid Mechanics, Vol. 56, Part 2, 1972, pp. 337-351.
54. Patel, V.C. and M.R. Head: "Reversion of Turbulent to Laminar Flow," Journal of Fluid Mechanics, Vol. 34, Part 2, 1968, pp. 371-392.

55. Zysina-Molozhen, L.M.; M.A. Medvedeva; and E.G. Rohst: "The Influence of Longitudinal Pressure Gradient and Turbulence of the Flow Upon Heat Transfer in Turbine Blades," Heat Transfer 1978, Hemisphere Pub. Corp., Vol. 2, 1978, Paper No. EC-13, pp. 73-84.
56. Dunham, J.: "Predictions of Boundary Layer Transition on Turbomachinery Blades," AGARDograph No. 164 on Boundary Layer Effects in Turbomachines, 1972, pp. 55-72.
57. Liepmann, H.W.: "Investigations on Laminar Boundary Layer Stability and Transition on Curved Boundaries," NACA ACR No. 3H30, 1943, also Wartime Report W-107.
58. Aroesty, J.; W.S. King; G.M. Harpole; W.W. Matyskiela; C. Gazley, and A.R. Wazzan: "Simple Relations for Stability of Heated-Water Laminar Boundary Layers," AIAA Journal, Vol. 20, No. 5, May 1982, pp. 728-730.
59. Wazzan, A.R. and C. Gazley: "The Combined Effects of Pressure Gradient and Heating on the Stability and Transition of Water Boundary Layers," Proceedings of the 2nd International Conference on Drag Reduction, London, 1977, BHRA Fluid Engineering, Cranfield, Bedford, England, 1977, pp. E3-E23.
60. Straziar, A.J. and E. Reshotko: "Stability of Heated Laminar Boundary Layers in Water," AGARD Conference Proceedings No. 224 on Laminar-Turbulent Transition, 1977, Paper No. 10.
61. Barker, S.J. and C.G. Jennings: "The Effect of Wall Heating Upon Transition in Water Boundary Layers," AGARD Conference Proceeding No. 224 on Laminar-Turbulent Transition, 1977, Paper No. 19.
62. Wazzan, A.R.; G. Keltner; T.T. Okamura; and A.M.O. Smith: "Spatial Stability on Stagnation Water Boundary Layer With Heat Transfer," The Physics of Fluids, Vol. 15, No. 12, Dec. 1972, pp. 2114-2116.
63. Wazzan, A.R.; T.T. Okamura; and A.M.O. Smith: "The Stability of Water Flow Over Heated and Cooled Flat Plates," ASME Journal of Heat Transfer, Vol. 90, No. 1, Feb, 1968, pp. 109-114.
64. Wazzan, A.R.; T.T. Okamura; and A.M.O. Smith: "The Stability and Transition of Heated and Cooled Incompressible Laminar Boundary Layers," Proceedings of the Fourth International Heat Transfer Conference, Elsevier Pub. Co., Amsterdam, Vol. II, 1970.
65. Görtler, H.: "Über Eine Analogie Zwischen Den Instabilitäten Laminarer Grenzschichtströmungen An Konkaven Wa Und An Erwarmten Wänden," Ingr. Arch., Vol. 28, 1959, pp. 71-78.
66. Lees, L. and C.C. Lin: "Investigation of the Stability of the Laminar Boundary Layer in a Compressible Fluid," NACA Technical Note No. 1115, 1946.

67. Lees, L. and E. Reshotko: "Stability of the Compressible Laminar Boundary Layer," *Journal of Fluid Mechanics*, Vol. 12, Part 4, 1962, pp. 555-590.
68. Mack, L.M.: "The Stability of the Compressible Laminar Boundary Layer According to a Direct Numerical Solution," *AGARDograph No. 97 on Recent Developments in Boundary Layer Research*, 1965, pp. 329-362.
69. Jordinson, R.: "The Flat Plate Boundary Layer. Part 1: Numerical Integration of the Orr-Sommerfeld Equation," *Journal of Fluid Mechanics*, Vol. 43, Part 4, 1970, pp. 801-811.
70. Liepmann, H.W. and G.H. Fila: "Investigations of Effects of Surface Temperature and Single Roughness Elements on Boundary-Layer Transition," *NACA Technical Note No. 1196*, 1947, also *NACA Report No. 890*, 1947.
71. Katinas, V.; J. Zlugzda; and A. Zukauskas: "An Investigation of Local Heat Transfer on Plates in the Transitional Flow Regime," *Heat Transfer - Soviet Research*, Vol. 5, No. 6, Nov.-Dec. 1973, pp. 34-43.
72. Kercher, D.M.; R.E. Sheer, Jr.; and R.M.C. So: "Short Duration Heat Transfer Studies at High Freestream Temperatures," *ASME Paper No. 82-GT-129*, 1982.
73. Gazley, C., Jr.: "Boundary-Layer Stability and Transition in Subsonic and Supersonic Flow," *Journal of the Aeronautical Sciences*, Vol. 20, No. 1, Jan. 1953, pp. 19-28.
74. Kobayashi, R. and Y. Kohama: "Taylor-Görtler Instability of Compressible Boundary Layers," *AIAA Journal*, Vol. 15, No. 12, Dec. 1977, pp. 1723-1727.
75. Whitfield, J.D. and N.S. Dougherty, Jr.: "A Survey of Transition Research at Arnold Engineering Development Center," *AGARD Conference Proceedings No. 224 on Laminar-Turbulent Transition*, 1977.
76. Boltz, F.W.; G.C. Kenyon; and C.Q. Allen: "The Boundary-Layer Transition Characteristics of Two Bodies of Revolution, A Flat Plate, and An Unswept Wing in a Low-Turbulence Wind Tunnel," *NASA Technical Note No. D-309*, 1960.
77. Bradshaw, P.: *Effects of Streamline Curvature on Turbulent Flow*, *AGARDograph No. 169*, 1973.
78. Tani, I. and Y. Aihara: "Görtler Vortices and Boundary-Layer Transition," *Zeitschrift Fur Angewandte Mathematik und Physik*, Vol. 20, 1969, pp. 609-618.
79. So, R.M.C. and G.L. Mellor: "Experiment on Convex Curvature Effects in Turbulent Boundary Layers," *Journal of Fluid Mechanics*, Vol. 60, No. 1, 1973, pp. 43-62.

80. So, R.M.C. and G.L. Mellor: "Experiment on Turbulent Boundary Layers on a Concave Wall," *Aeronautical Quarterly*, Vol. 26, No. 1, 1975, pp. 35-40.
81. Thomann, H.: "Effect of Streamwise Curvature on Heat Transfer in Turbulent Boundary Layer," *Journal of Fluid Mechanics*, Vol. 33, No. 2, 1968, pp. 283-292.
82. Simon, T.W. and R.J. Moffat: "Heat Transfer Through Turbulent Boundary Layers - The Effects of Introduction To and Recovery From Convex Curvature," ASME Paper No. 79 - WA/GT - 10, 1979.
83. Taylor, G.I.: "Stability of a Viscous Liquid Contained Between Two Rotating Cylinders," *Phil. Trans. Roy. Soc. (London)*, Series A, Vol. 223, 1923, pp. 289-343.
84. Tani, I.: "Production of Longitudinal Vortices in the Boundary Layer Along a Concave Wall," *Journal of Geophysical Research*, Vol. 67, No. 8, July 1962, pp. 3075-3080.
85. Wortmann, F.X.: "Visualization of Transition," *Journal of Fluid Mechanics*, Vol. 38, Part 3, 1969, pp. 473-480.
86. Bippes, H. and H. Görtler: Translation of "Dreidimensionale Störungen in Der Grenzschicht an Einer Konkaven Wand," *Acta Mechanica*, Vol. 14, No. 4, 1972, pp. 251-267.
87. Liepmann, H.W.: "Investigation of Boundary Layer Transition on Concave Walls," NACA Wartime Report No. W-87, 1945.
88. McCormack, P.D.; H. Welker; and M. Kelleher: "Taylor-Görtler Vortices and Their Effect on Heat Transfer," ASME Paper No. 69-HT-3, 1969.
89. Smith, A.M.O.: "On the Growth of Taylor-Görtler Vortices Along Highly Concave Walls," *Quarterly of Applied Mathematics*, Vol. 13, No. 3, 1955, pp. 233-262.
90. Nayfeh, A.H.: "Effect of Streamwise Vortices on Tollmien-Schlichting Waves," *Journal of Fluid Mechanics*, Vol. 107, June 1981, pp. 441-453.
91. Tobak, M.: "On Local Görtler Instability," *Zeitschrift für Angewandte Mathematik und Physik*, Vol. 22, 1971, pp. 13-143.
92. Herbert, T.H.: "On the Stability of the Boundary Layer Along A Concave Wall," *Archiwum Mechaniki Stosowanej*, Vol. 28, No. 5-6, 1976, pp. 1039-1055.
93. Aihara, Y.: "Stability of the Compressible Boundary Layer Along a Curved Wall Under Gortler-type Disturbances," *Aeronautical Research Institute, Tokyo University*, Report No. 362, Feb. 1961, pp. 31-37.

94. Hämmerlin, G.: "Über Die Stabilität Einer Kompressiblen Strömung Längs Einer Konkaven Wand Bei Verschiedenen Wand - Temperaturverhältnissen," Deutsche Versuchsanstalt für Luftfahrt, Bericht No. 1976, Nov. 1961.
95. Kahawita, R.A. and R.N. Meroney: "The Influence of Heating on the Stability of Laminar Boundary Layers Along Concave Curved Walls," ASME Journal of Applied Mechanics, Vol. 44, No. 1, Mar. 1977, pp. 11-17.
96. Aihara, Y.: "Nonlinear Analysis of Görtler Vortices," The Physics of Fluids, Vol. 19, No. 11, Nov. 1976, pp. 1655-1660.
97. Tani, I. and H. Komoda: "Boundary Layer Transition in the Presence of Streamwise Vortices," Journal of the Aerospace Sciences, Vol. 29, No. 4, Apr. 1962, pp. 440-444.
98. Rosenhead, L. (ed.): Laminar Boundary Layers, Oxford University Press, 1963.
99. Obremski, H.J. and A.A. Fejer: "Transition in Oscillating Boundary Layer Flows," Journal of Fluid Mechanics, Vol. 29, Part 1, 1967, pp. 93-111.
100. Miller, J.A. and A.A. Fejer: "Transition Phenomena in Oscillating Boundary Layer Flows," Journal of Fluid Mechanics, Vol. 18, Part 3, 1964, pp. 438-449.
101. Kobashi, Y.; M. Kayakawa; and K. Nakagawa: "Development of Disturbances in Unsteady Boundary Layers," Proceedings, Symposium on Unsteady Aerodynamics, Mar. 1975. Tucson, Ariz., Kinney, R.B. (ed.), Arizona Board of Regents, 1975, Vol. 1, pp. 131-153.
102. Walker, G.J.: "The Unsteady Nature of Boundary Layer Transition on an Axial Compressor Blade," ASME Paper No. 74-GT-135, 1974.
103. Cousteix, J.; R. Houdeville; and A. Desopper: "Transition D'une Couche Limite Soumise a Une Oscillation De L'Ecoulement Exterieur," AGARD Conference Proceedings No. 224 on Laminar-Turbulent Transition, 1977, Paper No. 17.
104. Pfeil, H.; R. Herbst; and T. Schröder: "Investigation of the Laminar-Turbulent Transition of Boundary Layers Disturbed by Wakes," J. of Eng. for Power, Vol. 105, Jan. 1983, pp. 130-137.
105. Obremski, H.J. and M.V. Morkovin: "Application of a Quasi-Steady Stability Model to Periodic Boundary Layers," AIAA Journal, Vol. 7, No. 7, July 1969, pp. 1298-1301.
106. Obremski, H.J.; M.V. Morkovin; and M. Landahl: "A Portfolio of Stability Characteristics of Incompressible Boundary Layers," AGARDograph No. 134, 1969.

107. Finson, M.L.: "On the Application of Second-Order Closure Models to Boundary Layer Transition," AGARD Conference Proceedings No. 224 on Laminar-Turbulent Transition, 1977, Paper No. 23.
108. Smith, A.M.O.: "Transition, Pressure Gradient and Stability Theory," IX International Congress for Applied Mechanics, Brussels, 1956.
109. Van Ingen, J.L.: "A Suggested Semi-Empirical Method for the Calculation of the Boundary Layer Transition Region," University of Technology Delft, Dept. of Aero. Eng., Report VTH-74, 1956.
110. Van Ingen, J.L.: "Transition, Pressure Gradient, Suction, Separation and Stability Theory," AGARD Conference Proceedings No. 224 on Laminar-Turbulent Transition, 1977, Paper No. 20.
111. Hall, D.J. and J.C. Gibbings: "Influence of Stream Turbulence and Pressure Gradient Upon Boundary Layer Transition," Journal of Mechanical Engineering Science, Vol. 14, No. 2, 1972, pp. 134-146.
112. Donaldson, C. DuP. and R.D. Sullivan: "A Computer Study of an Analytical Model of Boundary Layer Transition," Boundary Layer Transition Study Group Meeting, Air Force Report No. BSD-TR-67-213, Vol. II, 1967, Section 12.
113. Reynolds, W.C.: "Computation of Turbulent Flows," Annual Review of Fluid Mechanics, Vol. 8, 1976, pp. 183-208.
114. Forest, A.E.: "Engineering Predictions of Transitional Boundary Layers," AGARD Conference Proceedings No. 224 on Laminar-Turbulent Transition, 1977, Paper No. 22.
115. McDonald, H. and R.W. Fish: "Practical Calculations of Transitional Boundary Layers," International Journal of Heat and Mass Transfer, Vol. 16, 1973, pp. 1729-1744, also AGARDograph No. 164, 1972, pp. 29-53.
116. Wilcox, D.C.: "Alternative to the e^9 Procedure for Predicting Boundary-Layer Transition," AIAA Journal, Vol. 19, No. 1, Jan. 1980, pp. 56-64.
117. Daniels, L.D. and W.B. Browne: "Calculation of Heat Transfer Rates to Gas Turbine Blades," International Journal of Heat and Mass Transfer, Vol. 24, No. 5, 1981, pp. 871-879.
118. Martin, B.W. and A. Brown: "Factors Influencing Heat Transfer to the Pressure Surfaces of Gas Turbine Blades," International Journal of Heat and Fluid Flow, Vol. 1, No. 3, Sept. 1979, pp. 107-114.
119. Harris, J.E.: "Numerical Solutions of the Equations for Compressible Laminar, Transitional, and Turbulent Boundary Layers and Comparisons with Experimental Data," NASA Technical Report R-368, 1971.
120. Van Driest, E.R. and C.B. Blumer: "Boundary Layer Transition: Freestream Turbulence and Pressure Gradient Effects," AIAA Journal, Vol. 1, No. 6, June 1963, pp. 1303-1306.

121. Brown, A. and B.W. Martin: "Heat Transfer for Turbine Blades, With Special Reference to the Effects of Mainstream Turbulence," ASME Paper No. 79-GT-26, 1979.
122. Brown, A. and B.W. Martin: "A Review of the Bases of Predicting Heat Transfer to Gas Turbine Rotor Blades," ASME Paper No. 74-GT-27, 1974.
123. Brown, A. and R.C. Burton: "The Effects of Freestream Turbulence Intensity and Velocity Distribution on Heat Transfer to Curved Surfaces," ASME Journal of Engineering for Power, Vol. 100, Jan. 1978, pp. 159-168.
124. Brown, A. and B.W. Martin: "Flow Transition Phenomena and Heat Transfer Over the Pressure Surfaces of Gas Turbine Blades," ASME Paper No. 81-GT-107, 1981.
125. Martin, B.W.; A. Brown; and S.E. Garrett: "Heat Transfer to a PVD Rotor Blade at High Subsonic Passage Throat Mach Numbers," AGARD Conference Proceedings No. 229 on High Temperature Problems in Gas Turbine Engines, 1978, Paper No. 32.
126. Blair, M.F.: "Influence of Freestream Turbulence on Boundary Layer Transition in Favorable Pressure Gradients," J. of Eng. for Power, Vol. 104, Oct. 1982, p. 743-750.
127. Chen, K.K. and N.A. Thyson: "Extension of Emmons' Spot Theory to Flows on Blunt Bodies," AIAA Journal, Vol. 9, No. 5, May 1971, pp. 821-825.
128. Owen, F.K.: "Transition Experiments on a Flat Plate at Subsonic and Supersonic Speeds," AIAA Paper No. 69-9, 1969.
129. Sharma, O.P.; R.A. Wells; R.H. Schlinker; and D.A. Bailey: "Boundary Layer Development on Turbine Airfoil Suction Surfaces," ASME Paper No. 81-GT-204, 1981.
130. Debruge, L.L.: "A Theoretical Determination of Convective Heat-Transfer Coefficients During Transition on the Suction Side of Turbine Airfoils," Air Force Aero Propulsion Laboratory, Wright-Patterson Air Force Base, Ohio, Technical Report AFAPL-TR-69-95, 1970.
131. Lessmann, R.C.: "Intermittent Transition Flow in a Boundary Layer," AIAA Journal, Vol. 15, No. 11, Nov. 1977, pp. 1656-1658.
132. Kays, W.M. and M.E. Crawford: Convective Heat and Mass Transfer, McGraw-Hill, 1980.
133. Reynolds, W.C.; W.M. Kays; and S.J. Kline: "Heat Transfer in the Turbulent Incompressible Boundary Layer. IV-Effect of Location of Transition and Prediction of Heat Transfer in a Known Transition Region," NASA Memorandum 12-4-58W, 1958.

134. Coles, D.: "Measurement of Turbulent Friction on a Smooth Flat Plate in Supersonic Flow," Journal of the Aeronautical Sciences, Vol. 21, 1954, pp. 433-448.
135. Charnay, G.; J. Comte-Bellot; and J. Mathieu: "Development of a Turbulent Boundary Layer on a Flat Plate in an External Turbulent Flow," AGARD Conference Proceedings No. 93, 1971.
136. Graham, R.W.: "Fundamental Mechanisms That Influence the Estimate of Heat Transfer to Gas Turbine Blades," ASME Paper No. 79-HT-43, 1979.
137. Joslyn, H.D.; R.P. Dring; and O.P. Sharma: "Unsteady Three-Dimensional Turbine Aerodynamics," ASME Paper No. 82-GT-161, 1982.
138. Dring, R.P.; H.D. Joslyn; L.W. Hardin; and J.H. Wagner: "Turbine Rotor-Stator Interaction," J. of Eng. for Power, Vol. 104, Oct. 1982, p. 729-741.
139. Evans, R.L.: "Turbulence and Unsteadiness Measurements Downstream of a Moving Blade Row," ASME Journal of Engineering for Power, Vol. 97, No. 1, Jan. 1975, pp. 131-139.
140. Kestin, J. and R.T. Wood: "The Mechanism Which Causes Freestream Turbulence to Enhance Stagnation-Line Heat and Mass Transfer," Heat Transfer 1970, Vol. 2, Elsevier Publishing Co., Amsterdam, 1970, Paper No. FC 2.7.
141. Schmidt, E. and K. Wenner: "Heat Transfer Over the Circumference of a Heated Cylinder in Transverse Flow," NACA Technical Memorandum No. 1050, 1943.
142. Gorla, R.S.R.: "Effects of Unsteady Freestream Velocity and Freestream Turbulence at a Stagnation Point," ASME Paper No. 82-GT-69, 1982.
143. Sadeh, W.Z.; H.J. Brauer; and J.A. Garrison: "Visualization Study of Vorticity Amplification in Stagnation Flow," SQUID-CSU-1-PU, Colorado State Univ., Fort Collins, Co., 1977.
144. Boldman, D.R. and P.F. Brinich: "Mean Velocity, Turbulence Intensity and Scale in a Subsonic Turbulent Jet Impinging Normal to a Large Flat Plate," NASA TP-1037, 1977.
145. Hansen, A.G. and H.Z. Herzig: "Secondary Flows and Three-Dimensional Effects," Aerodynamic Design of Axial-Flow Compressors, NASA SP-36, 1965, pp. 365-411.
146. Chait, A.: "Surface Roughness Effects on the Boundary Layer of the Turbine Blade," M.Sc. Thesis, The Ohio State University, Dept. of Mechanical Engineering, 1979.

147. Mengütürk, M. and E.F. Sverdrup: "A Theory for Fine Particle Deposition in Two-Dimensional Boundary Layer Flows and Application to Gas Turbines," ASME Journal of Engineering for Power, Vol. 104, No. 1, Jan. 1982, pp. 69-76.
148. Han, L.S.; W.R. Cox; and A. Chait: "Investigation of the Boundary Layer Behavior on Turbine Airfoils," Air Force Aero Propulsion Laboratory Report AFAPL-TR-79-2011, Wright-Patterson Air Force Base, Ohio, 1979.
149. Moffitt, T.P.; F.S. Stepka; and H.E. Rohlik: "Summary of NASA Aerodynamic and Heat Transfer Studies in Turbine Vanes and Blades," NASA Technical Memorandum X-73518, 1976.
150. Stepka, F.S.: "Uncertainties in Predicting Turbine Blade Metal Temperatures," ASME Paper No. 80-HT-25, 1980.
151. Kuhl, W.: "Investigations on the Local Heat Transfer Coefficient of a Convection Cooled Rotor Blade," AGARD Conference Proceedings No. 229 on High Temperature Problems in Gas Turbine Engines, 1978, Paper No. 7.
152. Secondary Flows in Turbomachines, AGARD Conference Proceedings No. 214, 1977.
153. Binder, A. and R. Romey: "Secondary Flow Effects and Mixing of the Wake Behind a Turbine Stator," ASME Paper No. 82-GT-46, 1982.
154. Sharma, O.P. and R.A. Graziani: "Influence of Endwall Flow on Airfoil Suction Surface Mid-Height Boundary Layer Development in a Turbine Cascade," ASME Paper No. 82-GT-127, 1982.
155. Walker, L.A. and E. Markland: "Heat Transfer to Turbine Blading in the Presence of Secondary Flow," International Journal of Heat and Mass Transfer, Vol. 8, 1965, pp. 729-748.
156. Walker, L.A. and E. Markland: "Calculation of Heat Transfer to Turbine Blading in the Presence of Secondary Flow," International Journal of Heat and Mass Transfer, Vol. 10, 1967, pp. 499-518.
157. Unsteady Phenomena in Turbomachinery, AGARD Conference Proceedings No. 1977, 1976.
158. Lander, R.D.: "Evaluation of the Effect of Freestream Turbulence on the Heat Transfer to Turbine Airfoils," Air Force Aero Propulsion Laboratory Technical Report AFAPL-TR-69-70, Wright-Patterson Air Force Base, Ohio, 1969.
159. Jones, T.V.; D.L. Schultz; M.L.G. Oldfield; and L.C. Daniels: "Measurement of Heat Transfer Rate to Turbine Blades and Nozzle Guide Vanes in a Transient Cascade," Heat Transfer 1978, Hemisphere Pub. Corp., Washington, Vol. 2, 1978, Paper No. EC-12, pp. 73-78.

160. Köhler, H.; D.K. Hennecke; K. Pfaff; and R. Eggebrecht: "Hot Cascade Test Results of Cooled Turbine Blades and Their Application to Actual Engine Conditions," AGARD Conference Proceedings No. 229 on High Temperature Problems in Gas Turbine Engines, 1978, Paper No. 6.
161. Bayley, F.J. and R.W. Milligan: "The Effect of Freestream Turbulence Upon Heat Transfer to Turbine Blading," AGARD Conference Proceedings No. 229 on High Temperature Problems in Gas Turbine Engines, 1978, Paper No. 37.
162. Turner, A.G.: "Local Heat Transfer Measurements on a Gas Turbine Blade," Journal of Mechanical Engineering Science, Vol. 13, No. 1, 1971, pp. 1-12.
163. Dunn, M.G. and F.J. Stoddard: "Measurement of Heat-Transfer Rate to a Gas Turbine Stator," ASME Paper No. 78-GT-119, 1978.
164. Oldfield, M.L.G.; R. Kiock; A.T. Holmes; and C.G. Graham: "Boundary Layer Studies on Highly Loaded Cascades Using Heated Thin Films and a Transversing Probe," ASME Paper No. 80-GT-137, 1980.
165. Consigny, H. and B.E. Richards: "Short Duration Measurements of Heat-Transfer Rate to a Gas Turbine Rotor Blade," ASME Journal of Engineering for Power, Vol. 104, July 1982, pp. 542-551.
166. Litchfield, M.R. and R.J.G. Norton: "Heat Transfer Measurements of a Transonic Nozzle Guide Vane," ASME Paper No. 82-GT-247, 1982.
167. Nicholson, J.H.; A.E. Forest; M.L.G. Oldfield; and D.L. Schultz: "Heat Transfer Optimised Turbine Rotor Blades - An Experimental Study Using Transient Techniques," ASME Paper No. 82-GT-304, 1982.
168. Bayley, F.J. and W.J. Priddy: "Effects of Freestream Turbulence Intensity and Frequency on Heat Transfer to Turbine Blading," ASME Journal of Engineering for Power, Vol. 103, Jan. 1981, pp. 60-64.
169. Krishnamoorthy, V.: "Effect of Turbulence on the Heat Transfer in a Laminar and Turbulent Boundary Layer Over a Gas Turbine Blade," ASME Paper No. 82-GT-146, 1982.
170. Junkhan, G.H. and G.K. Serovy: "Effects of Freestream Turbulence and Pressure Gradient on Flat-Plate Boundary-Layer Velocity Profiles and on Heat Transfer," ASME Journal of Heat Transfer, Vol. 89, No. 2, May 1967, pp. 169-176.
171. Dyban, E.P. and E. Ya. Epik: "Heat Transfer in a Boundary Layer in Turbulized Air Flow," Heat Transfer, 1978, Hemisphere Pub. Corp., Washington, Vol. 2, 1978, Paper No. FC(a)-4, pp. 507-517.
172. Han, L.S. and W.R. Cox: "A Visual Study of Turbine Blade Pressure-Side Boundary Layers," ASME Paper No. 82-GT-47, 1982.

173. Kistler, E.L.: "Boundary Layer Transition: A Review of Theory, Experiment, and Related Phenomena," NASA Contractor Report No. CR-128540, 1971.
174. Wilcox, D.C.: "Turbulence-Model Transition Predictions," AIAA Journal, Vol. 13, No. 2, Feb. 1975, pp. 241-243.
175. Wilcox, D.C.: "A Model for Transitional Flows," AIAA Paper No. 77-126, 1977.
176. Moore, F.K. (ed.): Theory of Laminar Flows, Princeton University Press, 1964.
177. Mojola, O.O.: "Transition in a Streamwise Corner," AIAA Journal, Vol. 15, No. 3, Mar. 1977, pp. 427-429.
178. Arnal, D. and R. Michel: "Effect of Freestream Turbulence on Turbulent Boundary Layers and on Boundary Layer Transition," EUROMECH 72, Boundary Layers and Turbulence in Internal Flows, University of Salford, Salford, U.K., 1976.
179. Boundary Layer Effects in Turbomachines, AGARDograph No. 164, 1972.
180. High Temperature Turbines, AGARD Conference Proceedings No. 73, 1971.
181. Morkovin, M.V.: "Critical Evaluation of Transition From Laminar to Turbulent Shear Layers With Emphasis on Hypersonically Traveling Bodies," AFFDL TR-68-149, Mar. 1969.
182. Wells, C.S.: "Effect of Free-stream Turbulence on Boundary-layer Transition," AIAA Journal, Vol. 5, 1967, pp. 172-174.
183. Hislop, G.S.: The Transition of a Laminar Boundary Layer in a Wind Tunnel, Ph.D. Thesis, Cambridge University, 1940.
184. Feindt, E.G.: "Investigation on the Dependence of Laminar-Turbulent Transition on Surface Roughness and Pressure Gradient," Jahrbuch 1956 Der Schiffbantechnischen Gesellschaft 50, 1957.
185. Fage, A. and J.H. Preston: "On the Transition From Laminar to Turbulent Flow in the Boundary Layer," Proc. Roy. Soc., Vol. 178, Ser. A, 1941, pp. 201-227.
186. Hall, D.J.: Boundary-Layer Transition, Ph.D. Thesis, Liverpool University, 1968.
187. Garner, H.C.: "The Development of Turbulent Boundary Layers," ARC R AND M 2113, 1944.
188. HALL, P.: "On the Non-linear Stability of Slowly Varying Time-dependent Viscous Flows," Journal of Fluid Mechanics, Vol. 126, Jan. 1983, p. 357.

189. Betchon, R.: "Transition," Ch. 6 in Handbook of Turbulence (Frost and Moulden, eds.), Vol. 1, Plenum Press, 1977.
190. Turbulent Boundary Layers, Experiments, Theory and Modelling, AGARD Conference Proceedings No. 271, 1980.

END

FILMED

2-86

DTIC